JET PROPULSION LABORATORY

CALIFORNIA INSTITUTE OF TECHNOLOGY

PASADENA, CALIFORNIA

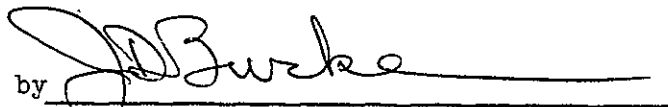JPL - 760-96

SCIENCE ASPECTS OF A 1980 FLYBY OF

COMET ENCKE WITH A PIONEER SPACECRAFT

May 20, 1974

L. D. Jaffe, C. Elachi, C. E. Giffin, W. Huntress,
R. L. Newburn, R. H. Parker, F. W. Taylor, T. E. Thorpe

Approved by _____

James D. Burke
Manager, Advanced Technical Studies

JET PROPULSION LABORATORY

CALIFORNIA INSTITUTE OF TECHNOLOGY

PASADENA, CALIFORNIA

FOREWORD

The study reported in this document was carried out
September 10 to December 15, 1973. The document reflects
technical inputs up to the latter date. Effort since then
has been confined to editing, coordination, and review.

CONTENTS

CONTENTS (Cont'd)

CONTENTS (Cont'd)

CONTENTS (cont'd)

TABLES

FIGURES

I. INTRODUCTION

At the request of the System Studies Division of Ames Research Center, JPL has carried out a study of science aspects of a 1980 flyby of Comet Encke using a Pioneer-class spacecraft. Areas covered in this study include:

- Science objectives and rationale

    Science observables

    Effects of encounter velocity

    Science encounter and targeting requirements

    Selection and description of science instruments

    Definition of a candidate science payload

    Engineering characteristics of suggested payload

    Value of a separable probe

    Science instruments for a separable probe

    Science payload integration problems

    Science operations profile

A guideline was that the spacecraft would be generally simi___ __ ____ concepts for Pioneer Venus as they existed at the start of this study (July 1973). Also, the study team was aware of a parallel study by Martin Marietta Corporation of 1980 missions to Comet Encke and asteroids using a spin-stabilized spacecraft; the Martin Marietta study was also for the Ames System Studies Division. The JPL study received many inputs from the Martin Marietta team and utilized these for definition of many spacecraft and mission characteristics. No attempt was made to be consistent with the Martin Marietta results in all respects; indeed, the final Martin Marietta report (Ref. I-1) was not available early enough to influence this work significantly.

Further, it was clearly desirable to keep the mission cost low. To this end, the mission and spacecraft should not be complicated unnecessarily and existing hardware designs should be usable where possible.

The model of Comet Encke used in this study is that of Taylor, Michaux, and Newburn (Ref. I-2).

A study of science aspects of a slow flyby of Comet Encke using a 3-axis-stabilized spacecraft was recently completed (Ref. I-3); other aspects of this slow flyby are under study (Ref. I-4). A mission design study of a fast (ballistic) flyby near perihelion with a spinning spacecraft has been published (Ref. I-5). A study of a fast Encke flyby with a 3-axis-stabilized spacecraft is in progress at JPL.

SUMMARY AND CONCLUSIONS

1. A 1980 fast flyby mission to Comet Encke using a Pioneer-type spinning spacecraft, without despin of the science instruments, could provide valuable scientific data and is scientifically worthwhile as an initial reconnaissance. (The engineering feasibility of conducting this mission with a Pioneer-type spacecraft was not examined in this study.)

2. Such a mission can determine the existence of a cometary nucleus and, if one exists, its approximate dimensions and albedo. This mission can determine the composition and concentration of neutral gases, ions, and solid particles in the coma and tail, and the interaction of the coma and tail with the solar wind.

3. With this mission it appears impractical to <u>assure</u> observations of topographic features of the nucleus, if any, measurements of nucleus or halo temperatures, or determination of nucleus mass or spin.

4. With this mission it appears impractical to <u>assure</u> imaging of the nucleus, if any, at 100-m feature resolution. There is some chance that a very few pictures with such resolution might be obtained, depending on the dust density and particle sizes actually encountered by the spacecraft close to the nucleus and on luck in its not suffering a destructive impact by a dust particle.

5. Encounter with Encke should take place before the comet reaches perihelion and between 0.45 AU and 0.9 AU from the sun. The spacecraft should fly through the shock front sunward of the nucleus, through the coma and the tail,

and, if possible, through the contact surface between the solar wind and the ionized cometary gas.

6. Imaging of the nucleus should be from as close as is considered safe, and from the sunward hemisphere. Mass spectrometer measurements should be obtained as close to the nucleus as is considered safe: if possible, within 500-1000 km. (No attempt was made in this study to determine whether such a close pass can be achieved by a Pioneer spacecraft.)

7. On the basis of the data available, a flyby at 5000 km from the nucleus, at velocities of 18-20 km/sec, appears to involve insignificant risk from the cometary environment (dust). At 500 km from the nucleus, the risk is not more than a few percent.

8. A mission is suggested that includes encounter near 0.53 AU from the sun, with approach from the sunward side and almost along the sun-comet line. It is suggested that the spacecraft be targeted for the nucleus and that on-board navigational aids be provided to insure flyby within 500-1000 km of the nucleus. If the risk of losing the spacecraft at encounter, and therefore the post-encounter tail data, is considered too high with this encounter design, an optional tail probe may be carried, which would be separated prior to encounter and targeted to fly by at 5000 km or more from the nucleus. This probe should communicate directly to Earth.

9. For the science instruments, a spin axis orientation approximately toward the comet during approach (therefore approximately along the sun-spacecraft line) is desirable with the mission design outlined.

10. The type of mission suggested involves encounter speeds of 18-20 km/sec
relative to the comet. These relatively high speeds are, on the whole,
disadvantageous scientifically. They decrease the spatial resolution for
in-situ measurements in coma and tail, tend to increase imaging smear and
the difficulty of properly pointing optical instruments, increase the dust
hazard and therefore the safe distance from the nucleus, reduce the accuracy
of measuring particle velocities relative to the comet, and necessitate
modifications in mass spectrometer design if the composition of undissociated
neutrals is to be measured. High speeds do, however, facilitate measurement
of composition of impacting dust by impact vaporization and ionization. Despite
the disadvantages, a mission with high encounter speed seems satisfactory for
initial reconnaissance of a comet.

11. A science payload is suggested which includes a (spinning) framing camera
using a charge-coupled-device sensor, an imaging photometer, ultraviolet spectro-
meter, mass spectrometer, optical dust detector, magnetometer, plasma probe,
plasma wave detector, Langmuir probe, micrometeoroid detector, and dust analyzer.
For most of these instruments, existing designs or equipment could be used. The
estimated mass of this payload is 56 kg, the estimated power usage and bit rate
at encounter are 56 W and 15 kbit/sec. A tape recorder is not needed.

12. If a separable tail probe is flown, as an optional add-on, the suggested science
payload for this probe consists of a mass spectrometer, magnetometer, plasma
probe, and Langmuir probe. Estimated mass, power, and bit rate for these instru-
ments on the separable probe are 13.8 kg, 20 W, 120 bit/sec, respectively.

13. If obtaining some nucleus pictures with 100-m feature resolution were to be
seriously attempted, on-board equipment would be needed to track the nucleus

optically during encounter, to automatically point the camera at it, and to automatically trigger the camera when the nucleus was within its field of view.

14. A preliminary science profile for the mission considered indicates that encounter science operations should commence about 5 days before closest approach. The period of maximum payload operation on the bus lasts about 1 hour. If a separable tail probe is carried, its science instruments should operate 11 hours or more to insure data through the coma and tail.

III. SCIENCE OBJECTIVES AND OBSERVABLES

A. SCIENCE OBJECTIVES

Science objectives that appear appropriate to this mission are:

To determine the existence of a cometary nucleus and, if
it exists, its dimensions and albedo.

To determine the composition and concentration of neutral
gases, ions, and solid particles in the coma and tail.

To determine the interaction of the coma and tail with
the solar wind.

The first objective is addressed to the most fundamental question about
comets amenable to direct observations: do comets have a solid nucleus, from
which coma and tail develop, or is the so-called nucleus merely a group of small
separated particles in independent but similar orbits (as believed by Lyttleton,
Ref. III-1)? This objective is also aimed toward characterizing any nucleus by
determining the general nature of its surface.

The second objective is addressed to determining the chemical and physical
nature of a comet -- water, other volatiles, silicates -- the manner in which
the constituents decompose and ionize under the effects of solar radiation
and solar wind, and the manner in which the particulate matter is affected
by its environment.

The third objective is addressed to understanding the plasma phenomena
associated with a comet and the origin and acceleration mechanism of the ion
tail.

hese objectives have been discussed by the Comet and Asteroid Mission Study
Panel (Ref. III-2) and by Clay et. al. (Ref. III-3).

B. SCIENCE OBSERVABLES

Properties of the comet that are pertinent to the objectives selected, and are considered practical to measure directly on a mission of the kind considered, include:

Nucleus existence

Nucleus size

Nucleus general shape

Nucleus albedo

Dust concentration vs. position

Dust mass distribution

Dust elemental composition (major elements)

Dust general mineralogical nature (from optical polarization)

Coma neutral gas composition vs. position (elemental, some
  molecules and radicals)

Coma and tail ion composition vs. position

Coma and tail ion temperatures and approximate direction of
  ion flow

Coma optical shape

Coma brightness along various lines of sight

Intensity of several optical bands, along various lines of sight

Ultraviolet spectrum and brightness, along various lines of sight

Magnetic and electrical fields vs. frequency and position

Solar plasma flux, energy distribution, and direction vs. position

Properties, on which measurements are very desirable but not considered practical for this mission, include:

Mass. No known techniques would give a useful measure with the
  flyby speeds and distances available (see Ref. III-2).

Nucleus spin. Duration of high-resolution imagery is insufficient
  on a fast flyby.

Other properties that may or may not be directly measurable include:

        Photometric function of nucleus. Some data may be obtained but the photometric function is difficult to measure with the very high angular rate between spacecraft and nucleus that arises from the fairly close encounter desirable for other objectives.

        Nucleus surface features. It is very difficult to obtain resolution of surface features with a small spacecraft at a distance considered safe for a fast flyby.

        Icy halo, if one exists. These measurements will be difficult unless the halo is quite thick and bright.

        Velocities of dust and of neutrals and ions in coma. These velocities would be difficult to determine accurately from a platform which is moving at much higher velocity, relative to the comet.

        Electron content along line of sight. Difficult because of low content expected in comet.

These various difficulties and limitations are discussed further in later sections.

IV. MISSION AND SPACECRAFT ASSUMPTIONS

Information from the Martin Marietta study as it progressed indicated that the following assumptions were reasonable for possible mission and spacecraft characteristics:

Encke encounter:	16-30 days prior to Encke perihelion.
Approach direction:	spacecraft approaches Encke from near solar direction.
Encounter speed:	18-26 km/sec.
Encounter distance:	Minimum is set by spacecraft safety. Navigation accuracy to be determined.
Spin rate and axis direction:	2-10 rpm or higher. Choice of direction.
Data transmission rate at encounter:	16 kbits/sec. X- and S-band transmission.
Data storage:	can carry Mariner 9 tape recorder, plus separate 1-frame buffer.
Science payload mass:	up to 75 kg or more.
Probes:	can also carry 1 to 3 deployable probes.
Probe data transmission rate:	for a single probe, 128 b/sec. Can be direct to Earth.

Not all of these assumed capabilities were utilized in the suggested science design.

V. SCIENCE REQUIREMENTS FOR ENCOUNTER

Encounter with the comet should take place at 0.45 to 0.9 AU from the sun, 10 to 40 days before Encke perihelion. The spacecraft should fly through the coma and tail, through the shock front sunward of the nucleus (estimated to be 10^5 to 10^6 km distant), and if possible through the contact surface between the solar wind and the ionized cometary gas (estimated as to be about 10^4 km from the nucleus); see Fig. V-1.

Imaging of the nucleus should be from as close a distance as is considered safe, and from the sunward hemisphere. Mass spectrometer measurements should be obtained as close to the nucleus as is considered safe; if possible, within 500-1000 km to insure a neutral gas density high enough for good analyses and to increase the chance of measuring undissociated parent molecules, originating at the nucleus.

A. TRAJECTORY

The Martin Marietta study (Ref. V-1) recommended an encounter at 0.53 AU from the sun, 16 days prior to Encke perihelion passage, with the spacecraft approaching the comet directly along the sun-Encke line (from the sunward direction). (See Figures V-2 and V-3). This appears to be a good choice for the mission class contemplated. At distances further from the sun than 0.9 - 1.0 AU (earlier encounter), the comet will be less active and less bright. At distances closer to the sun, the coma will be much smaller (Ref. V-2). After perihelion, Encke will be much less active and less bright (Ref. V-3). Whether this drop in activity occurs shortly before or shortly after perihelion is not known with certainty. An encounter at perihelion may therefore mean observing the comet after its activity has fallen sharply, and when its coma is very small. Moreover, higher launch velocity will be needed for encounters close to the sun: either the payload must be smaller or a larger launch vehicle will be needed.

BOW SHOCK FRONT

EDGE OF T.

EDGE OF COMA

COMA

TAIL

CONTACT SURFACE (?)

EDGE OF COMA

TO SUN

10^6 10^4 10^2 10^2 10^4 10^6 km

NUCLEUS

-12-
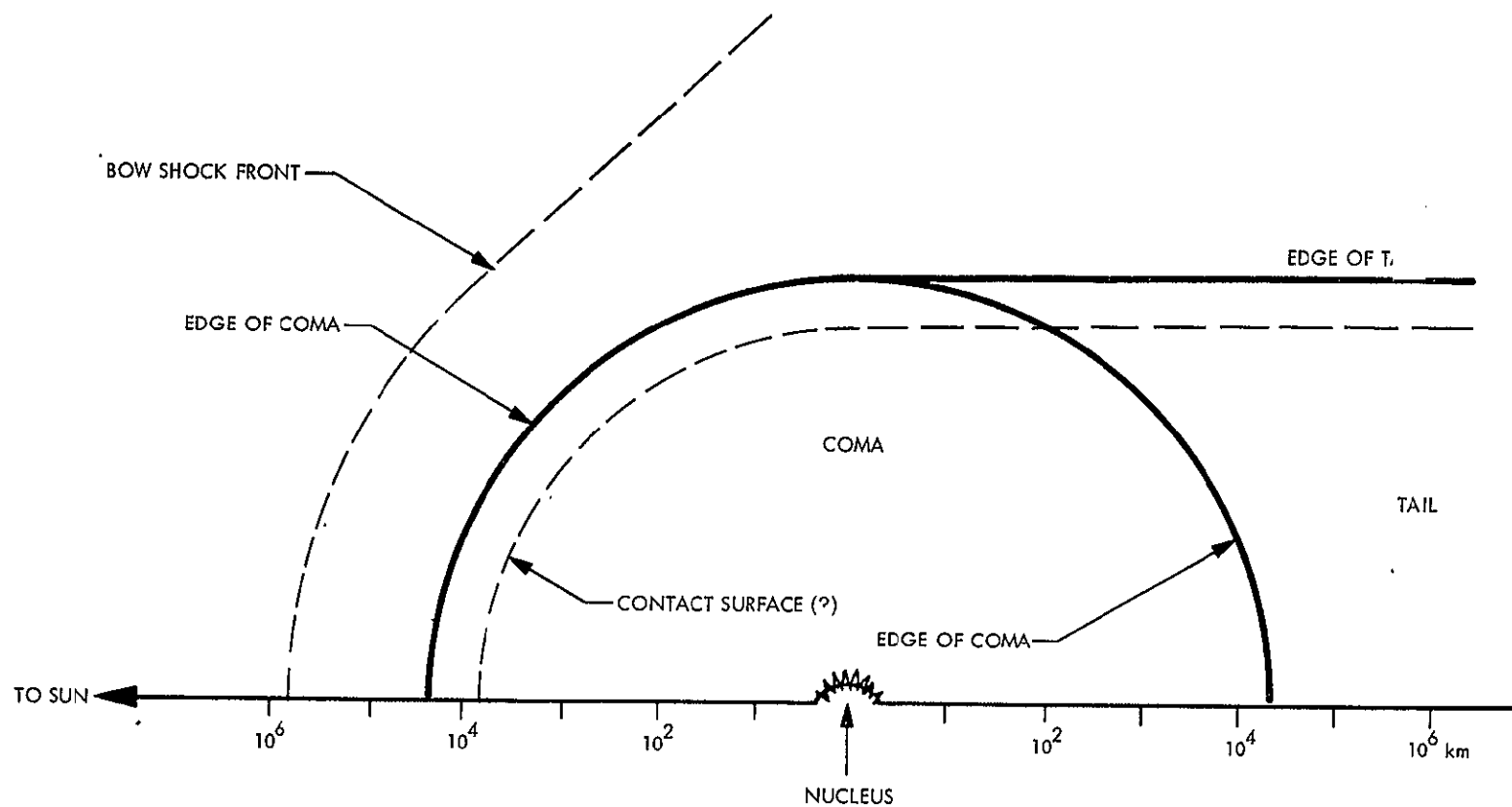
e V-1.   Schematic of Comet Encke.
Note log scale
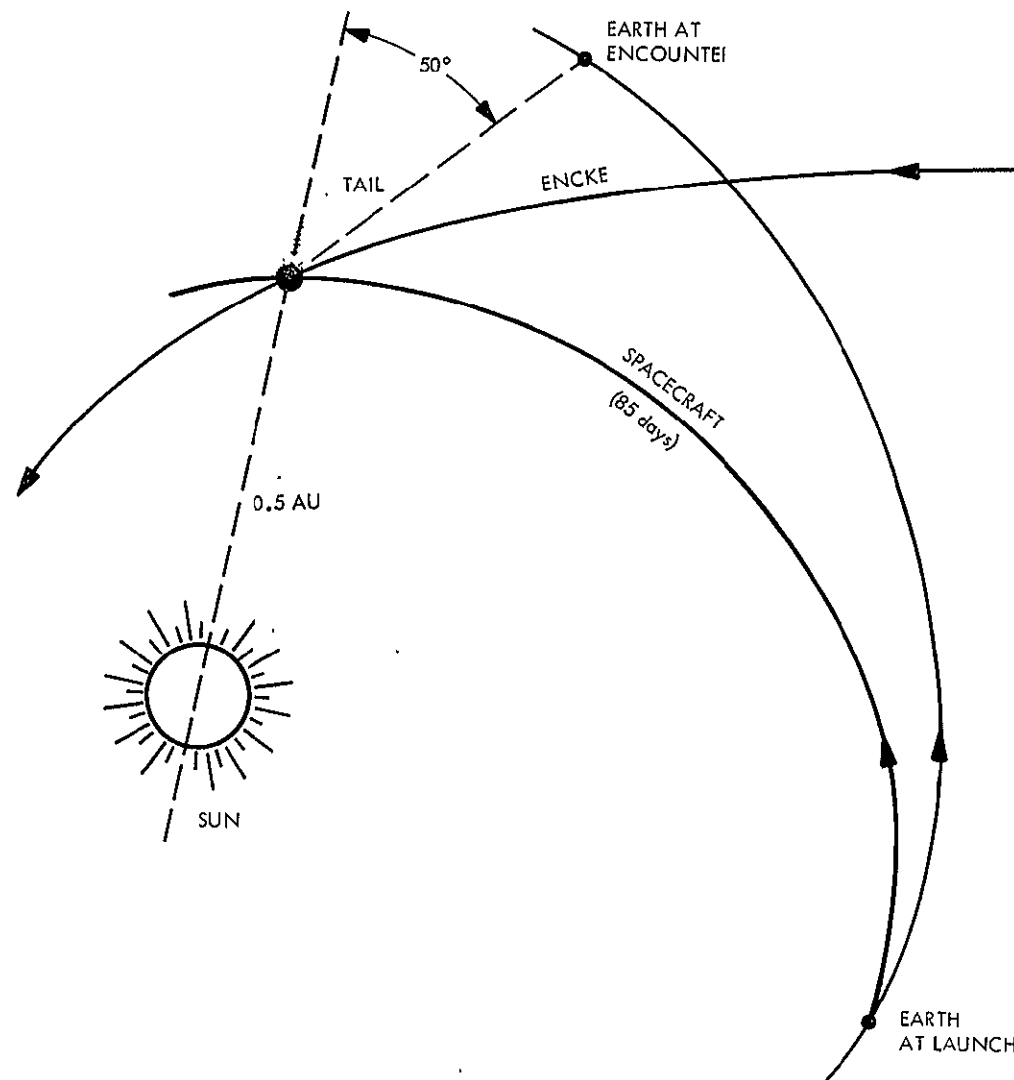
Figure V-2. Trajectory and tail direction. Heliocentric coordinates.

TAIL

TO EARTH

NUCLEUS

COMA

TRAJECTORY

TO SUN
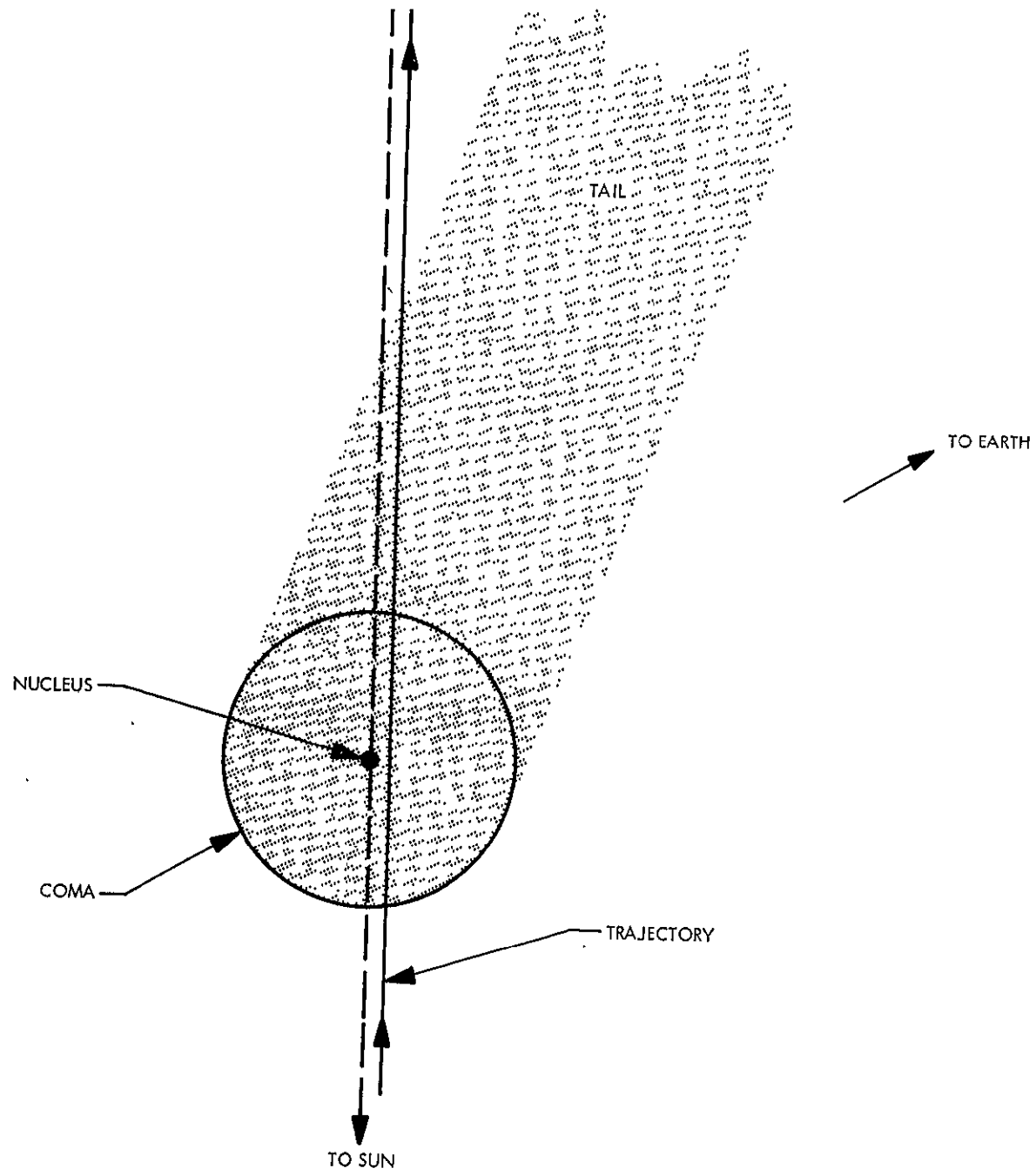
Figure V-3.   Trajectory in comet-centered coordinates.   Schematic.

Approach from the sun direction also seems advantageous. It maximizes the brightness of the nucleus as seen by the spacecraft during approach and so should maximize the range at which the nucleus is detected from the spacecraft. It tends to maximize length of path of the spacecraft through the tail, which at this helio-centric distance will point close to the anti-solar direction. Some other advantages are pointed out below.

For heavier spacecraft configurations, such as those carrying a despun science platform or a separable probe, the Martin Marietta study indicates that encounter 16 days prior to Encke perihelion cannot be achieved with the launch vehicle con-templated (Atlas/Centaur/TE 364-4). Such weights can be accommodated by a slightly earlier encounter, say 17 days before Encke perihelion. At this time, the helio-centric distance would be about 0.55 AU and the approach direction would be about 2° off the sun-Encke line. This also seems satisfactory.

The approach angles mentioned are for a selected launch date. Variations of a few days in launch date will change the approach angle, relative to the sun-comet line, by a few degrees (Ref. V-1).

B. ENCOUNTER SPEED AND ITS EFFECTS

The speed of the spacecraft relative to Encke, for the trajectories mentioned, is approximately 18.3 km/sec for an encounter 16 days before perihelion and about 19 km/sec for encounter 17 days before perihelion. These speeds are higher than optimum for most science measurements. Encounters further from the sun (as, for instance, at 0.9 AU) will involve even higher speeds.

The effects of high encounter speed upon various types of scientific measurements are as follows:

1. Mass Spectroscopy

    a. Dissociation. Molecules striking a mass spectrometer at high speeds will
        be dissociated by impact. This makes it difficult to determine the
        character of the molecules prior to impact. For some molecules of interest,
        the effect begins at about 5 km/sec; at 10 km/sec, most molecules of interest
        will be dissociated.

    b. Separation from background. Molecules originating from the spacecraft are
        expected to provide a relatively high background, which must be separated
        from the signal arising from cometary material. Spacecraft velocity
        relative to the cometary gas provides a convenient way to do so. (Note that
        even if the spacecraft were at rest relative to the comet nucleus, the
        outward flow of cometary gas would provide a relative speed of 1 km/sec or
        more). One technique utilizes a retarding potential behind the ionizer:
        the potential is set to exclude molecules with only thermal velocities
        but to admit molecules with higher incoming velocities. This technique
        is not yet fully developed or tested in flight.

    c. Loss of spatial resolution. The spatial resolution is degraded with increasing
        speed, due to the fixed cycle time needed to provide adequate signal, as
        discussed below.

2. Imaging

    A high spacecraft speed, and the accompanying high angular velocity near encounter
greatly increases the difficulty of maintaining proper pointing for imaging, pointing
both of a camera (or scan platform) and of the spacecraft itself (attitude control).
Also, with high velocity, there is less time to obtain pictures of the nucleus (if
any) at close range. The high angular velocity near encounter also tends to increase
imaging smear; this smear is, however, likely to be less than that arising from
spacecraft spin.

3. Charged Particles and Fields

A high spacecraft velocity reduces the spatial resolution of the measurements. Also, it somewhat reduces the accuracy with which the velocity of particles relative to the comet can be measured.

4. Dust Detection and Analysis

For impact-type dust detectors, a high spacecraft speed has several advantages:

a. Because incoming particles will have higher momentum and energy, the device will be sensitive to smaller particles at higher relative velocities.

b. As the speed rises above 5 km/sec, enough vaporization and ionization occurs on impact to permit analysis of the dust particle composition by a mass spectrometer.

Determination of the particle velocity relative to the comet becomes less accurate, however, as the spacecraft speed rises.

For optical dust detectors, the high spacecraft speed has several disadvantages:

a. Because of the shorter observing duration per particle, there will be less integrated signal per particle.

b. Because of the overall shorter observing time, there will be fewer particles observed.

c. Because of the higher relative velocity of particles and spacecraft, the accuracy of measuring the comet-centered velocity of the particles will be diminished.

5. General

Since the mass spectroscopy and imaging will probably provide the most critical measurements for understanding the nature of a comet, high relative speeds are generally undesirable. Moreover, for any spacecraft instrument, the time available to make measurements of the comet is decreased as the relative velocity is increased.

For any observing interval, dictated by integration time or data rate, the spacecraft moves further at high relative speeds, so the attainable spatial resolution is poorer. This applies generally to all measurements.

A high speed also greatly increases the hazard from cometary dust: the energy per particle varies as the square of the velocity. This increased hazard translates into a constraint on the minimum safe approach distance and so reduces the chance of obtaining measurements on characteristics of the region close to the nucleus: parent (undissociated) gas molecules, icy halo, if any, temperature and spectral measurements of the nucleus, and perhaps the contact surface (if it exists) between the solar plasma and the ions of the coma.

Nevertheless, for missions of the Pioneer class, with the launch vehicle selected, it is not practical to obtain significantly lower encounter speeds. Speeds of 18-20 km/sec are considered satisfactory for an initial reconnaissance of Encke.

C. TARGETING STRATEGY AND SEPARABLE PROBES

The Martin Marietta study selected a flyby distance of 5000 km from the nucleus. This choice was made primarily on the basis of the possible meteoroid hazard to the spacecraft of a closer approach; the dust density presumably varies inversely as the square of the distance from the nucleus. The dust density is uncertain by three orders of magnitude (Ref. V-4) and (assuming navigation and guidance are accurate enough to achieve it) the Martin Marietta flyby distance appears a conservative and reasonable choice for a first mission if the risk of losing the spacecraft by impact of cometary dust is to be kept very low. With this encounter geometry, the angular velocity of the nucleus as seen by the spacecraft at closest approach is 12.6°/min (Ref. V-1).

The value and use of separable probes has been considered at some length. Our

recommended mission strategy is:

A) Baseline: Spacecraft (bus) targeted directly for the nucleus.

B) Optional add-on: One tail probe biased to fly by at nominally

5000 km from the nucleus.

The sequence of reasoning that led to this recommendation is outlined in the succeeding paragraphs.

With a bus flyby at 5000 km, as selected by Martin Marietta, the primary value found for a probe was to explore portions of the coma close to the nucleus, seeking parent molecules, icy halo, and contact surface. (The contact surface, if it exists, may be more than 5000 km out, or it may be less; it may not exist, or it may not be stable). For this purpose, the probe would be required (if it survived) to go within 500 km of the nucleus, or at most 1000 km. Moreover, its position relative to the nucleus should be known as a function of time to within 100 km, after the mission; otherwise the data obtained on spatial distribution could not be adequately referenced to the nucleus. With this mission design, if the probe is destroyed, the bus should still survive and return its data. A fairly high risk of losing the probe would be acceptable; any data it returned on conditions closer than 5000 km from the nucleus would be a scientific bonus.

The use of 3 probes in a shotgun pattern has been suggested as one means of taking care of uncertainties in spacecraft position relative to the nucleus, to insure getting some data at 5000 km or closer. Because the data will mean very little unless the corresponding position is known accurately (relative to the nucleus), this shotgun technique is not considered desirable.

The next concept considered was to use a bus and a single probe but aim the bus directly for the nucleus and bias the probe to fly by with a miss distance of 5000 km or more. This risks destruction of the bus but should insure that the probe survives to obtain data anti-sunward of the nucleus, and especially in the tail.

The probe is adequate for tail measurements since the primary measurements needed in the tail are particles and fields and mass spectroscopy. The probe would have to communicate its data directly to Earth; such a data link is envisaged in the Martin Marietta study (Ref. V-1). Advantages of this mission design are:

- The angular rate of the nucleus, as seen from the bus, is considerably lower when the bus is 5000 km distant and aiming straight for the nucleus than it would be if the bus were to fly by at this distance. This helps considerably in reducing image smear, effectively increases imaging sensitivity, and helps significantly in pointing the camera and timing its exposure.

- The sensitivity of ultraviolet spectroscopy is effectively increased because it is relatively simple to scan a UVS over an arc centered close to the nucleus during each spacecraft rotation and integrate over this arc, which will be close to symmetrical about the sun-nucleus line. (This is discussed below, under "Ultraviolet Spectrometer").

- Higher spatial resolution is obtainable close to the nucleus on particles- and-fields and mass-spectroscopy instruments, because the higher data transmission rate available from the bus (as compared to the probe) permits more frequent sampling.

- If the bus survives to closer than 5000 km from the nucleus, imaging can be obtained at correspondingly higher resolution.

- Once the probe is separated, its trajectory presumably cannot be improved. The bus trajectory can be improved later, utilizing bus optical sensors and Earth-based observations for a series of approach maneuvers, if necessary. This capability may be essential to place the instruments within 500 km of the nucleus. (See navigation discussion below). A

much larger error can be tolerated in placing the flyby object (here the probe) without significant loss of science data. There is nothing critical about the suggested 5000 km probe flyby. The flyby distance should simply be small enough to bring the probe well within the coma and large enough to make the risk of damage by cometary dust very low.

Accurate post-mission knowledge of position, relative to the nucleus, is more important for close-in measurements than for those farther out. Position measurement should be more accurate for the bus, which could carry a transponder permitting 2-way doppler and ranging, as well as optical sensors for on-board navigation, than for the probe, which will carry no imaging or guidance capability and probably no transponder (probably no communications receiver).

It may be noted that, with the imaging system proposed below, a frame would be transmitted within 18 seconds after it is taken. Thus a picture taken at a 5000-km distance would be transmitted before the bus reached 4700 km from the nucleus; the risk of bus destruction before the picture is sent is thus not appreciably greater than if the bus stayed at 5000 km. Any pictures taken and transmitted inside 5000 km would be a bonus.

Disadvantages of targeting the bus to the nucleus include:

. If the bus is destroyed before closest approach, nucleus imaging will not be obtained at as high a phase angle. This would reduce image contrast and data on the photometric function.

. Polarimetry of dust close to the nucleus might likewise be restricted to lower phase angles, if the polarimeter is on the bus and the bus is destroyed.

. Risk of degraded spatial resolution for on-board instruments in anti-solar hemisphere (probe capability only).

. The risk of losing the bus at a given distance from the nucleus is
greater than for the probe, since the bus is a larger target for dust
particles.

. Even if the bus survives, the angular rate of the nucleus, as seen by
the bus, will be very high at phase angles not close to 0° or 180°.
It will therefore be more difficult to make optical observations at
these phase angles.

Weighing these advantages and disadvantages, the study made an interim choice
of a bus targeted at the nucleus and one separable probe biased 5000 km off. With
further consideration, it was noted that the likelihood of bus survival past encounter
with this strategy is fairly high. Martin Marietta calculations (Ref. V-1), based
on a model of cometary dust hazard that is considered very conservative, indicate a
survival probability greater than 0.98 if the flyby is at 500 km from the nucleus
at 20 km/sec, and, it appears, greater than 0.90 at 100 km distance and 20 km/sec.
The survival probability is appreciably higher at 18.3 km/sec than at 20. Also,
the expected miss distance due to navigation uncertainties is expected to be nearer
500 than 100 km. Thus, bus survival is very likely with the strategy proposed. The
flyby probe then serves essentially as a back-up to insure getting tail data for the
small chance that the bus is lost during encounter.

These considerations suggested a variant strategy: simply accept the risk of
bus loss on encounter (with resulting loss of tail data), omit the probe, and save
money. (With no probe, the nominal encounter velocity falls slightly, increasing
survival probability). This seems a very worthwhile alternative and was chosen as
baseline. The flyby probe is retained as an optional add-on.

Engineering aspects of separable probes, and their costs in competition with

a bus-only mission, were not covered in this work and should be the subject of separate studies.

D. DIRECTION OF AIM POINT AND TAIL PASSAGE OF OPTIONAL TAIL PROBE

For measurements in the coma, the direction of the comet-probe vector at closest approach (the "aim-point direction" of the optional separable probe) does not seem very significant. Since the rotation pole of the nucleus (if any) is unknown, it is not possible to select a polar or equatorial approach, nor, given our present knowledge, is it clear that this would make much difference. A flyby on the side farthest from Earth slightly increases the path length through the coma from probe to Earth and increases the sensitivity of plasma column measurements by radio. Since the probe would presumably transmit only at one frequency, plasma column measurements from it would not be very accurate and are not proposed.

Choice of aim-point direction for the tail probe is therefore based primarily on the desirability of maximizing times in the tail. The ion tail is not exactly in the anti-sun direction but in a direction determined by the solar wind and the comet motion. The tail deviation is in the direction opposite planetary motion (see Fig. V-2). The average angle from the radial direction for the bulk solar wind flow is 0°. However, during short periods (several hours), the solar wind velocity vector can be as much as 8.5° from the radial direction. The following discussion shows that, in consequence, the average deviation angle of the comet's tail at 0.5 AU is 6°, but it may get to be as much as 15° for short times.

The general statement is always made that comet tails stream back in the antisolar direction. This is approximately true for both Type I (ion) and Type II (dust) tails but is not precisely true for either. Long dust tails always have a curvature caused by the individual particles, which make up the tails, taking up their own independent Keplerian orbits around the Sun as they are slowly forced away from the comet and Sun by radiation pressure. (Of course the curvature may

not be obvious as seen projected against the sky). Ion tails are often very straight, which is one evidence of high acceleration. Even so, they do not point in exactly the antisolar direction; the angle between the axis of the tail and the antisolar radial is called the aberration angle.

"The orientation of Type I tail appears to be determined by the direction of the solar wind as seen by an observer on the comet" (Brandt & Hodge, Ref. V-5). The aberration angle α is given by (Ref. V-5):

$$\cot \alpha = \frac{(\vec{w} + \vec{V}) \cdot \vec{r}}{(\vec{w} + \vec{V}) \cdot -\vec{\phi}}$$

where $\vec{w}$ is the plasma velocity

$\vec{V}$ is the comet velocity

$\vec{r}$ is a unit radial vector

$-\vec{\phi}$ is a unit azimuthal vector (in a sense opposed

to the comet's motion, but $-\vec{\phi} \cdot \vec{r} = 0$

Using the latest elements for the orbit of P/Encke [a = 2.216485 AU and e = 0.847745] we can calculate the comet's radial velocity and its velocity perpendicular to the radius vector from

$$\dot{r}^2 = \frac{GM}{r^2 a} [a (1 + e) - r] [r - a (1 - e)]$$

$$\text{and} \quad (r \dot{\theta})^2 = \frac{GMa}{r^2} (1 - e^2)$$

where G = universal gravitational constant

M = mass of the Sun

r = heliocentric distance

$\dot{r}$ = radial velocity

θ = heliocentric azimuth

$r\dot{\theta}$ = velocity $\perp$ radius vector

Of course $V^2 = \dot{r}^2 + (r\dot{\theta})^2$

where V = orbital velocity

Using **GM** = $1.327125 \times 10^{11} km^3 sec^{-2}$ we find:

	r= 0.5	r = 0.8	r = 1.0
$\dot{r}$ (km/sec)	30.52	30.85	28.63
$r\dot{\theta}$ (km/sec)	47.08	29.43	23.54
V (km/sec)	56.11	42.64	37.06

Assume for the moment that we are dealing with a two dimensional problem (i.e., that solar wind velocity is in the same plane as the comet's orbit) and that the solar wind speed is 400 km/sec. Assume also that the wind direction is either radial (400 km/sec radial velocity) or, during a moderately large solar flare, has an $8\frac{1}{2}$ degree deviation (395.6 km/sec radial velocity and 59.1 km/sec velocity perpendicular to the radius vector). Then we find for the aberration angle:

	r = 0.5 AU	r = 0.8 AU	r = 1.0 AU
Solar Wind 400 km/sec	$6°.24$	$3°.91$	$3°.14$
Solar Wind 395.6 x 59.1 km/sec	$13°.99$	$11°.73$	$11°.02$

The distance (Fig. V-4) the separable probe will traverse through the coma and tail after closest approach is

$$R \csc \alpha + b \ctn \alpha$$

where R = radius of coma and tail

b = bias of flyby toward direction opposite planetary motion

α = angle between antisolar and tail direction, measured opposite direction of planetary motion
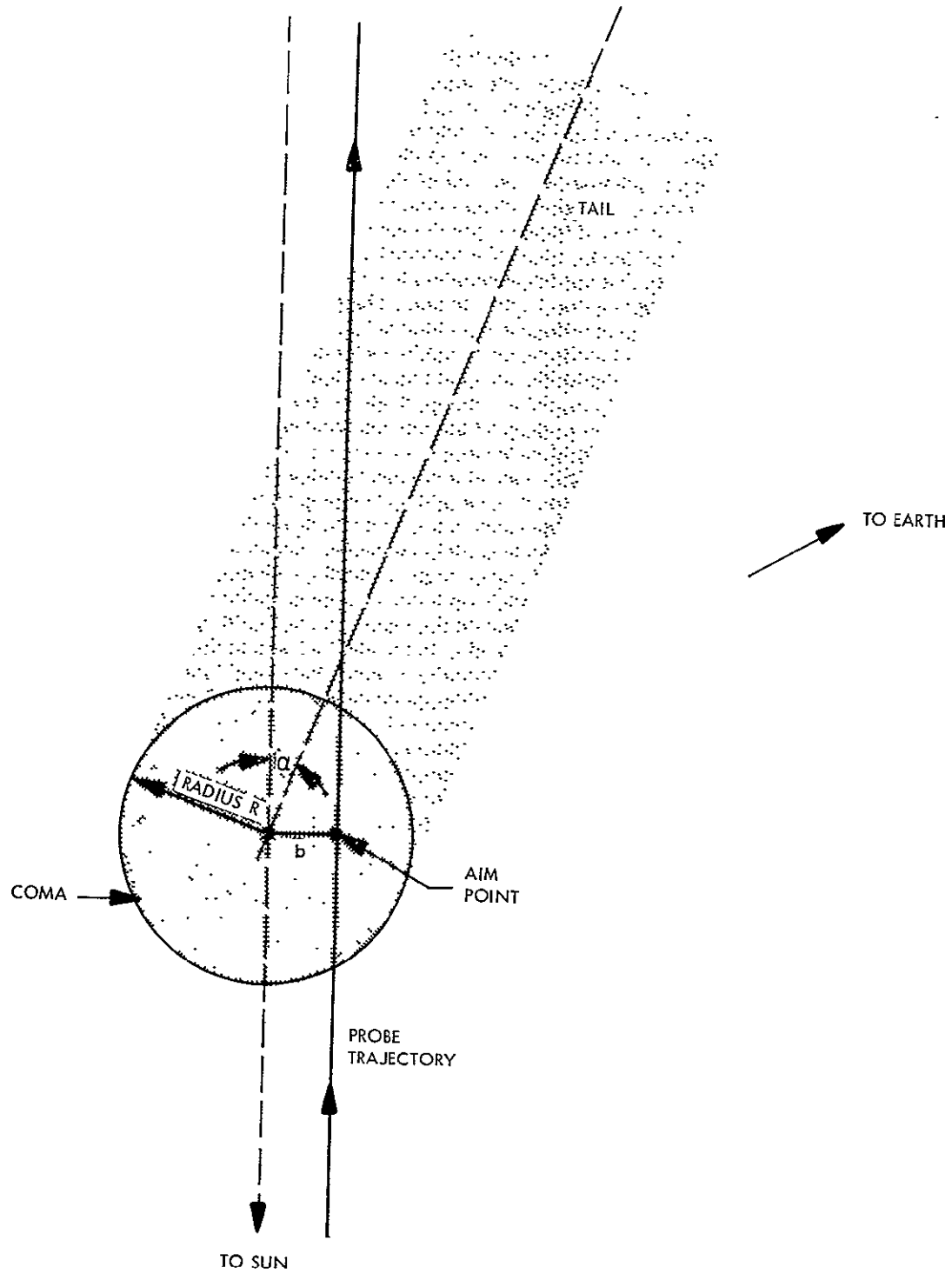
Figure V-4. Probe trajectory through the comet.

For an aberration angle of 15°, a coma radius of 20,000 km and a flyby bias, b, of + 5000 km, the distance between closest approach and tail exit is 100,000 km and the corresponding time is 1.4 hr. The bias contributes 0.3 hr for these conditions. Thus, biasing the tail probe toward the side opposite the direction of planetary motion is desirable; this is the direction toward the Earth during encounter (Figs. V-2 and V-4). More likely is an aberration angle of 6°; if the coma radius turns out to be as great as 50,000 km, and the flyby bias is unchanged, the distance to tail exit is then 500,000 km and the time 7.5 hr.

Curvature of the spacecraft flight path relative to the comet is in the same direction as the tail deviation. This curvature amounts to less than $2^{\circ}/$day (Ref. V-1) or $\frac{1}{4}^{\circ}$ in 3 hr., and can be neglected compared to tail deviation.

REFERENCES

IV-1 G. R. Hook, E. G. Howard, J. M. van Pelt, W. J. Bursnall,
      "Study of 1980 Comet Encke-Asteroid Missions using a Spin-Stabilized
      Spacecraft", Martin Marietta Corp., MCR 73-180, "Mid-Term Review"
      and MCR 73-260, "Final Oral Presentation", 1973.

IV-2 F. W. Taylor, C. M. Michaux, R. L. Newburn, Jr., "A Model of the
      Physical Properties of Comet Encke". JPL Tech. Rpt. 32-1590, 1973.

IV-3 Brandt, J. C. and Hodge, P., "Solar System Astrophysics," McGraw-Hill,
      New York, 1964.

VI. SPACECRAFT SPIN

A. DESPINNING SCIENCE INSTRUMENTS

Examination of possible imaging instruments, below, indicates that considerable improvement of imaging performance is possible by despinning the camera; that is, mounting it on a despun platform accurately stabilized in 3 axes with respect to celestial coordinates. The performance of such other potential instruments as an ultraviolet spectrometer and an infrared radiometer would also be increased somewhat by despinning (though the radiometer is probably not feasible; see below). However, a despun platform with the necessary accurate stabilization would add considerably to the weight (Martin Marietta estimate (Ref.VI-1): 26 kg), complexity, and cost of the spacecraft. Such an addition is felt to be inconsistent with the advantages of simplicity and relatively low cost offered by the Pioneer spacecraft. The study team accordingly recommended against a despun platform. For comparison, one of the options in the Martin Marietta study (Ref.VI-1) does include a despun platform, and can be examined as an alternative.

The Martin Marietta study also considered using a despun mirror. For imaging, this is merely a form of image motion compensation, and generally leaves the image rotating across the sensor surface. Image motion compensation internal to the imaging system is considered superior, as discussed in the Imaging Instruments section (Section VII A) of this report. Accordingly, a despun mirror is not recommended by the study team.

B. SPIN AXIS

The choice of spin axis direction has been considered. From the point of view of science measurements, it appears highly desirable to point the spin axis at, or very close to, the comet during approach. Optical instruments viewing the comet can then be pointed very close to the spin axis. For a given spin rate, the linear rate of motion of the comet across the optical sensors will then be much lower than if viewing were at 90° from the spin axis. (The rate of motion varies as sin θ, where θ is the view angle relative to the spin axis). This considerably increases the integration time available on each revolution of the spacecraft, which in turn increases the effective sensitivity of the optical instruments. As discussed below, this is extremely important; as otherwise the sensitivity of some instruments would be marginal.

Certain instruments, such as the mass spectrometer, should be pointed along the ram direction. With the spin axis toward the comet during approach, they need merely to be pointed along the spin axis.

Imaging instruments should not be pointed exactly along the spin axis. A spin scan imager would not scan, and, for a frame-imager, image motion compensation would involve the high relative rotation of various parts of the image. As discussed below, alignments within 6' arc of the spin axis may be desirable with the television camera proposed, but an offset of 1-2° seems satisfactory. During approach, the spacecraft-comet-sun angle is also 1-2° (for certain launch dates). Thus, a particularly simple form of implementation would be to point the spin axis at the sun during approach; this is recommended.

During encounter, as the spacecraft flies by close to the comet, the view angle of the comet, relative to the spacecraft trajectory and the sun, changes very rapidly. At a 5000-km miss distance, the rate of change of the view angle reaches 12.6°/min.; at a 500-km miss distance, it reaches 126°/min. Slewing the

spin axis at such rates, with the high accuracy that would be needed, does not

seem feasible. Moreover, if this were done, the ram direction relative to the

axis would also change, requiring a mechanism to point the mass spectrometer in

the ram direction. It seems preferable to keep the spin axis pointed at the

sun and use a hinged mounting for the television camera so that it will view

the nucleus once per rotation. The problem of keeping the camera mount at the

correct angle to the spin axis during flyby is also discussed below (Section IX F).

A despun antenna will be needed for data transmission to Earth; the Martin

Marietta study (Ref. VI-1) indicates that the weight required for antenna despin

is quite small.

VII. RECOMMENDED SCIENCE INSTRUMENTS AND PAYLOAD

The recommended science payload is summarized in Table VII-1. On the bus, the total science-payload mass, power, and bit rate are 56 kg, 56 W, and 15 kbit/s. On the optional separable flyby probe, the science-payload mass, power, and bit rate are 14 kg, 20 W, and 120 bit/s. No tape recorder is needed on the bus or separable probe.

If weight limitations necessitate reduction of the payload, the Langmuir probe is of lowest priority on the probe. On the bus, the instruments of lowest priority are probably one of the dust/micrometeoroid instruments and the ultraviolet spectrometer.

The reasoning that led to these recommendations, and the various techniques and instruments suitable for this mission that can meet the scientific objectives, are discussed in the following sections.

A. IMAGING AND PHOTOMETRY

The imaging requirements for the proposed mission center around recording faint sources from a spinning spacecraft. The dominant source of apparent angular displacement will be the spacecraft rotation of 2-10 rpm (0.2-1.0 radian/sec). The 18-20 km/sec motion of the spacecraft relative to the comet introduces a maximum angular displacement rate slightly less than 0.2 radian/sec even with a flyby distance as small as 100 km; for a 500 km flyby distance, the maximum rate from this source is 0.04 radian/sec. Instrumentation is restricted to an overall payload mass not much over 75 kg (plus detachable probe) with preference for existing hardware and technology implementation. Data rates of $\leq$ 16 kbs are anticipated; however, a tape recorder could permit faster video readout and storage. Highest priority among the science imaging goals is to confirm or disprove the

Table VII-1

CANDIDATE SCIENCE PAYLOAD

Instrument	kg	W	Average Bits/Sec	Type
Bus				
Framing camera	19	13	13,000	New
Imaging photometer	4.2	2.8	.205	Pioneer 10 (Mod)
Ultraviolet spectrometer	3	3	500	AAFE *
Mass spectrometer	5.3	9.0	250	Venus Pioneer
Dust analyzer	5.2	8	52	Helios (Mod.)
Optical particle detector	4	3	. 10	Pioneer 10 (Mod.)
Magnetometer	2.0	3	200	Pioneer 10
Plasma wave detector	5	5.0	300	OGO-6
Langmuir probe	1.5	3	200	OGO-6
Plasma probe	5	5	350	ALSEP (Mod)
Micrometeoroid detector	1.8	1	200	Pioneer 10
	56.0	55.8	15,267	
Flyby Probe (Optional add-on)				
Mass spectrometer	5.3	9.0	45	Venus Pioneer
Magnetometer	2.0	3	25	Pioneer 10
Langmuir probe	1.5	3	25	OGO-6
Plasma probe	5	5	25	ALSEP (Mod)
Total	13.8	20	120	

* AAFE: Advanced Applications Flight Experiment

existence of a solid cometary nucleus. Desirable reconnaissance also includes nuclear size, shape, albedo, and phase information.

Successful encounter requires comet ephemeris refinement based, in part, upon early optical observation from large distances (see Section IX E, below). Hence, optical navigation and post-flight analysis of the trajectory may require imaging capabilities. In the absence of established requirements for navigation sensor performance, the choice of imaging instrument is here based primarily on science needs.

The cometary model chosen to evaluate instrument performance is consistent with prior analysis (Ref. VII-1). The coma is in accordance with the model of Taylor, Michaux and Newburn (Ref. VII-2) at 0.53 AU solar distance, and is consistent with the 1980 predicted visual magnitude. The nucleus brightness is based on the aphelion observation of Roemer (Ref. VII-3): nominally a 4-km nucleus diameter with 20% albedo; a minimum nucleus diameter of 2 km with 80% albedo. The nucleus is assumed to exhibit a Martian phase function and be visible only by neutral reflectance of solar energy.

To confirm the existence of a cometary nucleus the postulated 4 km diameter nucleus of 20% albedo should be imaged with at least 6 feature resolution elements, and the "minimal" 2 km diameter nucleus with at least 3 feature resolution elements. Feature resolution elements should be distinguished from picture elements ("pixels"), which are essentially the instantaneous field of view of an electronic image scanner. For average contrast and equipment performance, the pixel size must be multiplied by a ("Kell") factor of about 2.5 to give the feature resolution. Thus, for the 600-m feature resolution needed to identify an Encke nucleus, the projected pixel size should be 250 m or smaller.

1. Instrument description

   a. Comparative analysis

      The impact of these mission constraints severely limits the
   choice of imaging instruments. Confirmation of the existence of
   a cometary nucleus requires comparatively long focal lengths to
   obtain sufficient image size, yet extreme sensitivity to produce
   exposures short enough to handle the high angular velocity of a
   rotating spacecraft. Numerous sensor trade-off studies have been
   generated to evaluate imaging performance for Pioneer and other
   planetary missions (Refs. VII - 4 to VII - 10). These analyses have
   been examined for potential comet application. Performance capabili-
   ties with various combinations of sensors, telescopes, and image
   motion compensation devices are described in Appendix A.

   b. Framing camera

      The recommended instrument capable of satisfying the primary
   science objectives is .a single solid-state camera (charge-coupled
   device) with partial mechanical image motion compensation and a 50 cm
   focal length f/1.5 telescope. As described in Appendix A, the
   requirements of resolution, sensitivity, and minimum weight do not
   favor alternative options for a spinning spacecraft. Various pay-
   load characteristics are displayed in Table VII-2. A complementary
   instrument to obtain coma measurements is discussed below ("Imaging
   Photometer"). A tape recorder is not needed.

      The suggested camera will satisfy all of the major scientific
   objectives subject to the spacecraft automatic sequencing capability.
   The feature resolution threshold is anticipated to be about 600 m at

TABLE VII-2

CAMERA DESCRIPTION*

Camera	Solid state (charge coupled device)
Sensor	200 x 200 element array
Sensitivity (S/N = 10:1)	10^{-3} fc-s
Data rate	13 k bit/s
Exposure time	0.5 ms - 0.5 s
Shutter mechanization	Electronic**
γ (slope of light transfer characteristic)	0.95
Modulation Transfer Function (20% Response)	15 lp/mm
Spectral response	3000 - 11000 Å
Encoding	6-bit/element
Dark current	2.5 nA/cm^2 at -40°C
Saturation current	86 nA/cm^2
Quantum efficiency	50%**
Telescope	50 cm f/1.5**
Total mass	19 kg
Power	13 W
Image Motion Compensation (IMC)	Mechanical
IMC correction distance	15 pixels
Instantaneous Field of View (IFOV)	52 μradian
FOV	0.6°
Dimensions	80 x 40 x 40 cm (with telescope)

*Based on demonstrated Fairchild 100 x 100 array solid-state camera performance.

**Considered feasible by Fairchild or other institutions.

5000 km distance. Hence, sufficient margin exists to identify a nucleus as small as 2 km in diameter, and to place six feature resolution elements across a nucleus 4 km in diameter.

1. Sensor Configuration

The framing camera is consistent with study guidelines to utilize existing technology. Current sensor evaluation and development programs by several institutions, including JPL, should provide a viable flight instrument within the schedule imposed by the Encke mission (Appendix B). This sub-section will define only the sensor configuration; i.e., one-dimensional vs. two-dimensional arrays and the number of elements per array.

Two options for photography of the comet nucleus provide the choice of a scanning camera dependent upon spacecraft rotation to achieve a two-dimensional image, and a framing camera that would produce an instantaneous two-dimensional record at each camera pointing direction. For small image formats (few picture elements per picture) video readout is primarily dependent upon spacecraft tape recorder or data transmission rates and either sensor configuration is satisfactory. However, the combination of high resolving capability and camera pointing control imposed by the Pioneer vehicle implies that moderate sized arrays will be needed. Figure VII-1 shows the number of adequate-size picture elements (pixels) necessary to provide 600-m feature resolution elements at 5000 km range as a function of the corresponding total field of view. Typical spacecraft slewing increment and pointing accuracy suggest that
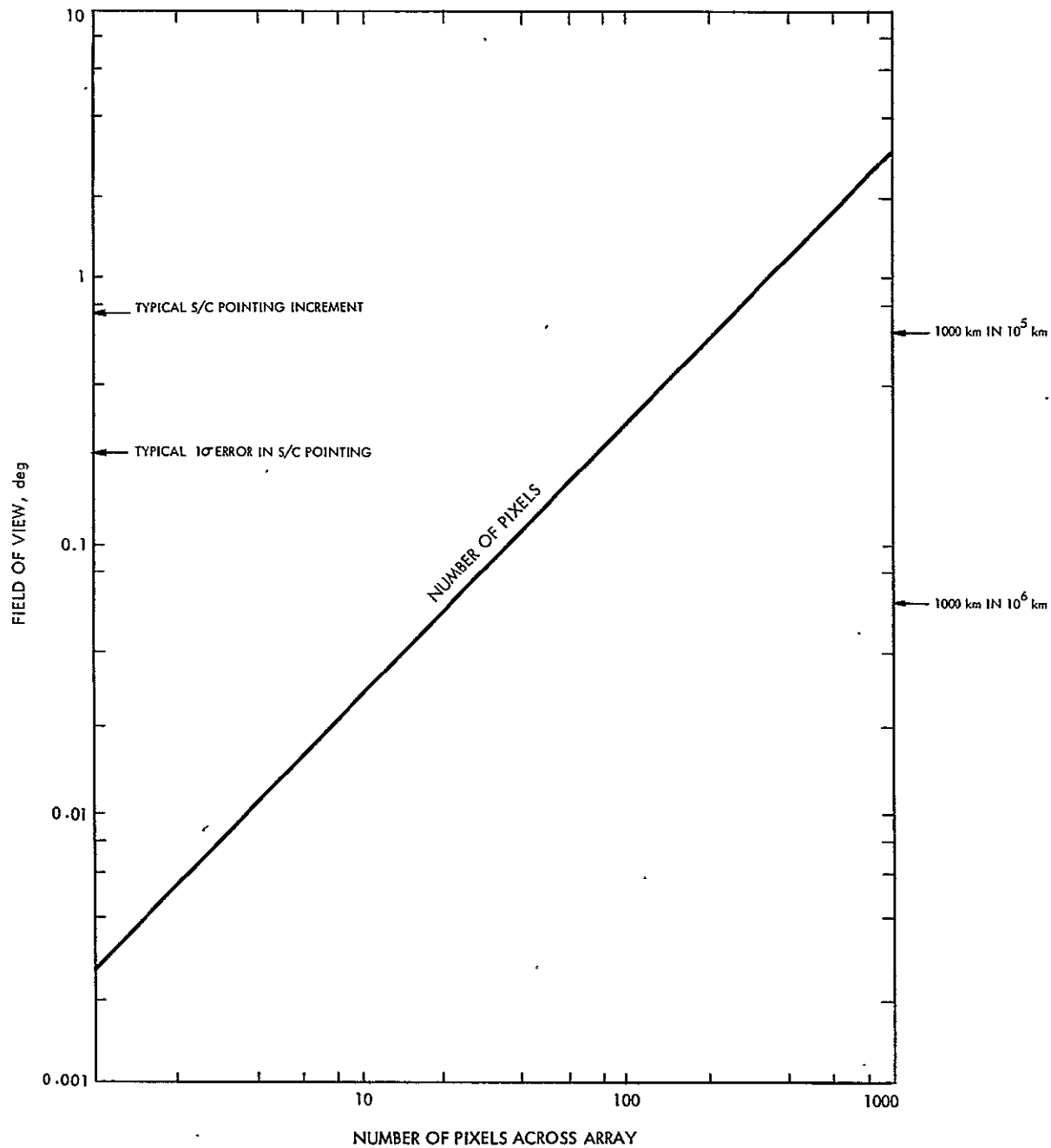
Figure VII-1. Number of pixels required to give 600 m feature resolution
at 5000 km distance, vs. total field of view. Pixel size
50 μ radian, equivalent to 250 m/pixel at 5000 km. Arrows
at right indicate angle corresponding to 1000 km uncertainty
in locating comet from spacecraft.

a field of view large enough to guarantee viewing of the Encke nucleus would include several hundred elements. Figure VII-2 illustrates that linear arrays of moderate size require readout at rates approaching 10^7 bps, using a minimal 6-bit data encoding at a spacecraft rotation of 10 rpm. This is an excessive readout rate even for input to a digital tape recorder. Consequently, a two-dimensional, 200 x 200 element array is preferred which will avoid excessive data rates and provide a field of view consistent with the camera pointing accuracy. Such arrays are within the current state of the art in CCD (charge-coupled device) technology; e.g., Fairchild Space and Defense Systems is developing a 400 x 400 array under a CCD imaging program for the U.S. Navy (Ref. VII-6).

Telescope

The requirement of 600-m feature-resolution elements at 5000 km range requires picture elements of less than 50 μr angular field of view. In addition, the sensor physical dimension (≤ 25 μm center-to-center spacing) implies a telescope focal length of ≥ 50 cm. To minimize image smear, the focal ratio must be kept as small as possible to maximize sensitivity and yet remain within the science-payload weight constraints. Figure VII-3 displays the expected signal-to-noise ratio using the Mariner 9 "B" telescope (f/2.35; 12 kg total instrument weight) and an f/1.5 50 cm focal length telescope (19 kg total weight) described in an earlier JPL study (Ref. VII-1). The latter telescope is considered the fastest and lightest practical flight instrument for the stated focal length which maintains an adequate optical modulation transfer function.
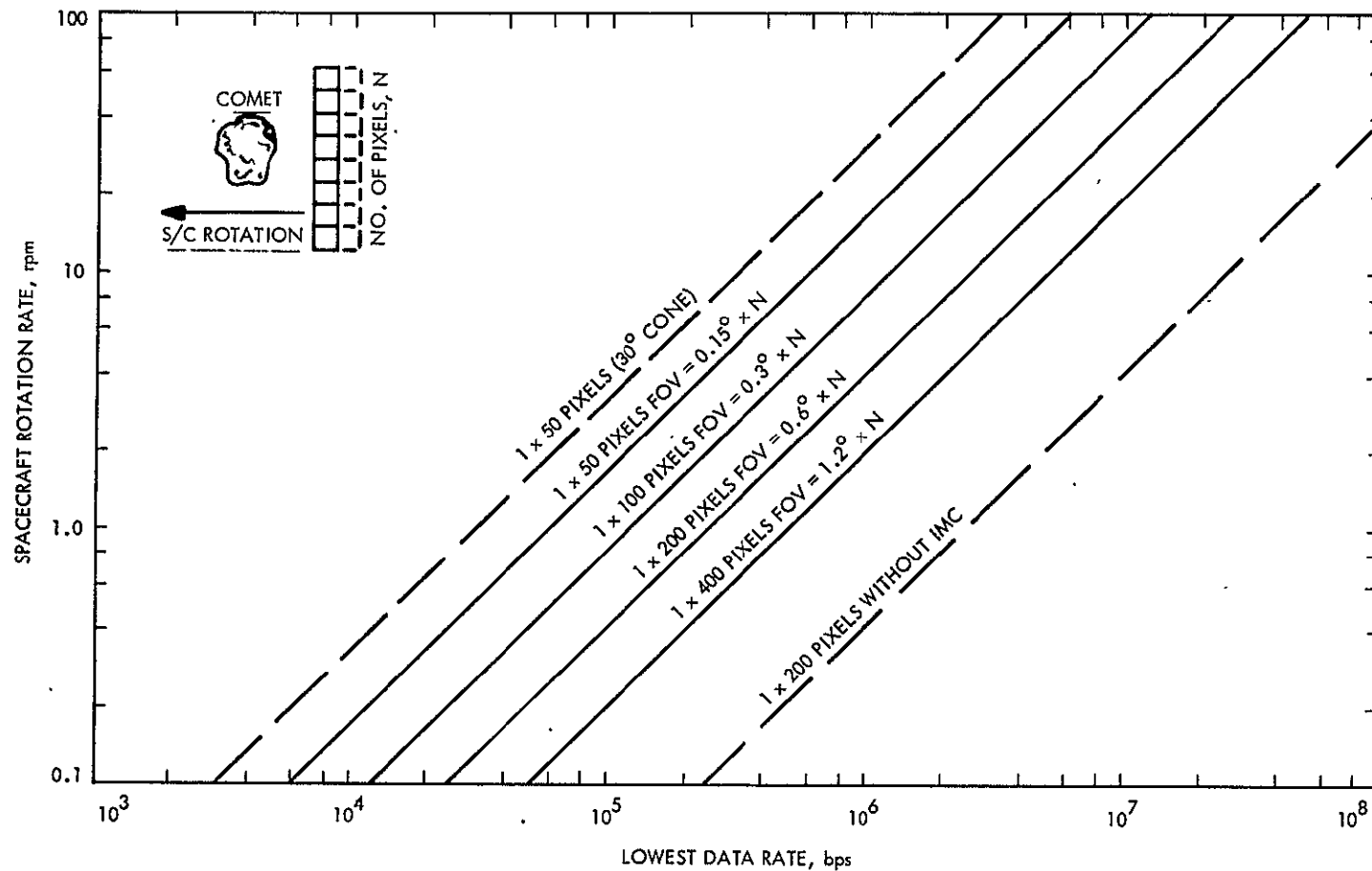
Figure VII-2. Readout data rate for various linear charge-coupled device arrays. Horizontal resolution equal to vertical. Viewing at 90° cone angle from spin axis, except as noted. Instantaneous field of view 50 μ-radian; 6 bit/pixel. Abbreviations: FOV = field of view; IMC - image motion compensation (10:1 ratio assumed present except as noted).
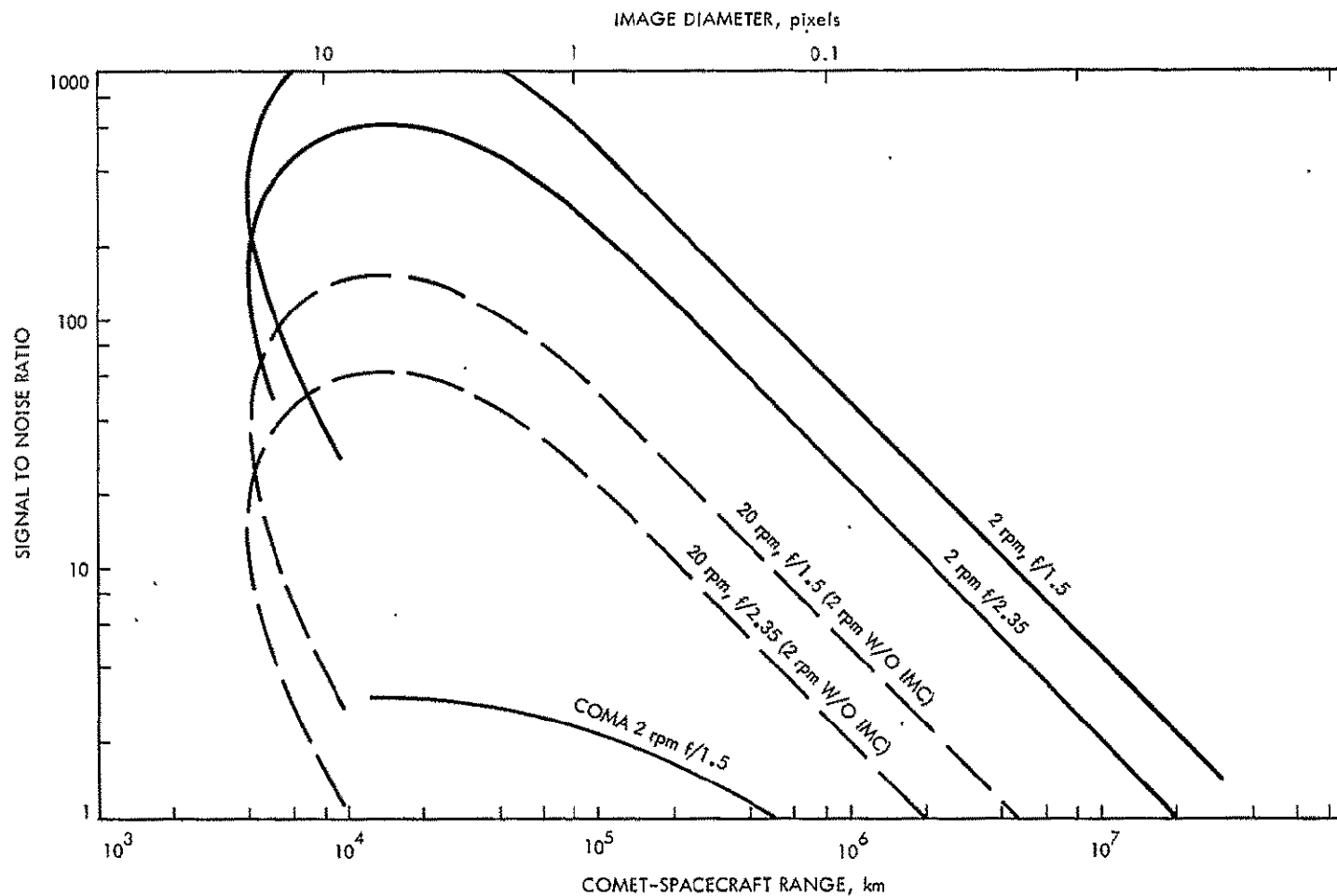
Figure VII-3. Camera signal-to-noise ratio vs. distance. Viewing 4-km Encke nucleus. Flyby distance 4000 km. Camera pointing 1° from spin axis. Image Motion Compensation (IMC) included except as noted. Effective shutter speed 0.5 ms at 20 rpm; 5 ms at 2 rpm. Coma viewed at 10 pixels from nucleus. Broad spectral bandpass.

3. Image Motion Compensation

Image Motion Compensation (IMC) may be used to offset some of the effects of spacecraft rotational motion. The apparent comet motion will vary as a function of pointing angle from the rotational axis (cone angle). Although this image motion traces an arc when close to the axial direction, the small field of view and short exposures anticipated should minimize the effect of a circular path and permit a linear motion compensation. A more important consideration is the capability of adjusting the IMC direction for various spacecraft-comet rotational orientations and cone angles. The requirement for good image quality together with weight and rotational moment characteristics appears to rule out IMC external to the camera, such as an external rotating mirror. Electronic IMC, possible with magnetically and electrostatically focused intensifiers, requires additional weight, bulk, and complexity. However, recent studies for the DOD have indicated that electronic transfer methods (sequential CCD image transfer) could increase the effective exposure by a factor of 200. While this option may be available during future sensor development, a simple mechanical IMC device will be adopted for this evaluation. Such a device was the product of a Viking-Mariner-Venus-Mercury commonality study (Ref. VII-7). It consists of a "nodding" plane-parallel prism (Appendix C) that could, for a small weight addition (1 kg) yield a factor of ten increase in effective exposure.

c. Imaging photometer

The Imaging Photopolarimeter Instrument (IPP) currently being flown aboard the Pioneer 10 spacecraft is an attractive candidate to supplement the framing camera for the Pioneer Encke mission. Imaging designed to

reveal properties of the nucleus from a spinning satellite is not capable of recording the diffuse coma (Fig. VII-3). Successful imagery using longer integration times could effectively be obtained by increasing the sensor field of view at the cost of spatial resolution.

Designed by the Santa Barbara Research Center, the IPP is a moderately-sized, low-weight instrument with three operational modes tailored to a spacecraft rotating at a 5 rpm rate. Table VII-3 lists the salient hardware specifications. Figures VII-4 and VII-5 display respectively the assembled instrument appearance and an exploded view of the optical parts.

Because of the coma's low brightness, only the zodiacal light and photopolarimetry modes are of science interest for the Encke mission. Figure VII-6 displays the standard operation with respect to a spacecraft-comet observation at 10^6 km from encounter (E-15 hours). The small coma suggests that little spatial information could be obtained prior to E-9 hours (6×10^5 km).

TABLE VII-3

SUMMARY OF IMAGING PHOTOPOLARIMETER SPECIFICATIONS
(As currently flown, with 5 rpm spacecraft spin rate)

Modes of Operation	1. Standby 2. Zodiacal light 3. Photopolarimetry 4. Imaging
Telescope	Maksutov-type, 2.5-cm aperture, 8.6-cm focal length
Instantaneous Field of View	40 mr (2.3°) square, Mode 2 (Zodiacal Light Mode) 8 mr (0.5°) square, Mode 3 (Photopolarimetry Mode) 0.5 mr (0.03°) square, Mode 4 (Imaging Mode)
Spectral Band	Blue, 390 to 500 nm Red, 595 to 720 nm
Polarization Analyzer	Mode 2, symmetrical Wollaston prism Mode 3, symmetrical Wollaston prism and achromatic half-wave retardation plate
Calibration	Mode 2, radioisotope - activated phosphor light source Mode 3, solar diffuser, tungsten filament lamp and Lyot depolarizer
Detectors	Two dual-channel Channeltrons (Bendix)
Look Angle Step	Mode 2, 40 mr every 20 rolls Mode 3, 8 mr, usually every 4 rolls Mode 4, 0.5 mr every roll Step direction or "no-step" commandable
Sampling Rate (Spin)	Mode 2, complete roll at 512 bps or higher telemetry rate Mode 3, 70° of roll at 1024 bps or higher telemetry rate Mode 4, 14° (29° at low sampling rate) at 1024 bps or higher telemetry rate Start of sampling in Modes 3 and 4; one of 64 commandable spokes or automatic from increase in light (threshold)

TABLE VII-3 (continued)

SUMMARY OF IMAGING PHOTOPOLARIMETER SPECIFICATIONS

Analog/Digital Conversion	Mode 2, 4 channels 10 bits each, after each integration period of 1/64th of roll
	Mode 3, 4 channels 10 bits each, after each 16-msec integration
	Mode 4, 2 channels 6 bits each, alternate channels every 0.5 msec (1 msec at low sampling rate)
	Five temperatures 10 bits each
Telemetry	Mode 2, 50 bits status, 50 bits temperatures, 2560 (max) bits detector data every other roll
	Mode 3, 50 bits status, 50 bits temperatures, 6044 (max) bits detector data every roll
	Mode 4, 50 bits status, 6094 (max) bits detector data every roll
	Data buffered by spacecraft DVU and sent in telemetry format D1 or D2
	One analog word (standby status) in science subcom
Commands	3 mode initiate, 4 telescope step control, 4 data sampling control, 2 gain control
Size	18 x 19 x 47 cm
Mass	4.2 kg
Power	2.8 watts

ELECTRONIC DATA
PROCESSING ASSEMBLY

SCANNING ELECTRO-OPTICAL
TELESCOPE ASSEMBLY

MOUNTING PLATFORM

Figure VII-4. Pioneer F/G Imaging Photopolarimeter. (After Santa Barbara Research Center, Ref. VII-12).

CHANNELTRON
DUAL CHANNEL

WOLLASTON PRISM

f/3.4 FOCAL PLANE OPTICS:
FIELD-OF-VIEW APERTURES
DEPOLARIZERS, RETARDER,
COMPENSATOR, CALIBRATION
SOURCE

ENTRANCE PUPIL

TELESCOPE OPTICS

FOLDING MIRROR

FIELD LENS

RELAY LENS

SPECTRAL FILTERING
COATING, RED TRANSMITTING

FOLDING MIRROR

DICHROMATIC MIRROR

RELAY LENS

SPECTRAL FILTERING
COATING, BLUE
TRANSMITTING

CALIBRATION LAMP

FOLDING MIRROR
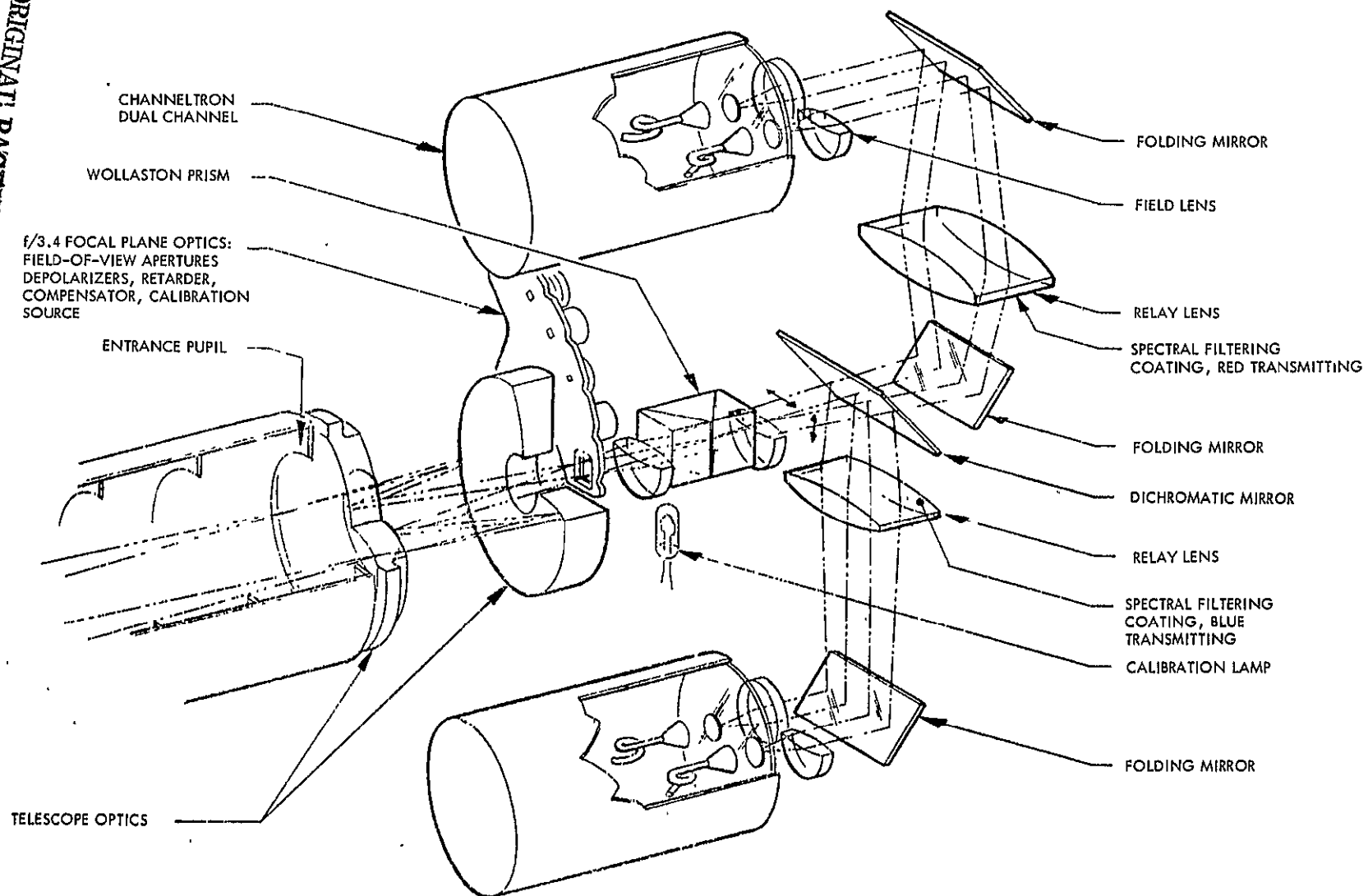
Figure VII-5. Exploded view of the Pioneer 10 Imaging Photopolarimeter. After Santa Barbara Research Center, Ref. VII-12.

ZODIACAL LIGHT MODE

PHOTO POLARIMETRY MODE

2.3°

5.5°

0.5°

0.5°

COMA
10^6 Km
E-15 h

COMA
E-15h

STEP 1.8°

STEP 0.5°

4 MEASUREMENTS (DETECTORS) PER
DIRECTION (2 ORTHOGONAL POLARIZATIONS
AT 2 WAVELENGTHS)

6-bit/DETECTOR 2640 BITS/ROLL

8 ROLLS + 2 CALIBRATION (PHOSPHOR)
PER CONE DIRECTION

5 rpm

4 ROLLS PER CONE ANGLE

1. CALIBRATION LAMP
2. HALF-WAVE PLATE
3. DEPOLARIZER
4. CLEAR

AUTOMATIC SEARCH MODE: STEP 0.5° UNTIL
0.5% SIGNAL, BEGIN 4 ROLLS/CONE
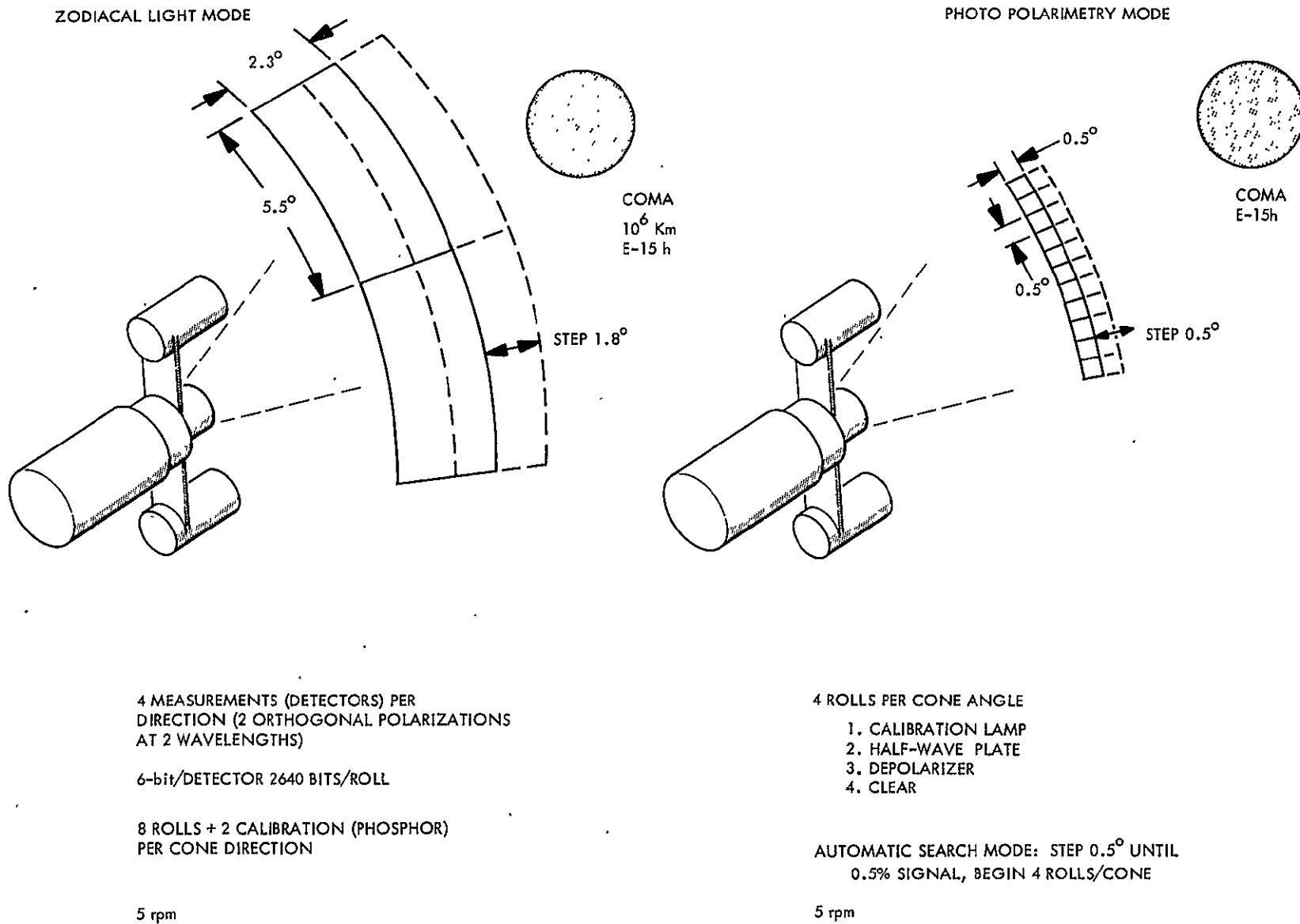
5 rpm

Figure VII-6. Typical operational modes of the Imaging Photopolarimeter. Existing instrument and spacecraft, 5 rpm.

Figure VII-7 verifies this conclusion, showing the expected signal-to-noise ratio as a function of pointing angle from the nucleus for both modes of operation. Spectral photometry of the integrated coma, including polarization measurement, is feasible from much greater distances. The polarization capability, however, requires a sufficiently large variation in phase angle of observation. IPP coma photometry would hence require instrument operation through encounter and occur at the same time as optimal television. Because Comet Encke is not considered to be a "dusty" comet, and because of the difficulties of targeting observations on the various near-encounter trajectories, it is suggested that the polarization experiment be replaced by simultaneous measurement at four narrow bandpass wavelengths. Deletion of several optical elements may then permit registration of selected coma emission lines at 3000 Å.

2. Camera integration

Early detection of the Encke nucleus is essential to refine the relative trajectories of the spacecraft and comet and to subsequently reduce the range at encounter (see Section IX E, below). At distances corresponding to several days prior to closest approach, the large angular velocity of a spacecraft spinning at only moderate rates prevents quick identification of the target. The framing camera revolving at 10 rpm and looking at a 90° cone angle would first detect the Encke nucleus (S/N=10) at a range of only 4×10^{5} km, 6 hours before encounter. Reducing spacecraft rotation to ≤ 2 rpm would permit imagery of the nucleus one day earlier. As the spacecraft continues its approach, the image of a 4 km nucleus becomes greater than 1 pixel in size 1.2 hours prior to closest approach.

Figure VII-7. Signal to noise ratio of Imaging Photopolarimeter. 5 rpm, solar distance 0.53 AU, comet distance 6 x 10⁵ km. Coma diameter 6 x 10⁴ km (6°). Nucleus assumed to be at center of coma.
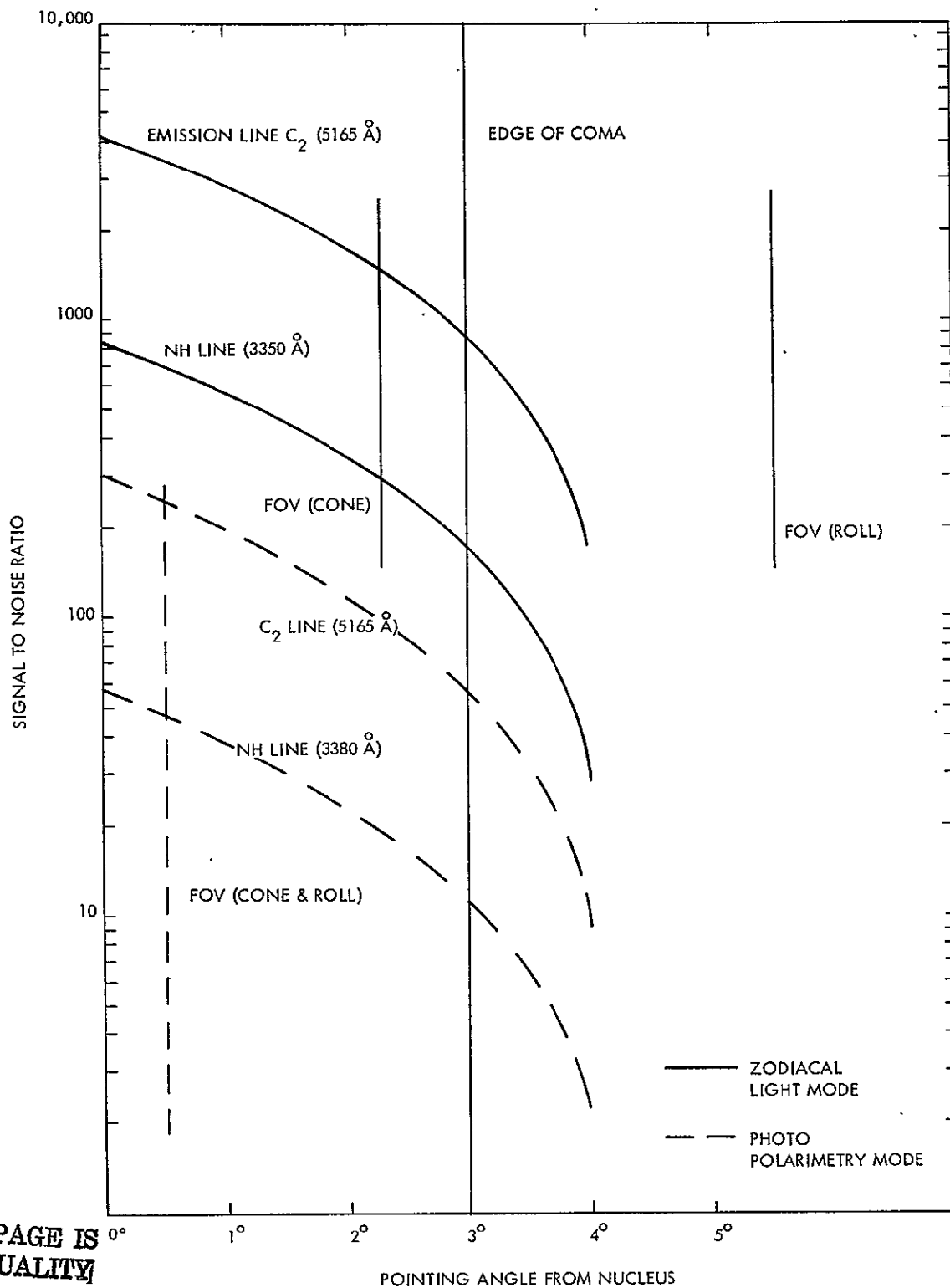
ORIGINAL PAGE IS OF POOR QUALITY

Information on phase function and shape is obtainable beginning five minutes prior to minimum range on the nearly anti-solar trajectory. The comet nucleus (if 4 km diameter) achieves a maximum size of 16 pixels at 5000 km distance (see Figure VII-8). The nucleu image drops below the detection limit five minutes after closest approach (phase angle $> 150^o$).

By pointing the pole of the spacecraft at Encke, however, a significant improvement in image motion may result. Because the field of view of the framing instrument is quite small ($< 1^o$) serious rotational smear will not occur until the comet is within 2' of arc of the polar direction: i.e., assuming 10 pixel image motion compensation along a linear path, a deviation of one pixel requires placing the comet within 2' of the rotational axis direction. Figure VII-9 illustrates the signal-to-noise ratio of the Encke nucleus during an exposure of the equivalent of 10 pixels image motion as a function of the angle from the axis of rotation, at 2 rpm. Much greater ratios are achievable at angles within 1° of the pole than at large angles. For example, at 10^6 -km range, the Encke image is 55 times brighter at 1° than at 60° from the rotational axis. Treating the Encke nucleus and halo ($< 10^3$ km) together, the increase in detection distance (S/N = 10) is more than 7 times, or an improvement to E-4.5 days at 2 rpm. Reducing the angl to $\frac{1}{2}^o$ would increase the detection distance to more than 10^7 km or E-6 days, at 2 rpm. Accordingly, to observe the target (500 km accuracy) at long range, the camera pointing angle should be kept between 2' and 1°.

0	0	0	0	0	0.	0	0	0	0
0	0	0	0	0	190	240	30	0	0
0	0	0	90	295	450	370	370	40	0
0	0	240	575	415	574	490	415	320	30
0	5	350	575	490	450	575	415	240	0
0	0	320	415	490	575	450	415	100	0
0	0	0	240	350	270	295	20	0	0
0	0	0	0	150	60	0	0	0	0

500 **500** **400 300 200** **100** **60**

SUN →
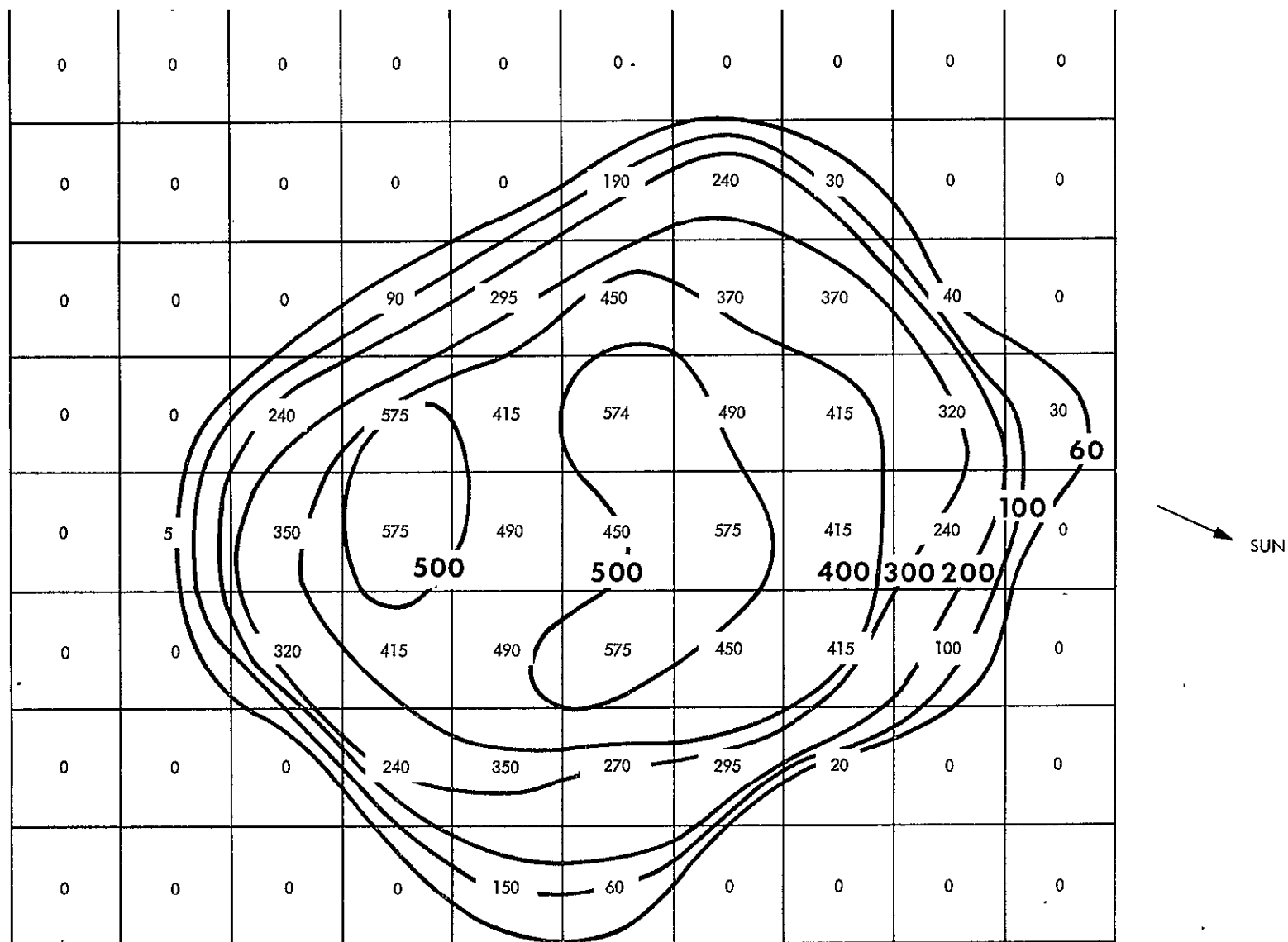
Figure VII-8. Luminous contours from a Mariner 7 image of Phobos, corresponding to an image of a 3-km Encke nucleus at 5000 km, with the recommended camera. Phase angle 20°. Units: foot-lamberts.
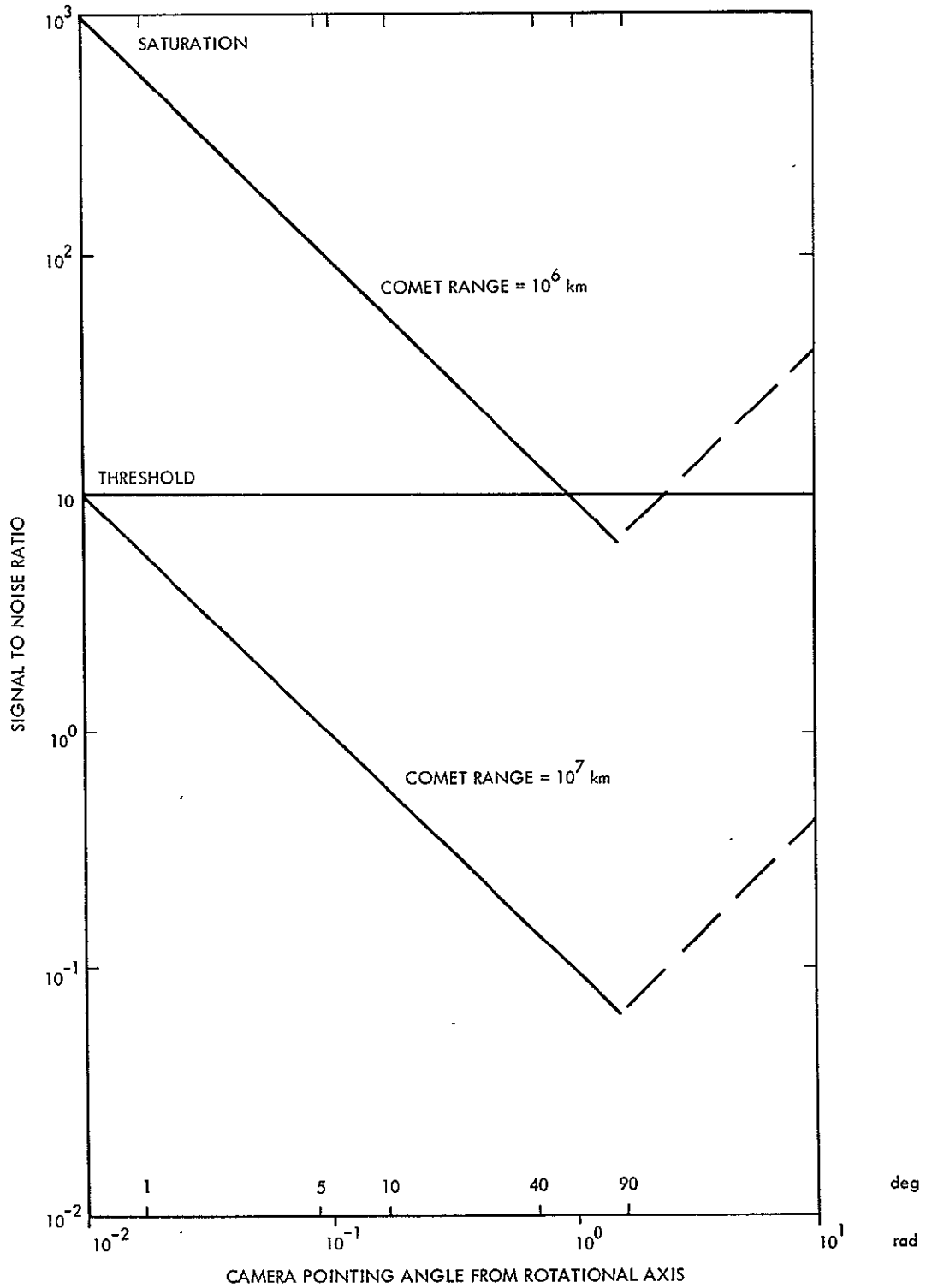
Figure VII-9. Nucleus signal/noise vs. observation angle from axis of rotation 2 rpm, 10 pixel IMC, f/1.5 telescope, CCD camera.

Another improvement of the imaging data return is the resolution obtainable from a collision-course trajectory ($\leq$ 100 km flyby), perhaps feasible with early ephemeris updates. Assuming a 13-kbs data rate, without a tape recorder, the framing camera (200 x 200 CCD array) would require only 18 seconds to transmit a single picture (6-bit encoding). Consequently, 15 additional pictures (at $\geq$ 3 rpm) could be taken at distances closer than 5000 km. However, considering a 100 km minimum distance flyby, the angular comet motion exceeds 1°/second while the comet range is still 1000 km. It may be difficult to achieve this slew rate while maintaining a 0.3° pointing accuracy. Hence, the last 3 pictures of the 15 may be lost. At 2 rpm, the minimum picture-taking interval would be 30 seconds. This would permit 9 pictures inside of the 5000 km distance of which two would be from closer than 1000 km. In either case, the resulting data return would include a maximum feature resolution of 130 m (50 m/pixel) and the elimination of post-encounter photography (the cone angle would be greater than 160° at 1000 km range post-encounter).

Several disadvantages of this sequence should also be considered. In addition to the difficulty of trajectory refinement capable of providing a 100 km encounter, the timing problems of sequence execution during the last few minutes near encounter, and the difficulty of placing the image consistently within the camera's field of view, obtaining certain types of data may require specific approach trajectories. Surface detail on the nucleus will be difficult to detect if the phase angle is small (or very high) when the spacecraft is 5000-1000 km from the nucleus. Phase function information, including polarization studies to determine particle

sizes, requires observations at a wide range of phase angles. This is difficult with a close encounter on a fast flyby, regardless of approach direction, because the angular velocity is so high at viewing angles of more than 20° from the approach and departure asymptotes. Hence, little phase information might be realized regardless of relative flight path.

It may be concluded that approaching the comet along the rotational axis of the spacecraft can offer significant benefits to the early ephemeris refinement necessary for successful encounter reconnaissance. Targeting towards the nucleus may not offer a greatly improved science imaging return within 5000 km. It is advantageous, however, in that the comet's angular motion at 5000 km and greater distances is reduced. For example, a 5000-km minimum encounter produces a 0.2°/sec angular rate. Targeting for a 500-km encounter produces a 0.02°/sec rate at a 5000-km distance.

3. Despun Platform Advantages

Despite the additional weight and complexity imposed by the option of a despun platform for the Pioneer spacecraft, such a configuration could significantly improve the science data return. Several different imaging instruments would offer better trajectory refinement and encounter sequence information. For example, the Mariner 9 camera/telescope used in a despun mode of operation would have the following advantages over a spinning camera:

1. Earlier detection of the nucleus or coma maximum intensity (E-13 days vs. E-5 days).

2. Better relative positional accuracy (15 μr vs. 170 μr with ATS V-slit optical navigation sensor, described in Section IX E below).

3. Coma spatial and spectral resolution with a single instrument: at a range of 10^6 km, the Mariner 9 camera angular resolution of 1' represents 1/216 of the coma vs. the IPP angular resolution of $0.5°$, which represents 1/7 of the coma.

4. Better nuclear resolution and less image smear without IMC and with smaller projected pixel sizes (30 ur vs. 50 ur).

5. More picture elements per image.

6. Better pointing control of camera. Can use Far Encounter Planet Sensor concept (see Section IX F below).

7. More pictures: ≤ 8-second integration time vs. 15 seconds between frames at 4 rpm or 30 s at 2 rpm.

4. 100-Meter Resolution

To obtain a feature resolution of 100 meters on the comet nucleus from the "safe" distance of 5000 km will require a telescope of greater focal length than the proposed 50 cm. The pixel size would have to be ≤ 40 m or 8 μradians. This would necessitate a telescope with a focal length greater than 3 m, which is not considered practical for a spacecraft of reasonable size.

A pixel size of 100 m (20 μradians at 5000 km; 250-m feature resolution) would require a 1.5-m focal length telescope. With a 200 x 200 element array, the field of view would be less than $0.25°$, which seems impractically small. It would apparently be necessary to go to a vidicon type sensor to provide the field of view. Sensitivity and smear problems would be much more severe; if the sensitivity of the optical system is to be maintained, the telescope

objective diameter would also have to be tripled, to 1 m, which seems quite impractical for this mission. Alternatively, the camera would have to be despun, allowing longer camera integration times but adding considerable complication and weight (about 25 kg for the despinning mechanism (Ref. VII-9) plus a 6-kg increment for the longer telescope and larger camera).

Another approach is to plan on taking pictures at distances closer than 5000 km, accepting the risk of dust impacts that could prevent obtaining or transmitting the pictures. The spinning CCD camera described above, with its 50-μradian pixel size, would give 100-m pixels at 2000 km distance and 40-m pixels (100-m feature resolution) at 800 km distance. At 800 km, an error of 4 km in relative position may place the nucleus outside the 0.6° field of view of the camera. Thus, continuous optical tracking of the nucleus during encounter would be necessary to keep the camera pointed at the nucleus and to trigger a frame at the proper instant. All portions of this tracking and pointing system (including recognition and logic) would have to be on board the spacecraft; the nine-minute round trip communications time to Earth (about 0.5 A.U. away) prohibits use of Earth-based equipment.

B. ULTRAVIOLET SPECTROMETER

The objectives of spacecraft ultraviolet spectrometry at Encke include identification of parent molecules and photochemical processes. Spatial resolution of UV emission features should be considerably better than is achievable from Earth orbit. Important weak lines may be detectable. The UVS should provide valuable support for on-board cometary gas analysis by distinguishing between ions or molecules difficult to separate by mass spectrometry, such as CO^{+} and N_2^{+}.

In principle, the UVS could also be used to observe the reflection spectrum of the nucleus, which could show the presence of ices, and for absorption spectroscopy of the cometary gas, looking back toward the sun. It is not clear whether observations of the nucleus are practical. Absorption measurements on the gas would require flipping the UVS to point toward the sun, or carrying two UV spectrometers. Again, it is not clear that this would be worthwhile.

For a spinning spacecraft, the ultraviolet instrument may require new development, depending upon the choice of trajectory and spin axis orientation. Present instruments might be used if they were mounted so as to be pointed directly along the spin axis, but the continuous rotation of the grating with respect to the comet would result in a cyclic change in the image of the slit reflected from the grating onto the PM tube, and would cause problems in calibration. For the purposes of the present exercise, a spin rate of 2 rpm is assumed, and it is assumed that the spacecraft approaches the comet directly along the sun-comet line.

The instrument evaluated is the Advanced Applications Flight Experiment (AAFE) 1/8 meter UVS. This instrument covers the band 1130-3650 $\overset{o}{A}$, over a field of view of 0.15° by 0.5°. Smaller fields of view may be available if required. The present minimum detectable source brightness is 40 R at a spectral resolution of 10 $\overset{o}{A}$. (One Rayleigh, R, is equal to 10^6 photons/cm^2-sec). The upper limit for source brightness is 10^6 R and gain change is available to prevent saturation for bright sources. (See Table VII-4). It is probably not necessary to search for emission lines below 1130 $\overset{o}{A}$ since only the rare gas lines are observed in weak plasmas below these wavelengths. The rare gases are not expected to be present in comets in detectable quantities, and the plasma temperature and excitation energy are probably insufficient to produce highly ionized lines in the extreme UV.

The AAFE instrument is a smaller version of that carried on Mariner 9, and is expected to fly on an Atmospheric Explorer. The advantage of this particular instrument is its flexibility. An electronic programmable drive provides for either slow or fast wavelength scan rates. The fastest scan rate presently available is 3 sec over the entire wavelength band covered by the spectrometer, and this may possibly be shortened to $1\frac{1}{2}$ sec. The programmable scan rate allows for the option of slow scans at long distances for increased sensitivity and fast scans nearer approach for spatial resolution. Also, the wavelength drive can be programmed in flight to stop at particular lines or to scan over narrower band widths. Thus, interesting lines or band systems found at longer distances can be examined at higher spatial resolution nearer to encounter because of decreased scan times.

For a fast flyby mission, it is necessary to orient the spectrometer toward the comet in order to greatly reduce the time required for obtaining a full wavelength scan. This arrangement requires that the spin axis be located along the spacecraft-comet line. The slow rotation rate of 2/min permits flexible operation of the instrument. Ten individual spectra may be taken over each revolution in order to obtain calibration data, and the instrument may be offset slightly from the spin axis in order to sweep over the various regions of the comet in order to obtain spatial distributions. The precise choice of offset angle, view angle, and scan rate will depend critically on the exact details of the trajectory. Large offset angles and high rotation rates are not compatible with the requirement for obtaining good spatial resolution. For a 1° offset angle, a view angle of 0.15° by 0.5° and a 500-km miss distance, the UVS footprints are shown for -1 day, -1 hr, and -30 min before encounter in Figure VII-10.

TABLE VII-4

ULTRAVIOLET SPECTOMETER PARAMETERS:

AAFE 1/8 meter Scanning Spectrometer

Mass	3.0 kg
Size	54 x 21 x 11 cm
Power	3 W
Data rate	500 bit/sec (nominal)
Wavelength range	1130-3650 Å @ 10 Å resolution
Scan time	3 sec nominal
Sensitivity	40 R - 10^6 R
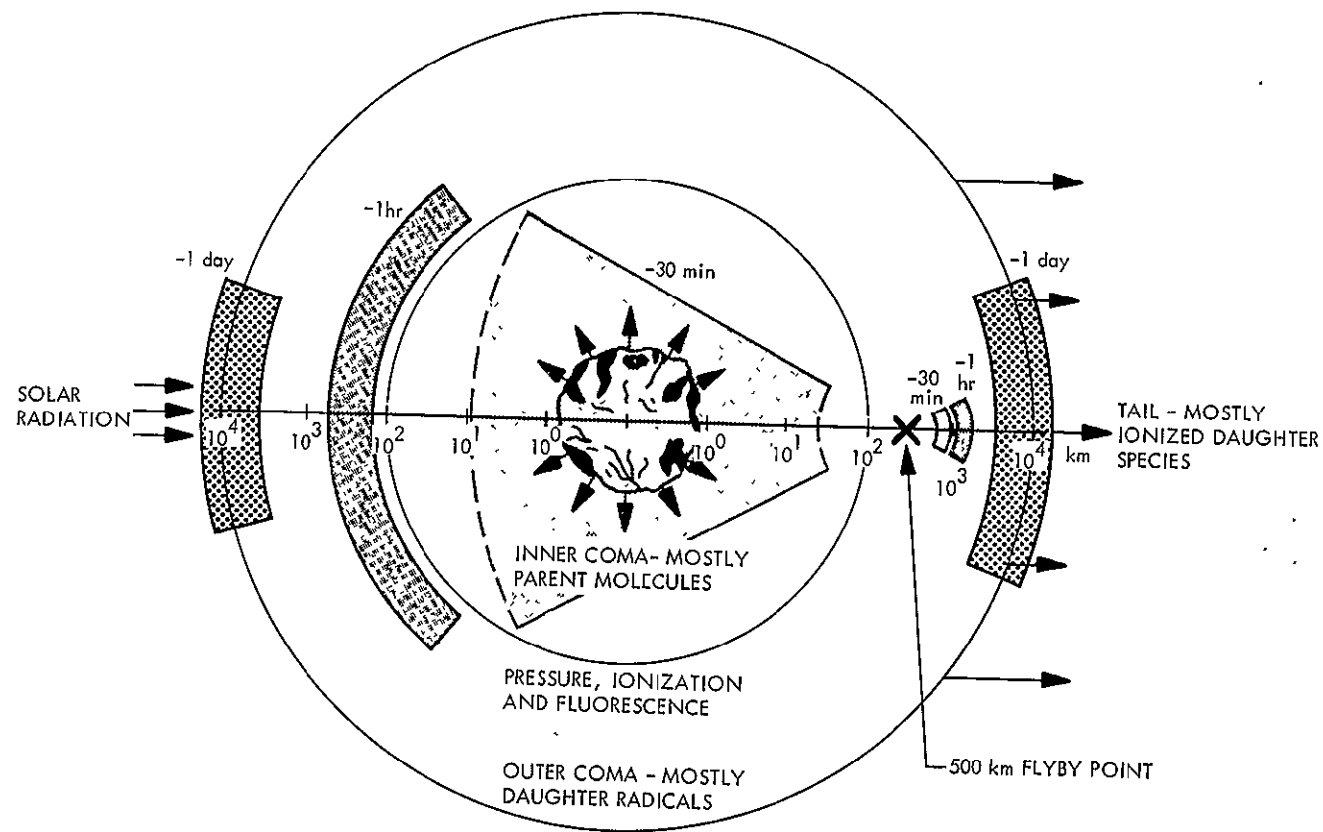
Figure VII-10. Ultraviolet spectrometer footprints, for 500-km miss distance. Instrument pointed 1° from spin axis. Note log scale.

C. MASS SPECTROMETER

A great deal can be learned about the nature of comets through in situ sampling of their composition as near as possible to the nucleus. A search for remnant parent molecules and an accurate, quantitative measurement of the radicals which are their first dissociation products is a most important remote study, related directly to the origin, structure, and evolution of the nucleus. Also of great importance in achieving a quantitative understanding of the physical processes occurring outside the immediate vicinity of the nucleus is the ability to measure the number densities of ions. The most highly developed, sensitive, accurate, flight proven technique for making both types of measurements is mass spectrometry. No true cometary payload could be justified without a mass spectrometer, given the present state of knowledge.

1. Instrument Description

Two major classes of mass spectrometer (MS) have flown in space, the electric quadrupole type and the double focusing magnetic sector type. Either could probably be developed to do the comet work, but the latter seems much the more satisfactory for this job in its present state of development and flight experience. Figure VII-11 depicts a block diagram of the experiment. It represents a double focusing magnetic sector, dual collector, mass spectrometer embodying ion counting as its mode of detection. The ion-source (and ion focusing) portion of the instrument is exposed to the ambient environment after launch via a pyro command which ejects a hermetically sealed protective cover. In the vicinity of the comet, ambient ions and neutrals enter the ion source where, in one mode of operation, the ambient ions are focused and mass-analyzed, and, in another mode of operation a portion of the ambient neutrals are ionized and then mass-analyzed. In this manner mass spectra of both ion and neutral species are obtained separately.
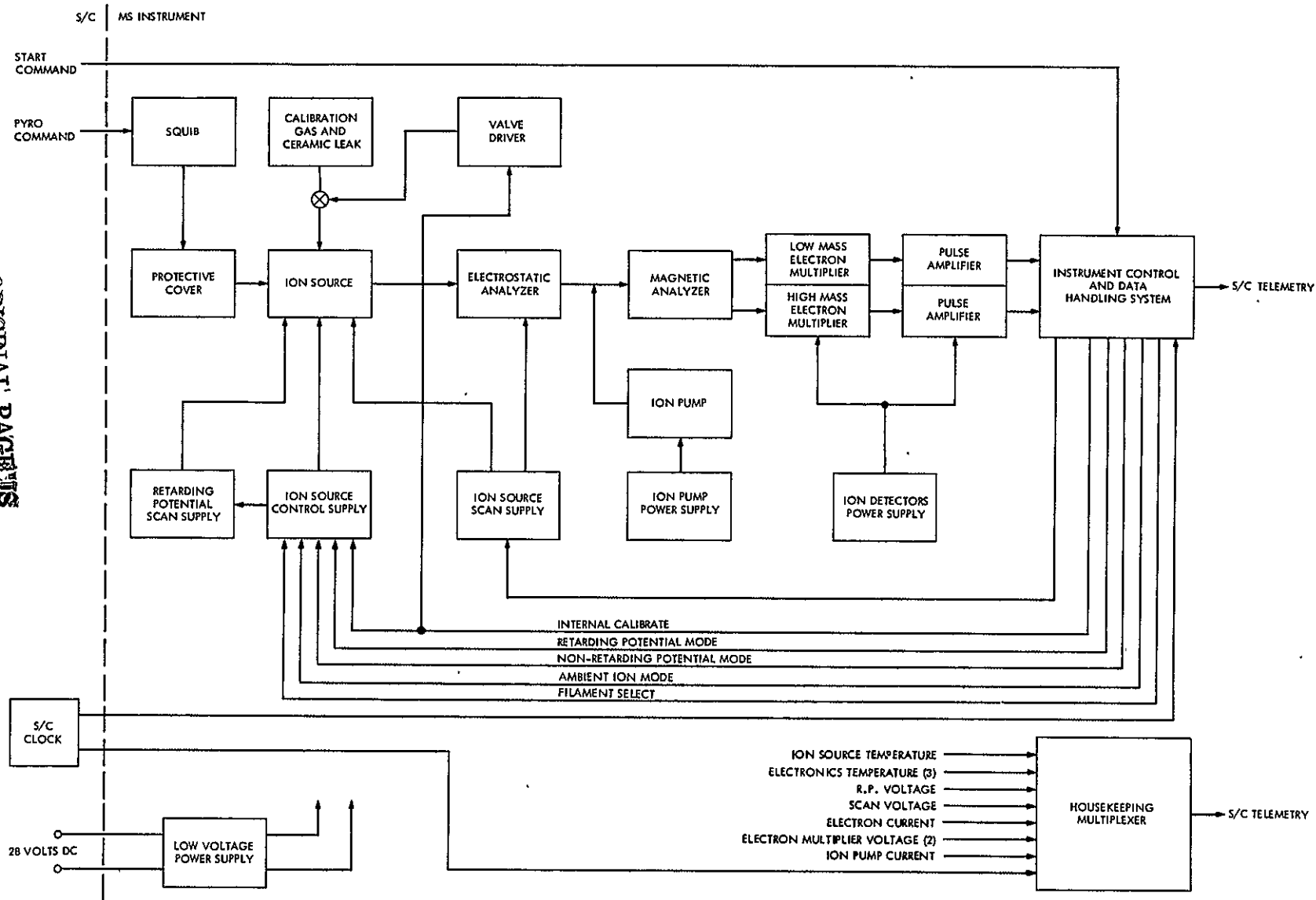
Figure VII-11.   Mass spectrometer block diagram.

High mass resolution and sensitivity are achieved through the use of tandem electric and magnetic fields whereby both energy and direction focusing occur to the first order. Ions exiting the ion source are initially dispersed according to energy by the electrostatic analyzer, and then refocused according to their mass-to-charge ratio by the magnetic analyzer (See Figure VII-12). By cyclical variation of the ion source potential, mass spectra in two different mass ranges are displayed at the outputs of the two electron multipliers simultaneously. Relative abundance of different mass species are determined by measuring the arrival rates of given ions at the electron multiplier detectors, and ratioing them to one another. This "ion counting" technique not only allows extremely low particle densities to be measured, but in turn allows a very wide range in density to be measured.
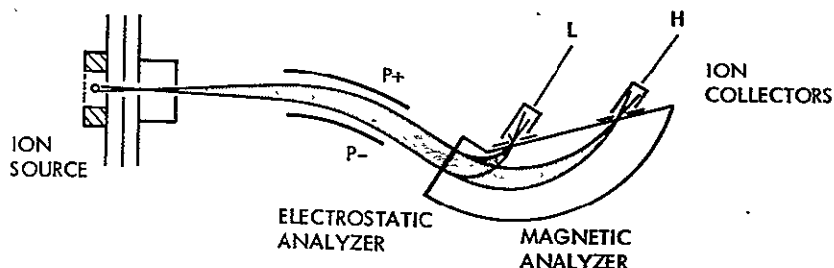
Figure VII-12.   Schematic drawing of Double-Focusing Mass Spectrometer showing ion source and electrostatic and magnetic analyzers. (Courtesy of A.O.C. Nier, University of Minnesota).

Since very low particle densities are likely to be encountered in the vicinity of the comet and since the composition of this cometary atmosphere is of extreme importance, techniques must be implemented to assure the accurate measurement of these gas species above instrumental background. The major background component will be the spacecraft's "atmosphere" (i.e., a cloud of gas traveling along with the spacecraft at the spacecraft velocity) which is due to outgassing of spacecraft components. In the fast flyby mission, the spacecraft will be moving with a relative velocity with respect to the comet of approximately 18.3 kilometers per second. This means that molecules of the cometary atmosphere will have an effective energy with respect to the mass spectrometer of approximately 1.75 electron volts per atomic mass unit (amu). On the other hand, molecules in the spacecraft's atmosphere will have effectively "zero" energy with respect to the mass spectrometer. Through the utilization of a retarding potential field in the mass spectrometer ion optics the "zero" energy molecules (and hence the background gases) can be effectively discriminated against. Figure VII-13 is a schematic diagram of the mass spectrometer ion source depicting this feature of the design.

At the cometary encounter velocity of 18.3 kilometers per second significant molecular decomposition is expected to occur due to molecular impacts with the instrument. Figure VII-14 presents a curve showing the spacecraft velocity at which certain bonds would be broken if all of the translational energy on impact were converted to vibrational bond energy (an obviously conservative estimate). One can see that at velocities as low as 9 km/sec, even the very strong carbon-oxygen bond would be broken. Hence an accurate analysis of the cometary atmosphere can be

EJECTABLE CAP

EXTERNAL GRID, S1

BUS OUTER SKIN

ION SOURCE CHAMBER, S3

REPELLER GRID, S2

ELECTRON BEAM
(AXIAL MAGNETIC FIELD)

RETARDING VOLTAGE GRID, S4

"J" FOCUSSING PLATES, S5

SHIELD (CONNECTED TO
ION SOURCE CHAMBER)

OBJECT SLIT, S6
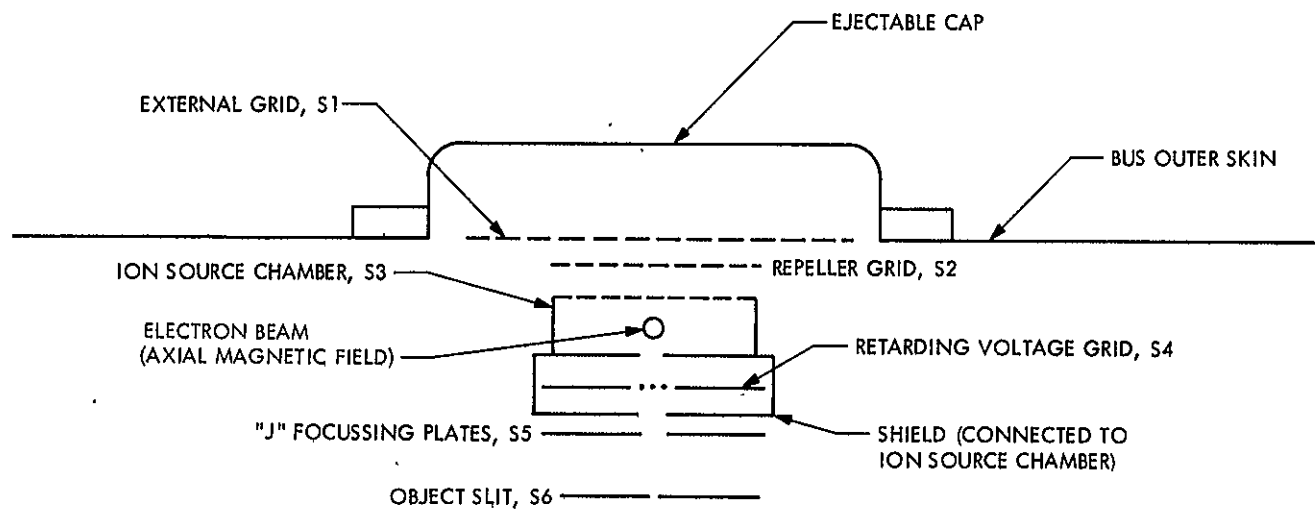
Figure VII-13.   Ion source details (Courtesy of J. H. Hoffman, University of Texas).

NOTATIONS SHOW MINIMUM VELOCITY
AT WHICH PARTICULAR BONDS WILL BREAK
IF ALL THE KINETIC ENERGY IS
TRANSLATED INTO VIBRATIONAL ENERGY

ENERGY, eV/AMU

$CH-H$ $C-O$

$N-N$ $HC-N$

$C-N$

$H-OH$

CH_2-H $C-C$, $NH-H$, $O-H$, $H-NH_2$ $C-H$, CH_3-H

$H-H$ $N-H$ $H-CN$

$O-O$

C_2H_5-H $O-CO$

SPACECRAFT VELOCITY, km/sec
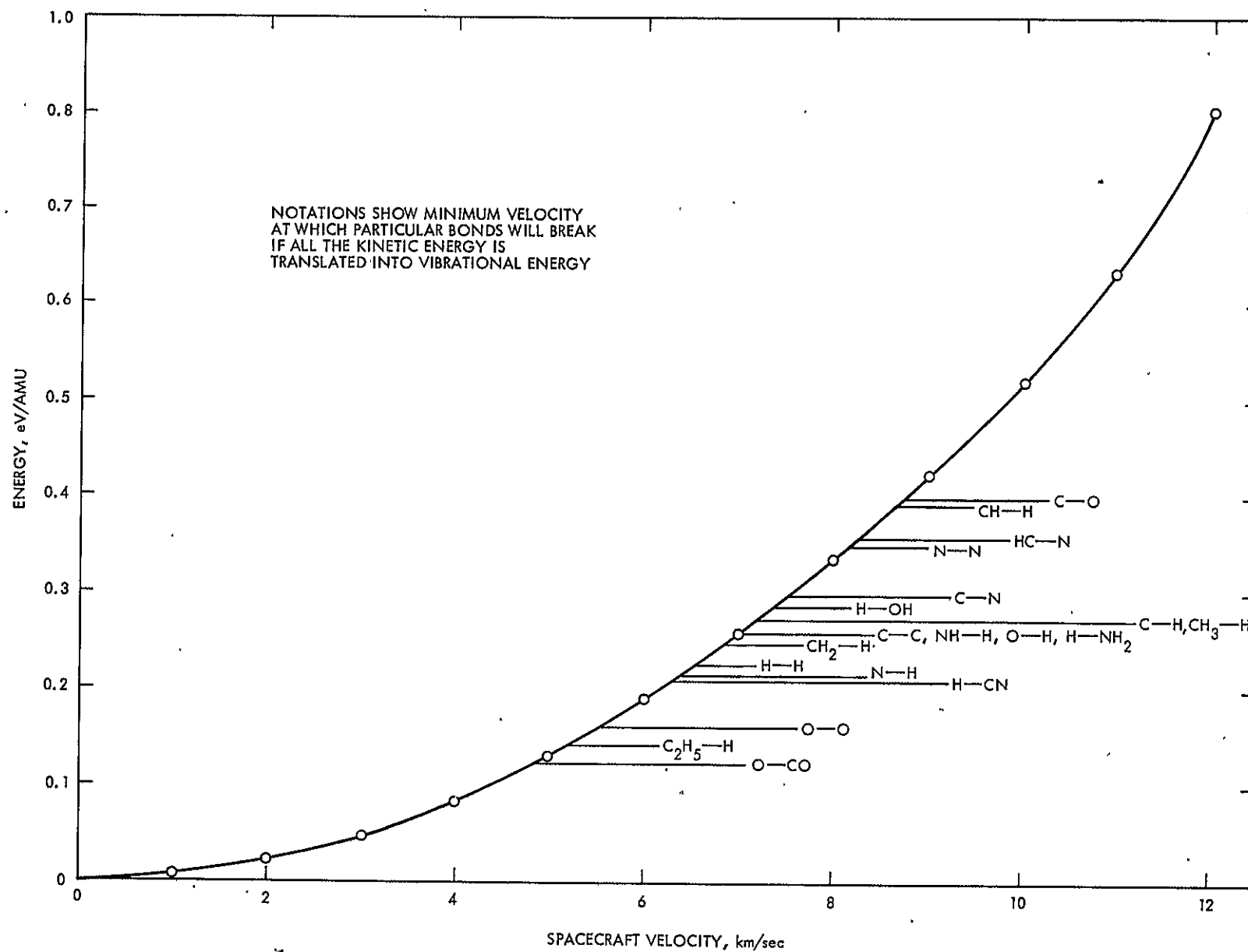
Figure VII-14.   Relative ambient molecule energy as a function of spacecraft velocity.

obtained only through the analysis of those species which have not previously impacted on the surface of the instrument. Since molecules striking the surfaces of the MS will undergo significant energy losses along with the production of fragments, the retarding potential ion optics will discriminate strongly against these molecules and their fragments, allowing a direct measure of the parent molecules in the cometary atmosphere.

Another feature of the instrument design is the capability for in-flight calibration. A reservoir of Ar^{38} & He^3 can be admitted to the instrument to confirm sensitivity and correct for any slight drifts that may have occurred in the electronics. A voltage drift correction must be used since "peak jumping" is employed whereby only integer mass numbers (and some selected non-integer mass numbers) will be analyzed to achieve maximum sensitivity and minimum data requirements.

The suggested mass spectrometer instrument is fully integrated and automatic, requiring only a start command to begin the analysis sequence (after removal of the ion source cover). Data handling is accomplished in the instrument package and presents two digital streams of data to spacecraft telemetry: science data and housekeeping data.

2. Modes of Analysis

The mass spectrometer is capable of three modes of analysis. These are:

a. Non-Retarding Potential Mode

This mode of analysis is useful only during calibration of the mass spectrometer. No retarding potential field is utilized, and Ar^{38} and He^3 are analyzed directly, the only source of these species being the on-board calibration gas reservoir. Redundant filaments

are incorporated in the ion source so that if one burns out the other is automatically switched in after a pre-determined time interval. Ambient ions are prevented from entering the ion source by biasing the repeller grid (S2, Fig. VII-13).

b. Ambient Neutral Composition with Retarding Potential

As detailed above, only in this mode can an accurate analysis of the neutral cometary atmosphere be obtained. Since the energy of the incoming atmospheric molecules is mass dependent, the retarding potential must be scanned along with the mass spectrometer scan.

It is common in analytical mass spectroscopy to acquire mass spectral data at more than one ionizing electron energy to enhance the ability to interpret the data where overlapping peaks occur from different species. In order to preserve the maximum spatial resolution, however, only a single ionizing electron energy can be utilized. This is an unfortunate compromise that must be made on a fast flyby mission.

c. Ambient Ion Composition

In this mode of analysis, the ionizing electron beam is biased to cut-off so that no ionization takes place within the ion source. Only ambient ions entering the instrument will be collected and analyzed. Due to the large energy spread of incoming ions, the retarding potential field is used in this mode of operation also.

3. Duty Cycles

Two duty cycle considerations must be taken into account to optimize the mass spectrometer experiment. These are:

i. Establishment of dwell time per mass peak, and

ii. Establishment of the absolute and relative times spent on neutral spectral scans versus ion spectral scans.

Both ion and neutral species are likely to occur in the cometary atmosphere over a very wide range of densities (see Figure VII-15). Complete mass scans over the ranges 1-8 and 12-100 amu will be accomplished simultaneously approximately every second. Ion scans and neutral species scans will be alternated so that the integrated data will be obtained over very nearly the same portion of the spacecraft trajectory. Data from many individual scans will be accumulated in a pair of buffer storage registers (one for ions, one for neutrals). Stored data from the buffers will be telemetered on completion of a set of scans while new data are being collected in another pair of buffers. Spatial resolution will be governed by the time required to complete a set of scans.

The basic equation for the signal-to-noise ratio assuming a Poisson distribution of events can be expressed as:

$$\frac{S}{N} = \frac{\dot{N}_s [TD]^{\frac{1}{2}}}{\left[\dot{N}_s + 2\dot{N}_n\right]^{\frac{1}{2}}}$$

where:

$\dot{N}_s$ = sample ion count rate

$\dot{N}_n$ = noise count rate

T = experiment integration time

D = Duty cycle

For a mass spectrometer sensitivity of 1 ion per second per 100 neutral molecules - cm^{-3} and a noise level of 1 noise pulse per second, a molecular species at a density of 500 molecules - cm^{-3} could be measured at a signal-to-noise ratio of 2 if 100 scans comprised a scan-set (i.e., $T = 100$ s, $D = 0.01$ for each amu).* The total distance traveled by the spacecraft during this time would be approximately 100 sec. x 18.3 $km\text{-}sec^{-1}$

*Private communication with A. O. C. Nier, University of Minnesota, indicates a factor of 10 less sensitivity than assumed in this document, because of dynamic effects on ion-source focusing characteristics.
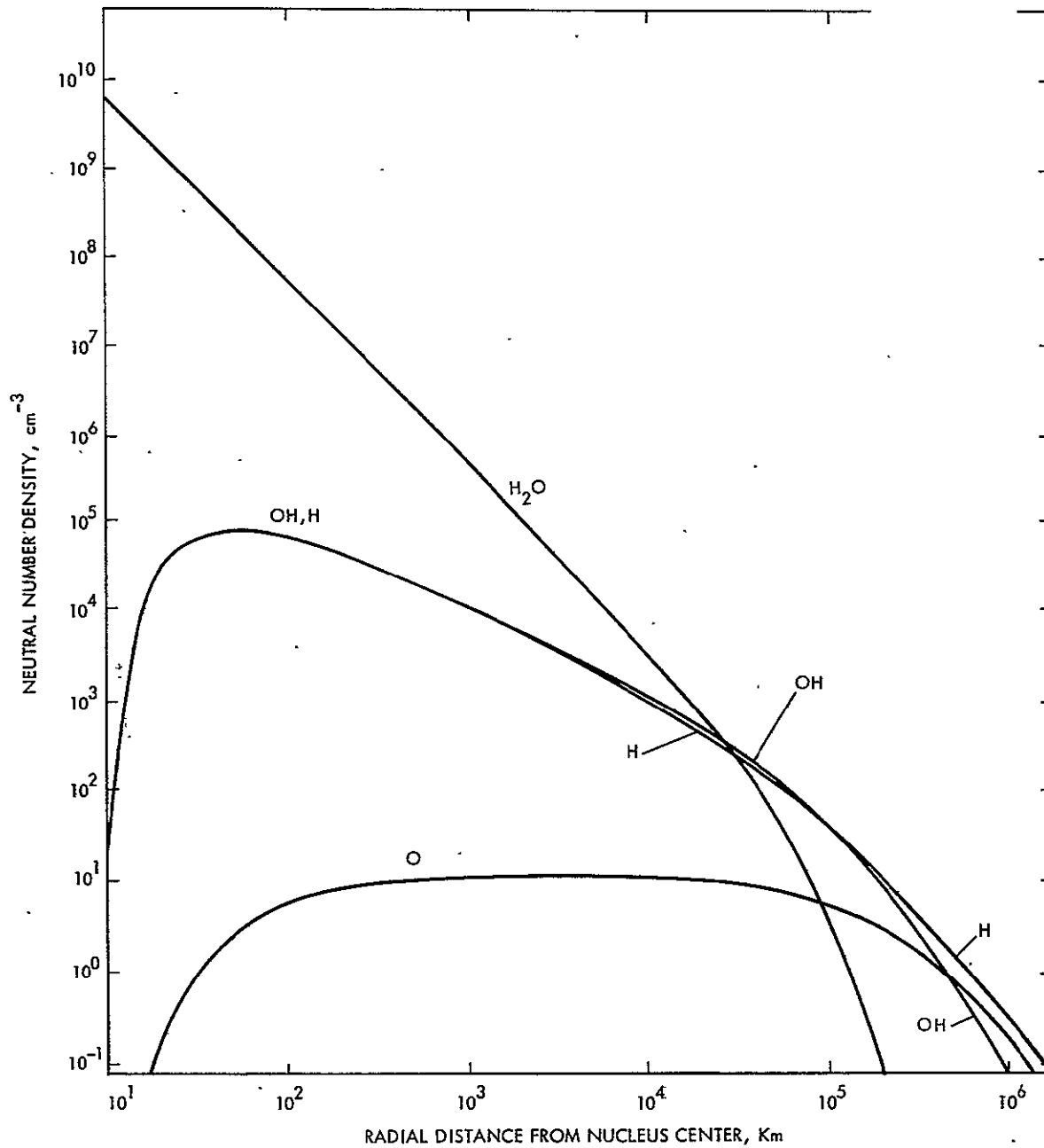
Figure VII-15. Neutral number densities at 0.5 AU from sun. Modified from Taylor, Michaux, and Newburn (Ref. VII-2) per data of Bertaux, Blamont, and Festou (Ref. VIII-3).

= 1830 km. Rather than accept such a degraded spatial resolution, it is proposed that the mass spectrometer be read out to telemetry at a more frequent rate at a sacrifice in real-time detectability. Summation of data through ground based data reduction would then be required to establish the presence of very low concentration species. With a 1×10^5 count channel capacity per amu, a dynamic range of 2×10^4 can be obtained for neutral species analysis based upon: (a) a closest approach distance of 500 km, (b) 10 mass scans per scan set (therefore a spatial resolution of ~ 180 km) and (c) a signal to noise ratio of 2 at the detectability limit of 5000 molecules $-cm^{-3}$ for each scan set. The telemetered data will be formatted to acquire only the 7 most significant bits (an additional 4 bits being required for encoding).

If the above analysis sequence were accomplished on a 500-km spacecraft flyby, the mass spectrometer on the probe flying by the nucleus at 5000-km closest approach could achieve comparable comet-centered angular spatial resolution by effecting 100 scans per scan set as noted at the beginning of this discussion.

For ambient ion measurements a strong "ram-effect" due to spacecraft velocity enhances the mass spectrometer sensitivity in this mode of analysis. Assuming all positive ions crossing a 0.1 cm^2 plane in the ion source can be analyzed, then an ion density of 0.01 ions-cm^{-3} would produce 0.01 ions-cm$^{-3} \times 0.1$ cm$^2 \times 18.3 \times 10^5$ cm-sec$^{-1} = 1.83 \times 10^3$ ions-sec^{-1} to the mass analyzer. A dwell time per mass channel of $1 - 10\%$ that used for neutral analysis would provide more than adequate sensitivity. Hence, the ambient ion analysis duty cycle on alternate scans would have minor effect on spatial resolution. To summarize then, a total "scan-set" would comprise:

Spacecraft:

>Ten (10) 0.88-sec neutral scans
>
>and
>
>Ten (10) 0.088-sec ion scans

Probe:

>One hundred (100) 0.88-sec neutral scans
>
>and
>
>One hundred (100) 0.088-sec ion scans

totalling approximately 9.7 and 97 seconds per scan set respectively on the spacecraft and probe with 0.010 seconds per mass per scan for neutrals and 0.001 seconds per mass per scan for ions.

4. Total number densities

In addition to utilizing the mass spectrometer for compositional analysis of ambient ions and neutrals, it is also possible to establish total number densities by integrating the output of the instrument in real time. This can be accomplished by two additional storage registers in the data handling system, which merely count all ions arriving at the detectors irrespective of their mass. By telemetering the data in these registers after each ambient neutral and ion scan, a factor of 10 improvement in real time spatial resolution can be achieved aboard the spacecraft and a factor of 100 aboard the probe.

5. Functional specifications - The functional specifications of the mass spectrometer experiment are listed below:

Mass Range

Low mass range	1 - 8 amu
High mass range	12 - 100 amu
Mass accuracy	$< \pm 0.5$ amu
Mass resolution $(M/\Delta M)$	
Low mass range	8
High mass range	100

Detection Threschold $(S/N = 2)$

Neutral species	
Probe:	500 molecules/c
Spacecraft	5000 molecules/cc

Ion species

    Probe: 0.0002 ions/cc

    Spacecraft: 0.002 ions/cc

Dynamic Range 2×10^4

Mass Scan Rate

    Probe: 88 seconds/telemetered spectrum (neutrals); 8.8 seconds/telemetered spectrum (ions)

    Spacecraft: 8.8 seconds/telemetered spectrum (neutrals)

                                      0.88 seconds/telemetered spectrum (ions)

Mass Peak Intensity
Accuracy

    Detection Threshold $\pm$ 50%

    > 20 x Threshold $\pm$ 10%

6.   Instrument physical specifications (see Figure VII-16)

<u>Weight</u>

Mass Spectrometer and base plate	2.2 kg
Electronics	2.5 kg
Ion pump	0.5 kg
Miscellaneous wiring, etc.	<u>0.1 kg</u>
TOTAL	5.3 kg

<u>Size</u> - (see Figure VII-15)

Base plate	25.4 x 22.9 cm
Average height	15.2 cm
Volume	8849 cm^3

<u>Power</u>

Mass Spectrometer electronics	5 watts
Ion source	2.5 watts
Ion pump	<u>1.5 watts</u>
TOTAL	9.0 watts average

EJECTING MECHANISM

EJECTABLE CAP

OBJECT SLIT

ION SOURCE

ION SOURCE FLANGE

ELECTROSTATIC ANALYZER PLATES

CUT LINE

IL/S ION PUMP ASSEMBLY

VACUUM HOUSING

PUMPOUT TUBE

2.02 R

LOW MASS

ELECTRONICS ASSEMBLY

25.4

5.72 R

HIGH MASS

ANALYZER MAGNET

COLLECTOR SLIT (TYP 2 PLACES)

COLLECTOR (TYP 2 PLACES)

CONNECTORS

MOUNTING FLANGE (TYP 2 PLACES)

22.9

13.3 MAX.

ANALYZER COVER

ELECTRONICS COVER

BASEPLATE

15.2

Figure VII-16. Principal parts of mass spectrometer (courtesy of J. H. Hoffman, University of Texas). Dimensions in cm.

7. Instrument Requirements

Thermal Requirements

Operating	$-20^{\circ}C$ to $60^{\circ}C$
Non Operating	$-50^{\circ}C$ to $85^{\circ}C$

Data Requirements

Peak Intensity (200 measurements
for ions and neutrals
combined including
selected "valleys") 2200 bits

Measurements of total ions
· and neutrals

Probe	2200 bits
Spacecraft	220 bits
Housekeeping	91 bits
Calibration	32 bits

TOTAL

Probe	4523 bits/scanset
Spacecraft	2543 bits/scanset

Date Rate

Probe:	$\sim$ 45 bits/second
Spacecraft:	$\sim$ 250 bits/second

Attitude Control

a) Pointing Accuracy - Entrance aperture must point along
velocity vector of S/C within $\pm$ 10°.

Post-flight documentation of attitude is necessary.

Special Requirements

a) MS must have direct access to ambient environment for
ion source.

D. DUST ANALYZER

The most widely accepted theory of cometary origin assumes comets to be made up of the primordial "stuff" of the solar system. If so, cometary solids and small asteroids may be the only sources of undifferentiated, unmixed primitive material available, and the elemental (and isotopic) composition of this material is of fundamental importance in geochemistry and cosmogeny. If not of solar system origin, the cometary solids must come from interstellar space, and an analysis of interstellar material is no less interesting.

The best way to measure the composition of the non-volatile fraction of the cometary nucleus during a flyby is probably to analyze the composition of the cometary dust reaching the spacecraft.

1. Instrument Description

Two major efforts have been carried out in recent years on the development of mass-spectrometric techniques for the compositional analysis of micrometeoroid material from spacecraft. The first of these (headed by H. Fechtig and J. Weihrauch of the Max Planck Institut fur Kernphysik, Heidelberg, Germany) is scheduled to be flown on the Helios Solar Probe. The second effort was under the leadership of J. F. Friichtenicht of TRW, Redondo Beach, California. The two approaches are identical in concept: a compositional analysis of micrometeoroid material is made through a time-of-flight (TOF) mass spectrometer analysis of the plasma generated when a small dust particle strikes a tungsten target at high velocity. Information on the size of the particle is gained through a measurement of the total integrated plasma charge and a measure of the relative particle velocity is made through the measurement of the rise time of the plasma "pulse."

The TOF mass spectrometer analysis assumes that the ionic composition of the impact-generated plasma is directly related to the bulk composition

of the micrometeoroid (or in this case the cometary dust particle). By
accelerating the plasma ions through a potential difference (V) and then
letting them pass along a field-free drift region of known length (L_2), the
atomic masses (M) of the ions can be determined by their respective arrival
times (t_M) at a detector through the approximate relationship:

$$t_M \approx (\frac{M}{2eV})^{\frac{1}{2}} (2L_1 + L_2)$$

where:

e = electronic charge

L_1 = distance over which ions are accelerated

$(L_1 < < L_2)$

$L_1 + L_2$ = distance between target and collector.

A simplified schematic of the instrument is shown in Figure VII-17. Upon
impact of a dust particle on the target, a plasma is generated, the time pro-
file and intensity of which is measured. The plasma-detection amplifier
sends a signal to the signal-conditioning electronics which starts a clock
for timing the arrival times of ion "bunches" as they reach the resolved
ion detector. The signal-conditioning electronics format the measurement
of the integrated charge in each ion "bunch" and time-label it for mass
identification.

It would be desirable to cover the mass range from carbon to nickel
which would necessitate the measurement of ions from 12 amu to 60 amu. Of
the elements in this region that are most likely to occur, the separation
of potassium and calcium is the most stringent. At a plasma-accelerating
potential of 1000 volts and a distance between the target and the collector
of 1 meter, the mean arrival times of K^{39} and Ca^{40} would be separated by $\sim$ 200
nanoseconds. The entire mass range is covered in $\sim 10^4$ nanoseconds. Therefore,
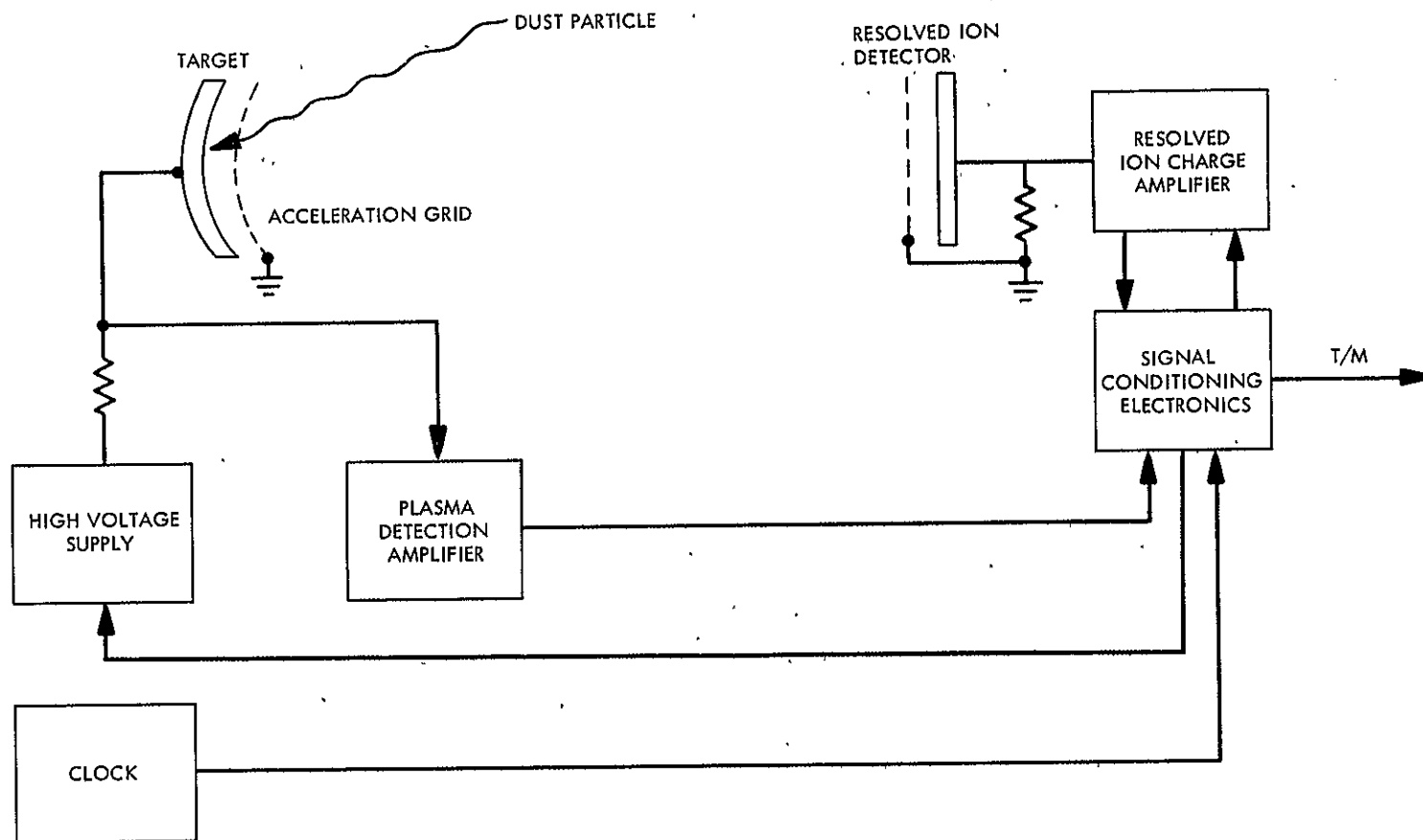
Figure VII-17. Simplified block diagram: Cometary Dust Analyzer

a 256-channel detector memory would provide sufficient time resolution at 40 nanoseconds/channel to reproduce the mass spectrum. However, the very fast gating required to achieve this performance may not be within the state of the art for this mission and resolution requirements may have to be relaxed. It is therefore felt that the "sample-and-hold" technique of Friichtenicht (Ref. VII-13) or the "pulse stretching" and pulse height analysis technique of Fechtig (Ref. VII-14) on the Helios Solar Probe are the most likely candidates for data acquisition at this time. Both of these approaches would strongly degrade mass resolution in their present configurations.

Based upon the dust model of Taylor et al., (Ref. VII-2) one can expect a peak dust-particle impact rate of 0.14 particles per second upon a target 20 cm in diameter at the closest approach distance to the comet of 500 km. This rate would be two orders of magnitude lower 1/2 hour before and after encounter using the symmetrical model. Hence one could expect that, during the hour centered on closest approach, approximately 250 impacts would be recorded. These would be comprised mostly of particles with diameters between 0.1 μm and 10 μm. Data of Friichtenicht et al., (Ref. VII-13) indicate that approximately 10^3 coulombs/kg of charge is released by a particle striking a target at $\sim$ 18 km/sec. Assuming a particle density of 2.5 gm-cm^{-3}, this would represent impact plasmas of $\sim 10^{-13} - 10^{-11}$ coulombs. To adequately cover the expected particle distribution estimated in Taylor's model, the instrument should be designed to detect plasmas in the range of 10^{-13} to 10^{-9} coulombs $(10^{-16} - 10^{-12}$ kg dust particles).

2. Functional Specifications

The functional specifications for the cometary Dust Analyzer are as follows:

Mass Range	12-60 amu
Mass Resolution	40 (Assumes ~ x 4 improvement in speed of A/D convertors. This will require significant instrument development effort.)

Dynamic Range

Target Plasma	10^4
Resolved Ion Charge	10^5
Detectability	10^{-16} kilograms

Accuracy

Target Plasma	$\pm$ 10%
Resolved Ion Charge	$\pm$ 10%

3. Data Requirements

Target Plasma	16 bits/impact

Resolved Ion Charge

Data	700 bits/impact
Gain Encoding	2 bits/impact
Housekeeping	35 bits/impact
Total	753 bits/impact
Assuming 250 impacts/3600 sec	52 bits/second

4. Physical Configuration and Constraints (after Helios)

Weight	5 kg
Power	8 watts

Size

Sensor diameter	20 cm
length	100 cm
Electronics	10cm x 10cm x 20 cm
Operating Temperature	- 40°C to + 50°C

E. OPTICAL PARTICLE DETECTOR

Spectra of the heads of long-period comets invariably exhibit a continuum of light between the molecular emission bands, the continuum being sunlight scattered by small dust particles and icy grains. Usually such comets also exhibit a long tail of dust, a so-called Type II tail, which is quite distinct from an ion tail (a Type I tail) but which may coincide with it or be projected together with it against the sky as seen from Earth. Short period comets often show little or no continuum, implying a much lower density of particles present. Comet Encke, in particular, has shown a very weak continuum, visible (using ordinary photographic techniques) only on spectra taken when the comet was about 0.8 AU of the Sun. It has never exhibited a discernible dust tail. There are no reliable quantitative figures on the size and number density of dust given off by Encke. Crude estimates used in this section are taken from the Encke model of Taylor et al., (Ref. VII-2).

A large uncertainty in understanding comets then is the contribution of particulate matter to their makeup. This orders-of-magnitude uncertainty is also of obvious concern in the proper design of space vehicles for comet exploration. Slight reddening of scattered sunlight in brighter comets indicates the presence of many particles whose size is comparable to the wavelength of visible light, making them difficult to detect individually, even from a spacecraft. A quite sensitive instrument is needed for simple detection. In order to determine the size distribution, a statistically significant number of particles must be observed; yet a large flux implies a potential spacecraft hazard.

The best particle detector in existence for comet studies is probably the optical particle detector called Sisyphus by its designers (Ref. VII-15). A version of Sisyphus is currently in flight on Pioneers 10 and 11, and another version was proposed to fly on Mariner-Jupiter-Saturn. The instrument described here (a modification of the MJS form) consists of three small telescopes and detectors. The MJS form is shown in Figure VII-18. A logic system determines both the apparent brightness and the angular rate of particles seen by the detectors. Since, in the flyby mission, the component of angular velocity due to the velocity of the spacecraft itself will be 20 to 40 times as large as that due to the velocity of the dust, to a first approximation the latter can be ignored, and a true distance can be computed to each particle that is seen. Given the distance to the particle, the particle size can be computed from the brightness by assuming an albedo. With the predicted capability of the instrument, a velocity uncertainty of $\pm$ 3% in the field-of-view plane and $\pm$ 15% normal to the field-of-view, the intrinsic velocities of the dust particles can be measured in a limited sense.

On a spin-stabilized S/C, the background due to coma irradiance will be modulated if the instrument's field of view rotates such that it is alternately pointed toward and away from the denser coma region. Although Sisyphus has a dynamic range of 10^6 when viewing against an average stellar background, it is less versatile against the radiant coma background. The instrument has a field-of-view which is at an angle of 30° from the spin axis. The spin axis is assumed to be oriented along the comet-relative velocity vector of the S/C. The background light will vary in a sinusoidal fashion as the field-of-view passes through the coma. The range-to-radius ratio of 10^6 (assuming a geometric albedo of 0.2) is reduced to $\sim 8 \times 10^4$ at 10^5 km from, and on the sun side of, the nucleus during the portion of the S/C rotation when the field-of-view passes through the brightest portion of the coma.
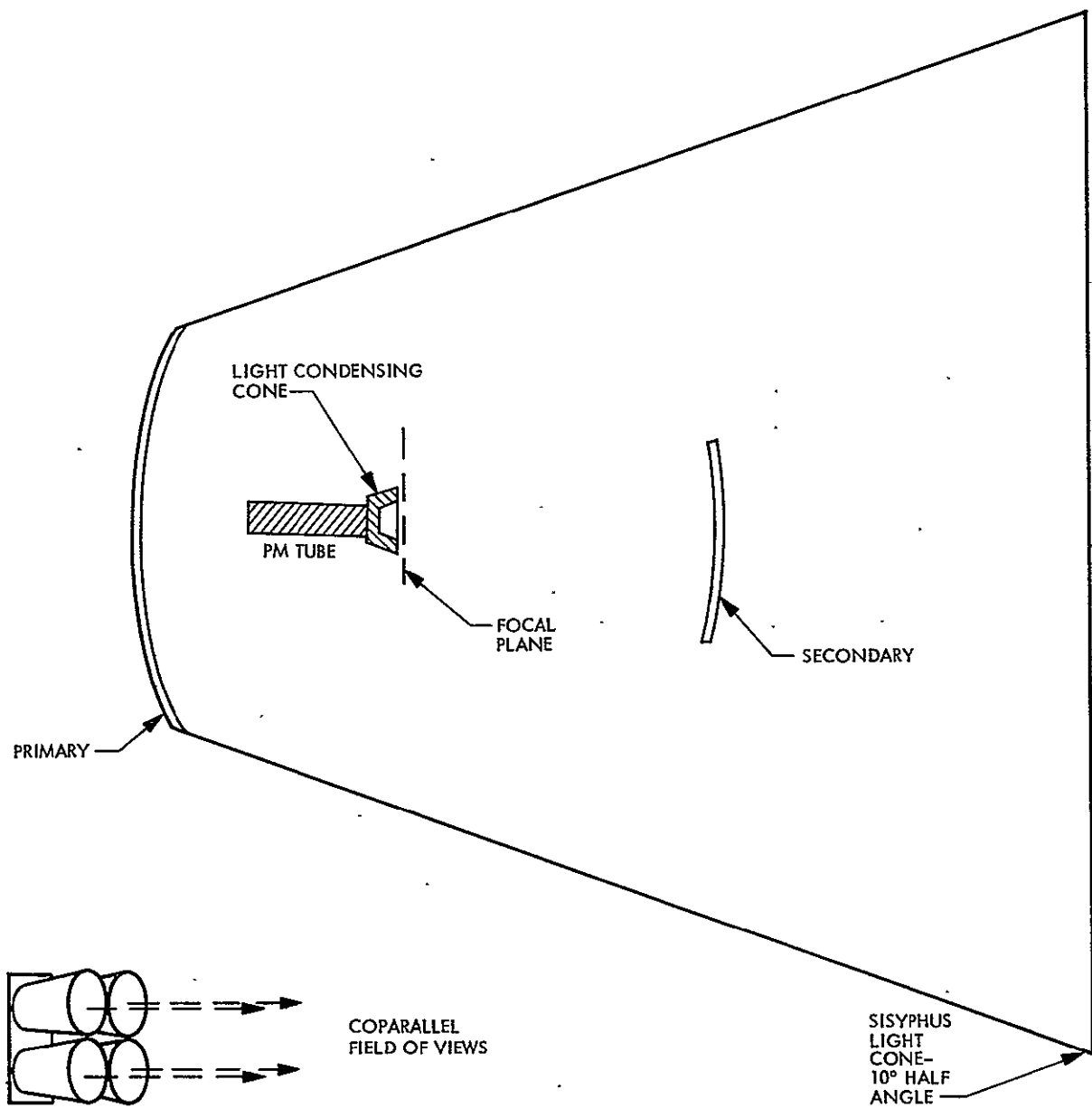
Figure VII-18. Schematic of Sisyphus: Telescope, Sensor and Arrangement of Four Telescopes; modified version of that proposed for Mariner-Jupiter-Saturn

(Here we have used the photometric model of Reference VII-2 multiplied by the broad band factor of 4.6). Further reduction occurs near closest approach, bringing the ratio to $\sim 2 \times 10^3$ near closest approach. During the portion of the S/C rotation when the field-of-view passes through the least bright portion of the coma the range-to-radius ratios will increase by a factor of ~ 10 at 10^5 km from the nucleus and by a factor of ~ 5 at closest approach.

Using the nominal Taylor model (Ref. VII-2), we can estimate the maximum detection rates of particles of various sizes which enter the field-of-view and range, assuming a $20°$ FOV cone angle and a range-to-radius ratio of $\sim 2 \times 10^3$. This means that a 10-micron particle would have to be within 2 cm of the telescope to be detected, which is too close to be out of the spacecraft shadow. Table VII-5 shows the detection rates and maximum ranges for particles using the various ratios of range to particle radius corresponding to background irradiance variations within the coma using the Sisyphus detector. The upper limit model increases all rates by 10^3.

The background noise current in the photomultiplier tube is described by

$$i_n = (2i_B ef)^{\frac{1}{2}}$$

where e is the unit electrical charge

f is the instrument circuit noise bandwidth defined by $(2\pi \tau)^{-1}$, where

τ is the circuit time constant (about 1 megahertz),

$$i_B = B_I \eta \left(\frac{\pi \alpha D}{2}\right)^2 (1 + b_c \sin \theta)$$

and where B_I is the background intensity in watts/(radian cm)^2

η is the phototube efficiency in amperes/watt

α is the half angle of the field of view cone (radians)

D is the optical aperture (cm)

b_c is the ratio of non-coma background to coma background (a function of S/C position in the coma)

θ is the pointing angle with respect to the nucleus (a function of time or spin position)

Table VII-5. Sisyphus Capabilities at Encke

Distance from Nucleus	10^6 km			10^5 km			10^3 km		
Look Direction	Before coma, 30° from anti-sun.			Looking into coma, 30° from anti sun.			Looking in, 30° from anti-sun.		
Ratio, Particle Range/ Particle Radius	10^6			8×10^4			2×10^3		
Particle Size (m)	10^{-6}	10^{-4}	10^{-2}	10^{-6}	10^{-4}	10^{-2}	10^{-6}	10^{-4}	10^{-2}
Peak Rates (Detection/sec)	2.1×10^{-6}	4.6×10^{-6}	3.5×10^{-7}	1.3×10^{-6}	2.7×10^{-6}	2.0×10^{-8}	1.8×10^{-6}	2.2×10^{-6}	7.6×10^{-8}
Detection Range (m)	10	100	10^4	.8	8	800	.02	.2	20

Distance from Nucleus	10^5 km			10^3 km		
Look Direction	Looking out of coma, 30° from sun.			Looking out, 30° from sun.		
Ratio, Particle Range/ Particle Radius	10^6			1.3×10^4		
Particle Size (m)	10^{-6}	10^{-4}	10^{-2}	10^{-6}	10^{-4}	10^{-2}
Peak Rates (Detection/sec)	2.0×10^{-3}	4.3×10^{-3}	3.2×10^{-6}	1.4×10^{-3}	1.6×10^{-3}	5.7×10^{-6}
Detection Range (m)	10	100	10^4	.13	1.3	130

Since the signal can be expressed as

$$i_s = I\eta \frac{\pi D^2}{4}$$

where I is the particle irradiance on the aperture (w/cm^2), the signal-to-noise ratio is given by

$$\frac{i_s}{i_n} = \frac{I}{2}\frac{D}{\alpha} \left(\frac{\eta}{2qfB_I(1 + b_c \sin\theta)} \right)^{\frac{1}{2}}$$

The prospects for positive results are quite good if the field of view is not shadowed by the space vehicle. Any sensor improvements and emission line filtering can improve the prospects to the point where almost any reasonable model can be tested. We anticipate that the instrument problems apparent on Pioneers 10 and 11 will have been satisfactorily overcome in the next generation of instruments.

Basic engineering parameters are:

Weight:	4 kg
Size:	40 x 30 x 20 cm
Power:	3 watts
Thermal:	$-40°$ to $75°C$ operating electronics $> -200°C$ optics and non-operating electronics
Mounting:	Body mounted pointing $\sim 30°$ from spin-axis which should be along anti-solar direction. The telescopes must be parallel within 10 arc seconds. No sunlight can be allowed to be reflected from the spacecraft into the light cone.
Field of View:	$10°$ half cone angle
Pointing Accuracy:	$\pm 5°$
Stability	± 100 μ rad/sec
Data rates:	6 kbps into buffer $\lesssim 10$ bps average rate

F. FIELDS AND CHARGED PARTICLES

For the fields and plasma scientists, comets are a particularly fascinating challenge and a unique opportunity. The physical processes by which cometary radicals are ionized (other than photoionization) and interact with the solar wind to form part of the outer coma and ion tails are still in dispute even on a qualitative basis. The spacecraft trajectory passing through the sun side, close to the nucleus, and through the tail region is ideal for the study of cometary fields and particles, since it passes through the region where one might expect a shock front ($\sim 3 \times 10^5$ to 10^6 km from the nucleus toward the Sun), through the region of a possible contact surface ($\sim 10^4$ km from the nucleus), and through the tail.

The instruments which make up the particles-and-fields group will address both the quantitative and qualitative understanding of solar wind interaction, tail formation and coma formation. Data from these instruments may possibly be applicable to other areas as well: for instance, the structure and properties of the nucleus may be inferred from magnetic properties. Whereas a comet flyby is largely a reconnaissance mission, the particles-and-fields package can be expected to produce definitive experimental results in several areas of plasma physics related to coma and solar wind interaction phenomena.

The minimum charged-particles-and-fields instrument set consists of a magnetometer, a plasma probe, a plasma-wave detector, and a Langmuir probe on the bus, and, as an optional add-on, a magnetometer, a plasma probe and a Langmuir probe on a small separate probe targeted for a 5000-km miss distance, to insure obtaining data during tail passage. Table VII-6 summarizes the measurements to be made by the recommended particles-and-fields instruments. The charged-particles-and-fields instrument set was selected to measure parameters which will sort out the several possible models of cometary interaction

Table VII-6

Particles and Fields Measurements

Instrument	Measurements
Magnetometer	Magnetic fields 0.1 nT to 200 nT, coma structure
Langmuir Probe	Electrons and protons 0 - 20 eV, low energy flows, structure
Plasma Probe	Protons 10 eV - 10 keV, flow and coma structure
Plasma Wave	Dynamic features in coma structure, 10^{-8} nT/$\sqrt{Hz}$
Optical Particle Detector	Dust particle density and velocity, 10^{3-6} range/radius, $\pm .3\%$ velocity $\perp$, $\pm 15\%$ velocity along velocity vector; $\geq 10^{-6}$ gm particles .
Micro-Meteoroid Detector	$\geq 10^{-9}$ gm particles

with the interplanetary plasma and magnetic-field environment. Though it is likely that there is a strong interaction between the cometary atmosphere and interplanetary environment, it is necessary to establish the existence and properties of a shock front and contact surface and, in addition, to place upper limits on any magnetic field associated with a "nucleus." If further justification can be developed for higher-energy charged particles as a source of coma ionization, an instrument capable of measuring 200-keV to 500-keV protons and electrons would be an important addition to the payload.

1. Magnetometer

The objectives of the magnetometer measurements are to investigate the magnetic properties of the solar-wind interaction with Comet Encke and the properties of the intrinsic cometary magnetic fields. Features such as the possible bow shock, the comet's coma region, the cometary tail, and the contact surface will be investigated. Dynamic changes of the magnetic-field properties in these interaction regions would also be detected. If the interplanetary fields are excluded at or near the contact surface, probe penetration through this surface will allow an upper-limit determination of the magnetic moment of the comet nucleus. The measurement of the magnetic-field strength and direction are vital to the plasma-probe and plasma-wave measurements and would be necessary for their proper interpretation. The magnetometer, plasma-probe, plasma-wave and Langmuir-probe instruments collectively will be able to ascertain which magnetospheric model of Encke (if any) is correct; such a collective picture will greatly advance the understanding of the origin and evolution of the cometary structures.

To be able to make the above-stated measurements to sufficient accuracy, a flight-proven vector-helium (Ref. VII-16) or fluxgate-triaxial magnetometer (Ref. VII-17) with a sensitivity of at least 0.1 nT is desirable. The instrument (Ref. VII-17) will have a dynamic range from 0.01 nT to

~ 200 nT, a sensitivity of at least 0.01nT and will be capable of making several vector measurements per second. Such an instrument has been flown on Pioneers 10 and 11 and is shown in Figure VII-19. In order to cover the region close to the nucleus, to allow for dynamic measurements, and to allow for more areal coverage, a similar instrument is recommended for an add-on probe.

The S/C magnetic environment at the sensors should be either a) ≤ ± 1.0 nT with a fluctuation less than ± 0.1 nT if smaller than 1.0 nT fields are to be measured, b) ≤ the smallest expected field measurement with a variation of less than or equal to ± 0.1 nT. These constraints are necessary to set a reasonable upper limit on any cometary fields and to measure the extent of interplanetary-field exclusion inside the contact surface.

To achieve the desired sensitivity requirements, the instrument should be boom-mounted; preliminary estimates indicate that only a short boom is required for the expected bus fields.

The magnetometer package will have an approximate weight of 2.0 kg, and will require 3 watts of power and approximately 200 bits per second of telemetry on the bus. For the probe, a reduced bit rate (~ 25 bps) is considered acceptable, at the expense of spatial resolution (from ≲ 1 km to ~ 5 km).

2. Plasma-Wave Detector

The plasma-wave instrument will investigate the modes of interaction of the solar wind with Encke and the role that wave emissions and absorptions play in the dynamic processes that occur in the plasma regions surrounding the comet (e.g., possible instability of contact surface). The instrument will investigate possible generation of wave due to plasma instabilities; waves such as electron-cyclotron and ion-cyclotron electromagnetic waves (Ref. VII-18), and electrostatic plasma waves (Refs. VII-19, VII-20) among others have been commonly detected in the plasma region of the earth's environment. The electromagnetic cyclotron waves are important in the pitch angle
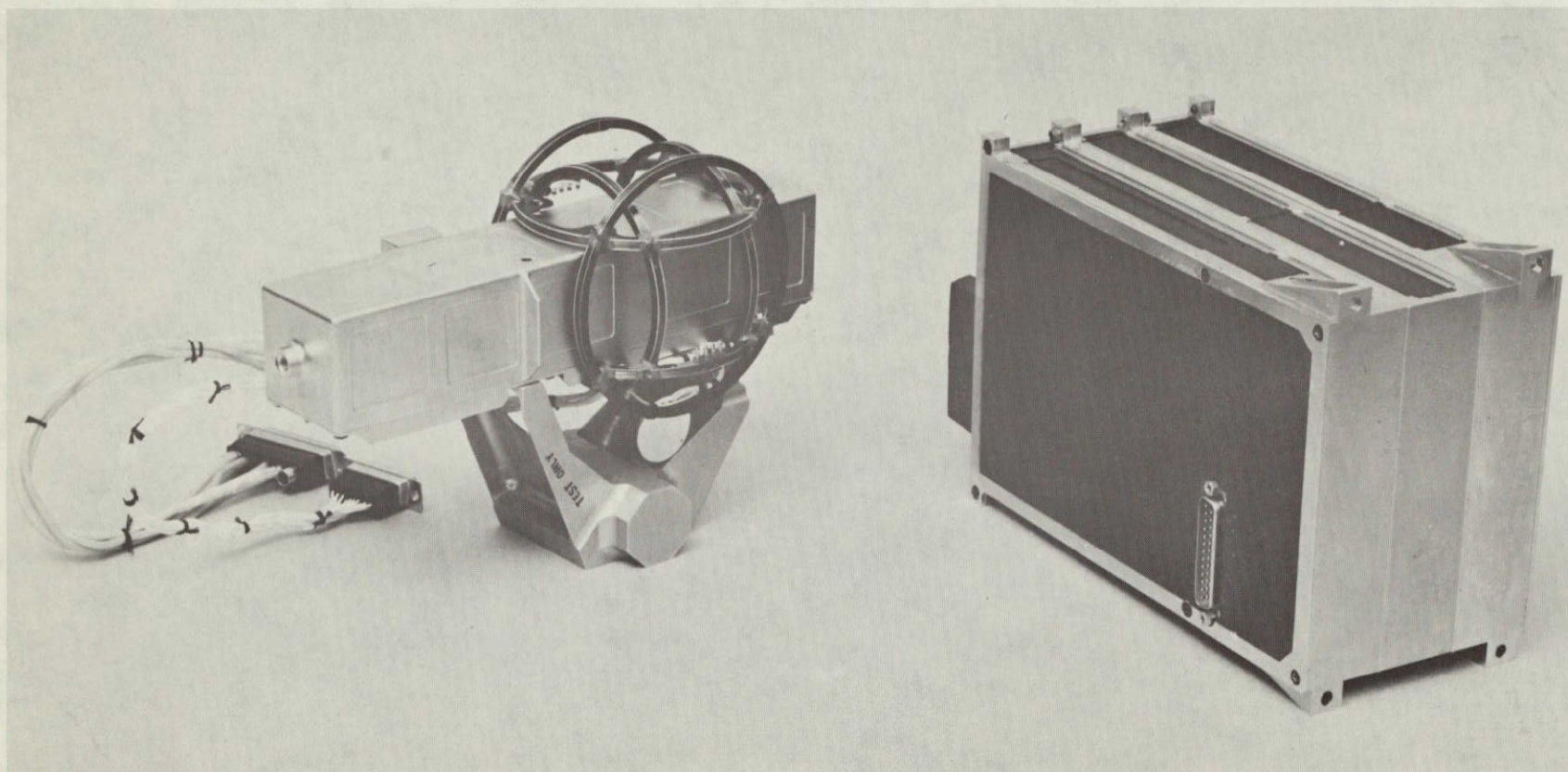
Figure VII-19. Magnetometer used on Pioneer 10 and 11
(courtesy of A. M. A. Frandsen)

scattering of energetic particles; by breaking of their first or second adiabatic invariants the particle velocity distribution can be altered, which in some cases leads to particle losses. Electrostatic plasma waves are important in the heating and acceleration of the electrons and ions. The plasma waves are indications of instabilities that relieve plasma anisotropies (e.g., loss cone, temperature, pressure, density, etc.). Many particle features could not be understood without wave observations. The plasma-wave investigation will observe and identify any wave structures at the shock front, at the contact surface, and in the plasma flow either in the coma or tail. Wave generation associated with magnetic-field-line reconnection in the tail region at x-type neutral points is a possibility and will be investigated. The plasma-wave observations will be an integral part of the particles-and-fields measurements, and, as part of a collective experiment, will make an accurate determination of the shock, magnetosheath, magnetosphere, atmosphere interior to the contact surface, tail, and neutral-sheet properties to the first order.

The sensitivity needed in order to observe the expected phenomena is 10^{-8} nT^2/Hz at 100 Hz, assuming an f^{-3} noise requirement; this is consistent with the magnetometer requirement of $\leq \pm 0.1$ nT in the range 0-1 Hz. Preliminary estimates of the spacecraft field indicate that the plasma wave sensors should be located on a boom away from the S/C body. This boom can be shared with the magnetometer, but the two instruments must be at least two meters apart. Magnetic-wave measurements will be made in the 1 to 10 kHz and 5 to 200 kHz ranges using a search-coil magnetometer and a loop antenna, respectively. The electric-wave range of 10 Hz to 200 kHz is a possibility for the electric-dipole antenna. Flight-proven instruments with the necessary sensitivity and weight-power requirements have been flown on OGO-6. The schematic of these instruments is shown in Figure VII-20.
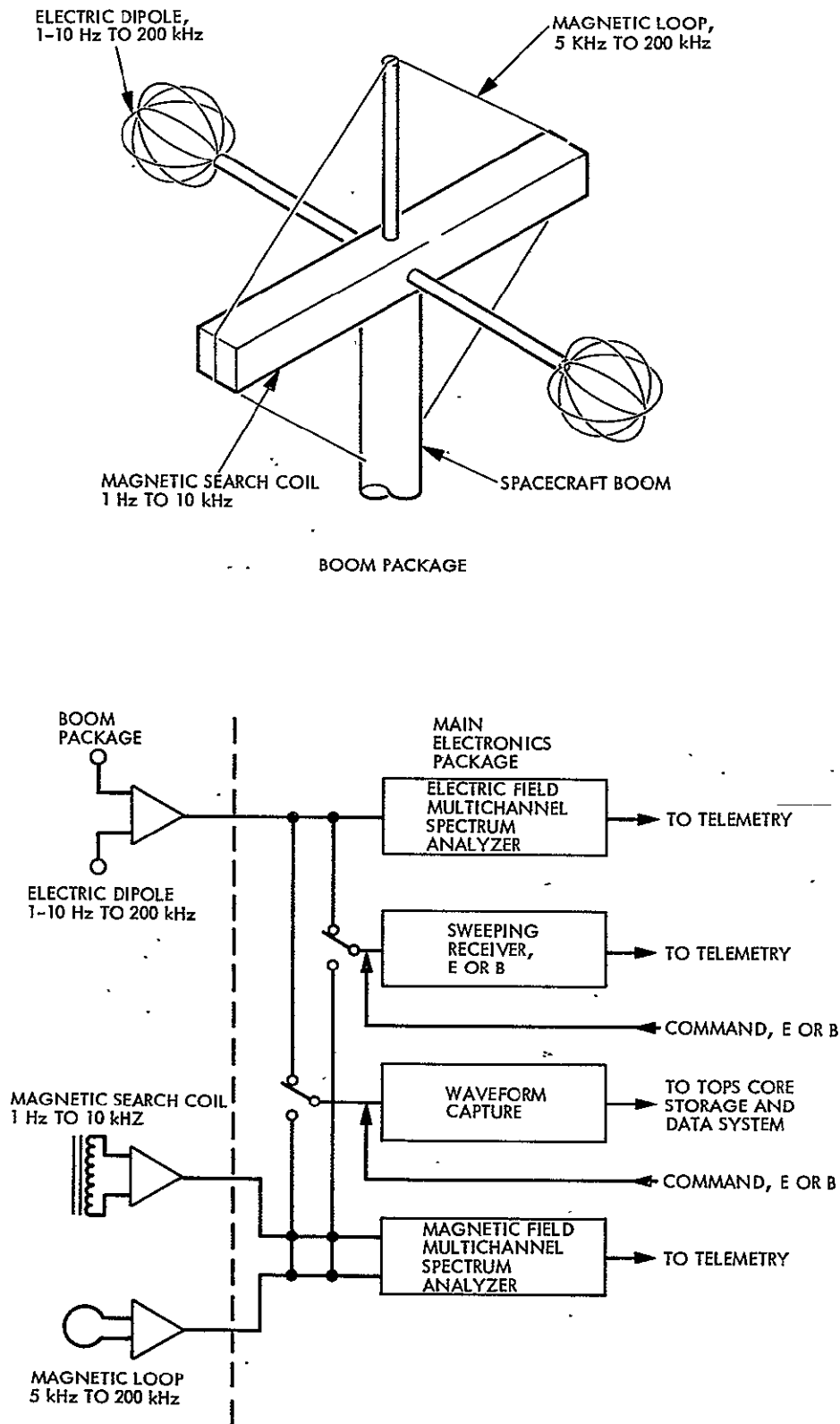
Figure VII-20. Plasma Wave Instrument Schematic and Block Diagram

The plasma wave detector will have a mass of 5 kg, use a power of 5.0 watts, and will require a data rate of 300 bps.

3. Langmuir Probe

The objectives of the Langmuir probe measurements are to determine the density and temperature of low-energy electrons and ions and the bulk velocity of ions in Encke's inner coma and tail. These data will contribute to knowledge of the flux and spatial distribution of electrons and ions which form the inner coma, and of the processes which generate the solar wind interaction and tail formation. It is anticipated that the regions of greatest interest for these measurements will be encountered during the nearest approach of the nucleus, particularly inside the possible contact surface which may extend into the tail, but measurements would extend for several days before and after encounter. Thus, two duplicate instruments (one on the main spacecraft bus and one on the optional flyby probe) are suggested for this type of experiment.

These results will help establish the existence and position of the contact surface, will help determine the contribution of the ion portion of mass movement and/or mass loss from Encke, and will help determine the charge movement or global current flow.

The instrument sensor selected for this experiment is a charged particle trap of planar geometry similar to those flown on OGO-6 (Ref. VII-21). The bi-polar operation (for electrons and ions) is based upon the use of such probes on IMP-1 (Reference VII-22). A retarding potential of + 20 to - 20 volts is used to establish parameters of electrons and ions from 15 V down to spacecraft induced noise levels. The noise value is dependent upon the details of spacecraft design or neutralization methods employed, but it is expected to be a few volts or less (Ref. VII-23).

A schematic diagram of such a charged-particle trap is shown in Figure VII-21. The retarding voltage is varied and those charged particles which can penetrate this barrier are collected and sensed by an electrometer. The position of the suppressor grid in the Langmuir probe is above the retarding grid, since the secondary-electron problem is greatly reduced by this configuration (Ref. VII-24). The suppressor voltage can be highly negative for ion-measurements, while the collector voltage can be positive for electron measurements, either of which will effect suppression of secondary-electron currents. The shield grids are present to the extent required to make negligible the capacitive pickup on the collector from the changing retarding or modulator voltage. This type of sensor does not function properly in the electron-detection mode when solar UV can enter and strike the interior surfaces. Consequently, the orientation of this sensor must be such that the field of view is away from the sun.

There are several conflicting requirements on the look direction for the sensor. In general, the ion mode of operation requires detecting-slow (less than S/C velocity of ~ 18 km/sec) ions which are in the forward, or probe-velocity, direction. In addition, when inside the contact surface, there may be a significant component of velocity radially away from Encke. The electron anisotropy dictates looking in an orthogonal direction. All of these require-ments can be satisfied by a two sensor instrument, each sensor with a 45-degree half-cone angle oriented (1) along the spin axis in the velocity-vector hemi-sphere, and (2) perpendicular to that axis. With this configuration, each sensor faces at least 90° from the sun.

Some of the significant physical parameters for this instrument are included in Table VII-7.

MODULATOR GRID

ENTRANCE GRID

CUP

MODULATOR OR RETARDING VOLTAGE

SUPPRESSOR VOLTAGE

TO ELECTROMETER AMPLIFIER

SUPPRESSOR GRID

COLLECTOR

SCREEN GRID
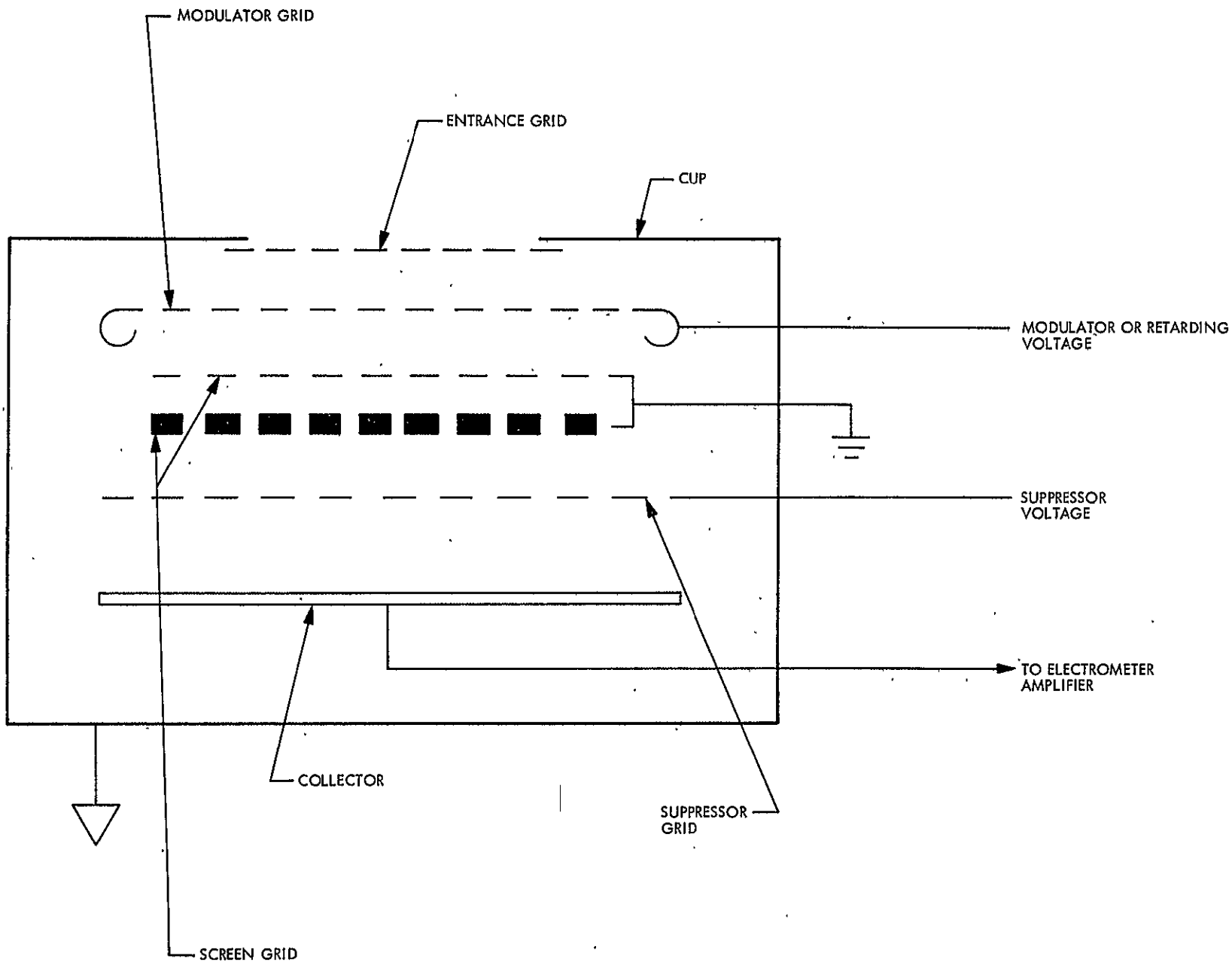
Figure VII-21. Faraday-Type Sensor

Table VII-7. Instrument Characteristics for Plasma and Langmuir Probe

Instrument Characteristics	Plasma Probe	Langmuir Probe
Weight (kg)	5	1.5
Power (watts)	5	3
Data rate (bit/sec) Bus:	100 - 350	75 - 200
Flyby probe:	25	25
Size:		
Electronics (cm x cm x cm)	20 x 20 x 15	20 x 10 x 10
Each sensor: diameter (cm)	10	4
length (cm)	10	2.5
Thermal limits (^{o}C)	-20 to +70	-20 to +70
Field of view:		
No obstruction	$\pm 45^{o}$ at sun, $\pm 45^{o}$ at 60° from sun*	$\pm 45^{o}$ antisun, $\pm 45^{o}$ at 120° from sun*, $\pm 45^{o}$ normal to plane*
"Some" obstruction OK	$\pm 65^{o}$ at sun, $\pm 65^{o}$ at 60° from sun*	$\pm 65^{o}$ antisun, $\pm 65^{o}$ at 120° from sun*, $\pm 65^{o}$ normal to plane*
Ion energy range (ev)	5 to 3000	0 to 20
Ion speed range (km/sec)	30 to 740	0 to 52
Ion flux range (charges/ cm^{2}-sec)	8×10^{5} to 4×10^{9}	5×10^{7} to 5×10^{12}
Electron energy range (ev)	N/A	0 to 15
Spectrum period (seconds)	10 to 20	20 to 30
Number of sensors	2	2
Current sensitivity (amperes)	1.5×10^{-13}	1×10^{-12}

* Directed in plane determined by sun, instrument, Encke on the side nearest Encke before encounter.

4. Plasma Probe

The objective of the plasma-probe measurements is to determine pertinent parameters for the solar-wind plasma flow and its interaction with the coma. These parameters, which include proton density, bulk velocity, and thermal speed, are to be measured in unperturbed interplanetary space and at various distances from Encke. These data will test for the existence and location of a shock front and for temporal and spatial variations which may indicate plasma instabilities and mechanisms for energy and/or momentum transfer within the coma. Although the model of the interaction region, for example, predicts a shock front at $\leq 10^6$ km (i.e., at about E - 15 hr), the uncertainties in the model are large. Again, within the tail, ions may reach detectable speeds at 10^4 - 10^6 km from the nucleus or E + 10 min to E + 15 hr. The value of these measurements will be increased if simultaneous data from an instrument measuring interplanetary solar wind conditions are available.

The basic sensor for the instrument selected is a modulated-grid Faraday cup that measures the ion flux entering the cup. By collecting these ions and using a sensitive current amplifier, the resultant current flow is determined. Energy spectra for the plasma are obtained by applying fixed sequences of retarding potentials to the modulator grid and measuring the resulting changes in current. Schematically, the cup is similar to that for the Langmuir probe (Fig. VII-21), having the same functional parts. The suppressor grid for this sensor is immediately above the collector. Similar detectors have flown on a variety of space probes, including ALSEP (Ref. VII-25), from which this instrument is patterned. The significant differences between this instrument and ALSEP's spectrometer are three: 1) six collectors within 2 cups instead of 7 collectors in 7 cups; 2) extended ion energy range

from 5 to 3000 eV (in order to measure bulk velocities corresponding to 10 to 2500 eV) in 21 windows instead of 75 to 9600 eV in 21 windows (14 positive and 7 negative); 3) increased electrometer sensitivity from 35×10^5 to 3×10^5 particle/cm^2-sec.

The changes to the sensor cup are flight-proven on the OGO-5 plasma spectrometer (Ref. VII-26). The lowered high voltage makes the design even less critical as regards corona or arcing, but increased sensitivity requires about the same degree of shielding and circuit-design care.

One of the areas for special concern for this instrument is the look direction and the field of view with respect to the angle measurement of the bulk velocity. These considerations require either a large-field-of-view detector or a narrow-field detector, such as cylindrical curved-plate analyzer, mounted on a programmable scan platform. The former was selected. To cover the range of angles anticipated for the velocity direction, two modified cups are required -- one facing the solar direction and one facing about 60° from the solar direction. The half-cone angle for each identical cup will be about 45°, with reduced sensitivity to about 60°. Each cup will have three pie-shaped, segmented collectors so that angle determination can be deduced from the ratios of currents. The field of view of each detector must not be obstructed for a half-cone angle of 45° with an additional 15° to 20° where no major obstruction may appear.

Some of the details for this instrument are indicated in the block diagram, Figure VII-22, where the techniques of preamplification by a sensitive electrometer, low-noise tuned amplification, synchronous phase-sensitive detection, and logarithmic compression are employed.
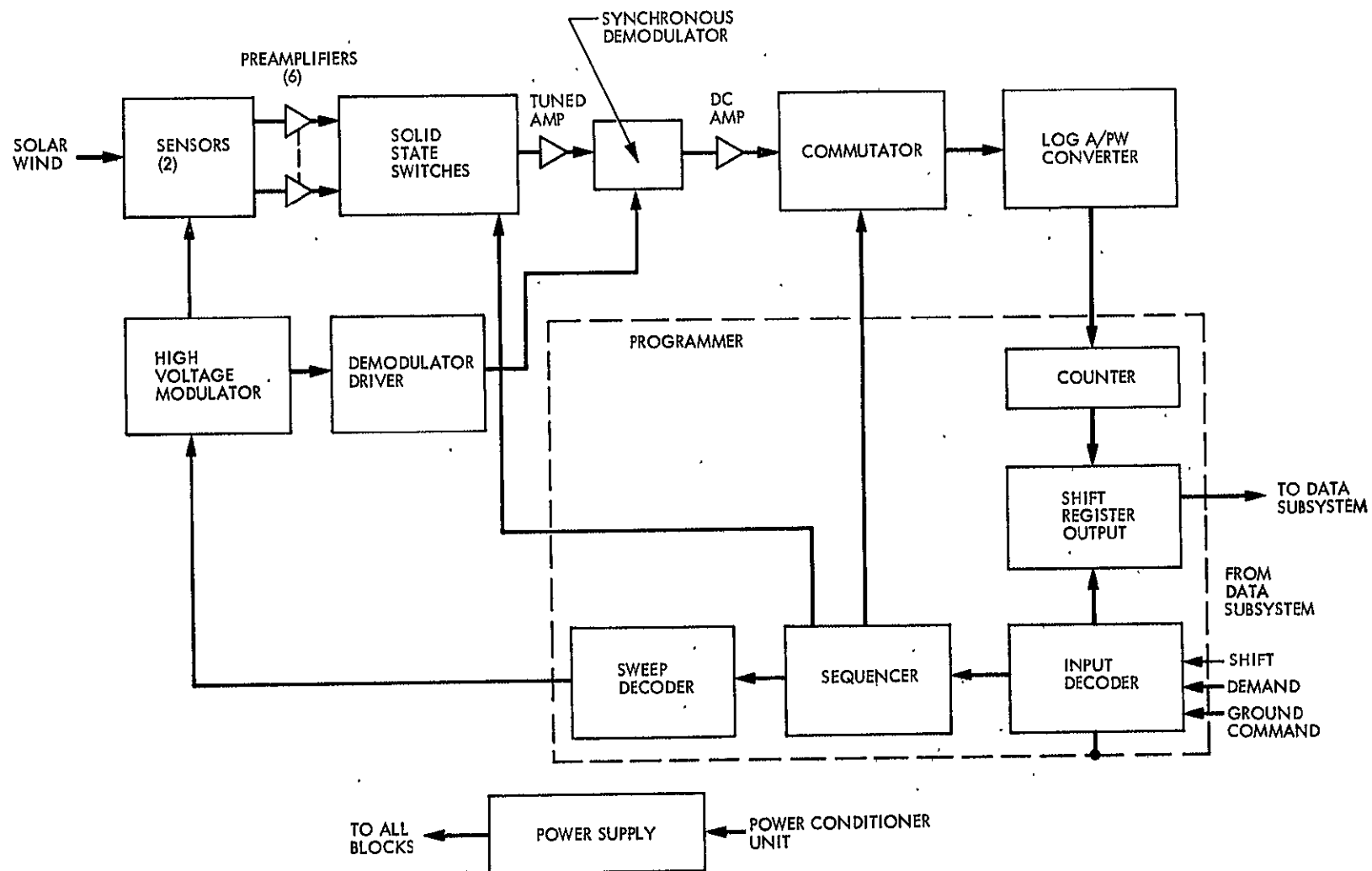
Figure VII-22. Plasma probe block diagram

Some of the significant physical parameters for this instrument are included in Table VII-7.

G.   MICROMETEOROID DETECTOR

The purpose of the micrometeoroid detector is to measure flux levels, spatial distribution, and particulate size of cometary dust too small to detect readily by optical means, and to perform a preliminary study of the meteoroid-penetration hazard to future spacecraft traversing the inner coma regions.

This instrument consists of 12 banks of penetration cells, attached on standoffs to the spacecraft's exterior. Each bank is constructed like an air mattress, with 18 individual cells in each bank. Each cell contains a pressure-sensitive transducer and is filled with neon prior to sealing. Penetration by a particle in the mass range under study causes a gradual pressure loss, with an evacuation time ranging from a few seconds to as long as 30 minutes. The transducer detects this pressure loss as a critical pressure is reached and a plasma discharge takes place across the cell. These events are counted to indicate meteoroid population, and the cell discharge is timed to give an indication of penetration-hole size and thus of particle size and incident energy. The signal processing, logic, power, and interface circuitry are contained in a housing located in the spacecraft equipment compartment.

This type of penetration detector has been flown on a number of space-craft. The above description is based on the instrument of Pioneers 10 and 11 (Ref. VII-27).

The engineering parameters are summarized below:

Mass:	1.8 kg total (cell banks, electronics, and interconnecting cabling.)
Power:	1 W (average)
Dimensions:	12 cell banks each 20.3 x 30.5 cm 1 electronic box 7.6 x 7.6 x 7.6 cm
Bit rate:	200 bit/s (average)

VIII. INSTRUMENTS NOT INCLUDED IN RECOMMENDED PAYLOAD

A number of other instruments were considered during this study which are not included in the recommended payload. Some of these are discussed in this section.

A. LYMAN-ALPHA PHOTOMETER; D/H RATIO

The addition of a Lyman (Ly) alpha photometer to the bus payload as a supplement to the UV spectrometer (UVS) has been considered. The potential advantages offered by a gas cell instrument of the Mariner-Jupiter-Saturn (MJS) type are: 1) H-atom velocity and temperature measurement and 2) D/H ratio measurement. Both the UVS and a Ly alpha photometer are capable of obtaining spatial resolution on the comet for these measurements although the field of view of the photometer (approximately 0.05° x 1.5° for the MJS instrument) may give somewhat better results.

The real advantage of the gas-cell MJS-type Ly alpha photometer is the capability to measure line shape at 0.10 Å - 0.01 Å resolution. For atmospheric lines, this feature works because the H and O lines are narrow: less than 0.02 Å wide for temperatures less than about 3000°K. It appears, however, that auroral lines arising from H atoms produced in the photodissociation process can be more than 1 Å wide because of the very large kinetic energies released. These are the type of lines most likely to be observed in a comet, since the H atoms are almost certainly produced by photodissociation. For lines as broad as 1 Å, the H/D ratio cannot be measured (H = 1215.66 Å, D = 1215.33 Å), Doppler shifts ($\sim$ .05 Å) cannot be measured, and the line profile is related more to the dissociation process rather than to the ambient temperature.

Some recent work, however, (Ref. VIII-1) indicates that the hot H atoms formed by the photodissociation processes are rapidly thermalized. H-atom velocities as low as 5 km/sec have been observed for the comet Tago-Sato-Kosaka. For velocities this low, the Ly-alpha photometer may be capable of determining a deuterium abundance for sufficiently high D/H ratios ($>10^{-5}$). More observations from earth orbit might be valuable before this possibility can be adequately assessed. The source density and radial velocities of H atoms can be deduced from cometary isophotes measured by the spacecraft UVS.

B. INFRARED SPECTROMETER AND RADIOMETER

Possible objectives for a spectrometer are

(1) Detection of emission features from parent molecules (H_2O, NH_3, CH_4, etc.) in the thermal infrared.

(2) Detection of absorption features from parent molecules by viewing Sun through coma, or by observing reflected sunlight.

(3) Relative abundances of parent species from (1) or (2).

(4) Reflection spectroscopy of solid materials (especially the surface of the nucleus) for identification of ices and silicates, etc.

For a radiometer:

(1) Temperature measurement of the nucleus.

(2) Optical thickness profiles of the coma.

(3) Angular distribution of reflected and re-emitted solar energy.

1. Spectrometry

Existing spaceworthy infrared spectrometers have the following problems

when they are considered for the above objectives on the proposed mission:

(a) The minimum detectable abundances are too high. Consider H_2O, which is probably the most abundant volatile in all comets (refs. VIII-2, VIII-3, VIII-4). The maximum path length is obtained either by viewing the sun through the center of the comet or by looking at sunlight reflected from the nucleus. In either case, the total abundance of water vapor along the line of sight is the same, and can be calculated if the rate and velocity of release of H_2O molecules from the nucleus and the characteristic distance for their dissociation by solar radiation are known. Taking these data from Ref. VIII-2, we find a column abundance of 10^{-2} precipitable μm. From similar calculations, Ip and Mendis (ref. VIII-4) find values in the region of 1 precipitable μm for the much larger and more active comet Kohoutek (1973 f). The value for Encke is well below that which could be detected with existing instruments, and even that for Kohoutek is marginal. The modifications needed to obtain the necessary increase in sensitivity on a spacecraft are beyond the current state of the art.

(b) The dwell times required to obtain spectra are typically of the order of tens of seconds and are therefore incompatible with the spacecraft spin rate (2 rpm).

(c) The instruments are in general bulky, massive and expensive. While (c) can be tolerated and (b) overcome by despinning, (a) would seem to rule out infrared spectroscopy for objectives (1) through (3).

Now consider the possibilities for reflection spectroscopy of solids. The possible targets are (1) the nucleus and (2) the cloud of dust and icy grains which surrounds it. Adopting the criterion that the nucleus should be resolved first at a distance of 5000 km, a field of view of not more than

0.3 mrad ($\sim 0.017°$) is required. The motion of the spacecraft sweeps the field of view across the background at such a rate that the nucleus fills this field of view, if it does so at all, for only about 1.5 msec. The small field of view and short dwell time make infrared spectroscopy of the nucleus energetically unfeasible. Also, the forward velocity of the space-craft is so high that successive sweeps are not contiguous. In fact, the probability of any swath including any part of the nucleus is only about 1% (see fig. VIII-1).

The target could be ~ 100 times larger if an extended, optically thick halo is present. Then the field of view and dwell time could be increased to $\sim 1°$ and ~ 100 msec respectively, making the objective energetically feasible at low resolution over a limited spectral range. In ref. VIII-2 the geometrical optical thickness at the center of Encke's halo is computed to be in the range 1 to 10^{-4}. This means that the probability of the halo being transparent to infrared radiation is high. The effect is to reduce the signal intensity by a factor which is most probably $\sim 10^{-2}$. Again we conclude that, while infrared spectroscopy of a large and active comet may be marginally feasible, it is not likely to succeed on Encke except possibly for approaches to ~ 100 km or platforms with complex pointing guidance, unless cooled detectors are used (see below).

2. Radiometry

Radiometry to determine the temperature of the nucleus is more easily attempted than spectrometry because a single broad spectral pass band can be employed to maximize the throughput, and the instrumentation is relatively simple. Energy is still a problem, however, because the trajectory and high spin rate restrict the field of view and dwell times useable to ~ 0.3 mrad
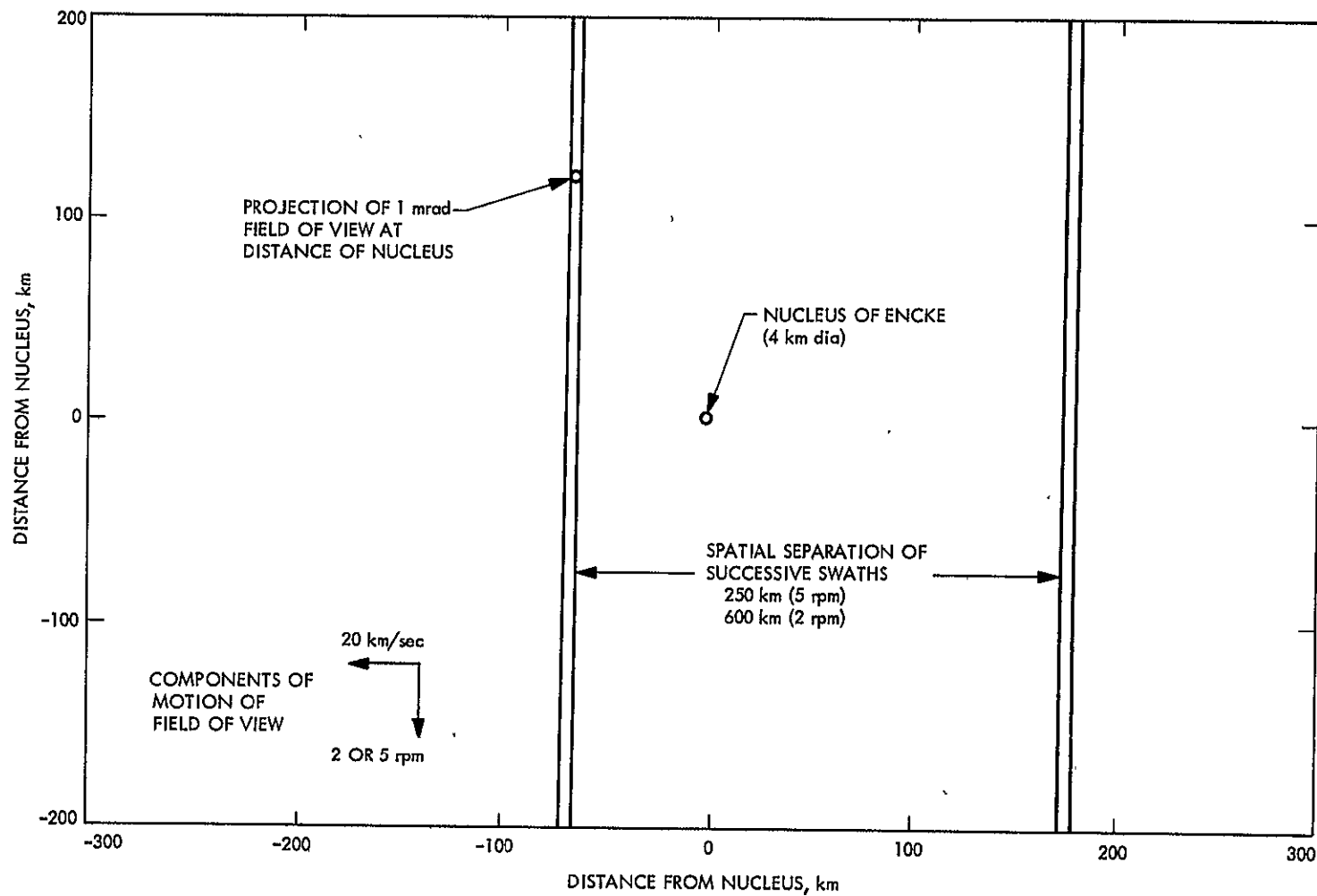
Figure VIII-1. Scans with a 1 mrad. field of view at a distance of 5000 km from the nucleus.
To scale for a 5 r.p.m. spin rate and 20 km/sec relative velocity.

and 2 msec, respectively, as before. We calculate approximately that, using uncooled detectors, a telescope of 50 cm diameter would give a useful signal-to-noise ratio. The biggest problem here is that of pointing the instrument accurately at the target.

In order to perform useful quantitative radiometry, it is essential that the instrument should be able to resolve the nucleus. Otherwise, uncertainties in the fraction of the field of view filled, and the variation in sensitivity of the radiometer across its field of view, give the results a very dubious validity. Attempts to estimate the filling factor, orientation and location of the target as it is smeared across the field of view by using the imaging system are unlikely to be satisfactory and are not recommended. This is especially true if the source is diffuse due to contributions from dust particles and icy grains surrounding the nucleus. Finally, the scientific usefulness of a single mean nuclear temperature, even if it could be measured with moderate precision, is not very high unless the surface is homogeneous.

The arguments presented above and in Figure VIII-1 concerning the probability of the nucleus ever filling the field of view, if guidance is not available, apply equally here. The results for the probable optical thickness of the coma also apply: it is unlikely that a measurable signal will be obtained from the coma except when viewing the nucleus directly.

3. Possible Mission Improvements

The above discussion indicates that no infrared science is feasible with the baseline mission. We now consider the potential advantages of reducing the approach distance, adding an instrument pointing guidance system, and using cooled detectors.

(a) Approach Distance: Reducing the approach distance has the advantage of increasing the angular size of the target. We can make use of this by either (i) increasing the field of view and the dwell time

and so increasing the signal/noise ratio or (ii) keeping the field of view small and increasing the chance that the nucleus can be resolved without guidance. Option (i) is not realistic because the probability of resolving the nucleus is vanishingly small for any approach distance, even though the S/N can be raised to a useful level with a modest telescope (Figure VIII-2). Considering option (ii), if the field of view is fixed at 0.3 mrad (implying the use of a large telescope to obtain adequate S/N) then the probability that the nucleus will be resolved is a <u>maximum</u> of

$$p = \frac{ds}{v} \times 100\%$$

d = diameter of nucleus ≈ 5 km

v = spacecraft velocity ≈ 18 km sec^{-1}

s = spin rate ≈ 0.033 sec^{-1}

or less than 1%. Close approach in itself, then, does not guarantee success; it is necessary also to make sure that the instrument is looking in the right direction when the nucleus goes past.

(b) Instrument Pointing Guidance

If it could be assumed that some kind of servo system was installed on the spacecraft to keep the instrumentation pointing at the nucleus, for example if the instrument views along the spin axis and this is aimed directly at the nucleus, then the curves of Figure VIII-2 apply. Figure VIII-3 shows the pointing accuracy (this is just one-half of the angular size of the nucleus as a function of distance) and the slew rates which are required. The requirements are very stringent.

(c) Cooled detectors

The arrangement of the spacecraft spin axis along the sun-comet line allows the instruments to remain permanently in the shadow of the spacecraft. Cooling of the infrared detectors would then be feasible by the relatively straightforward and inexpensive procedure of radiation
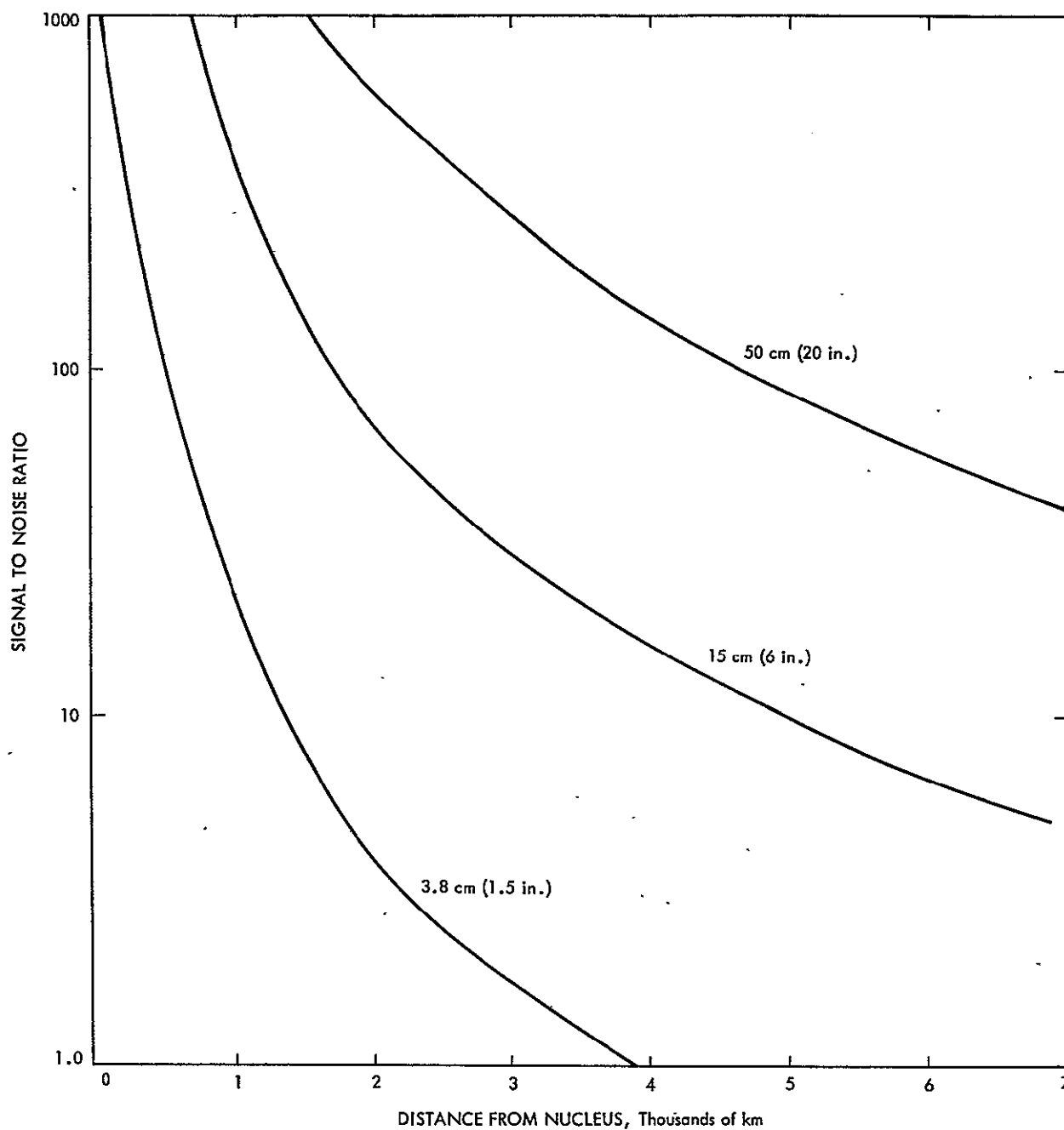
Figure VIII-2. Maximum achievable S/N ratio as a function of approach distance for a broad-band (4-100 μm) radiometer with uncooled detectors. The curves assume that the field of view and dwell time are matched to the maximum angular size of the nucleus, so are upper limits since trajectory uncertainties prevent this from being done in practice. The parameter is the telescope aperture.
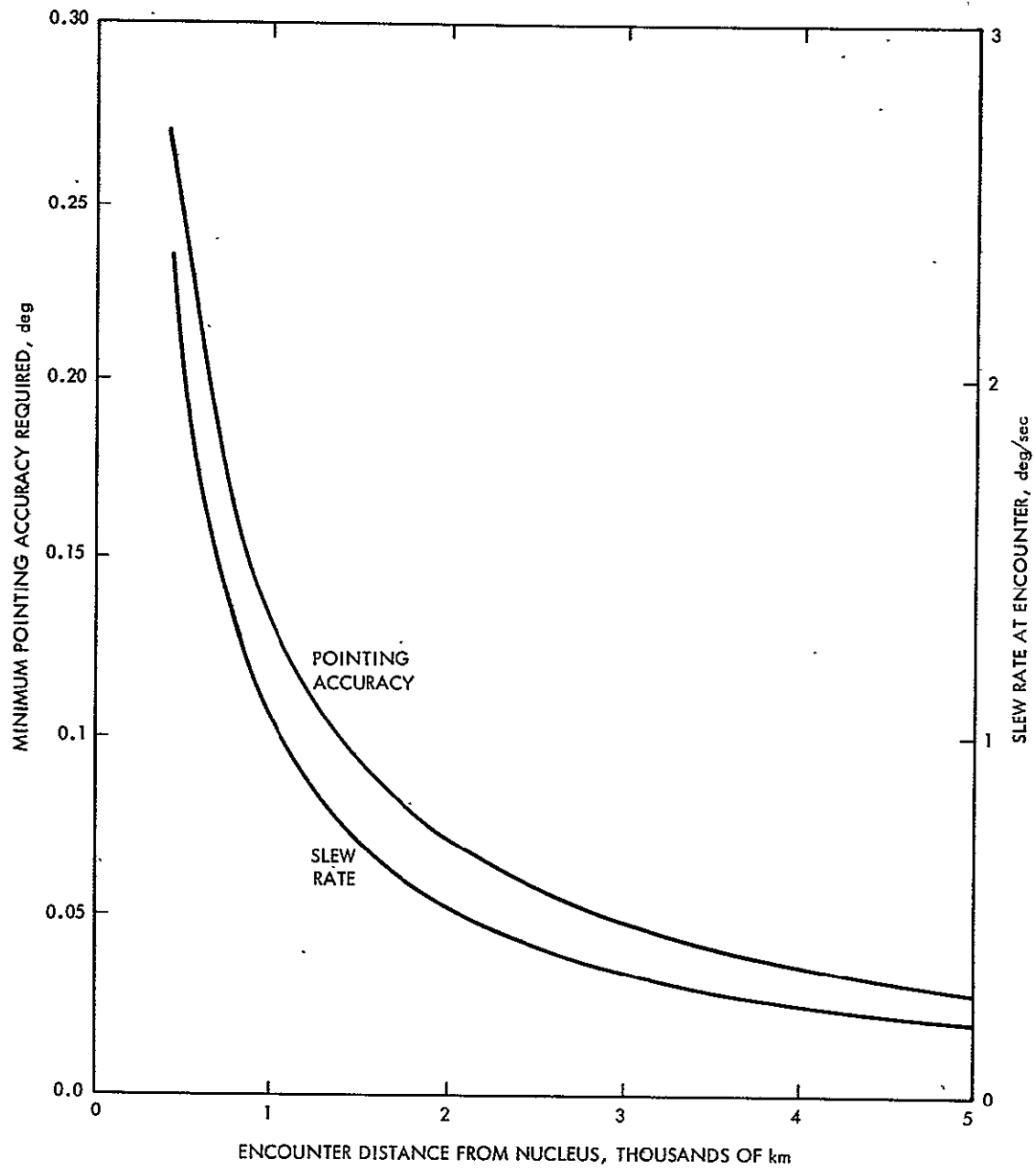
Figure VIII-3. Requirements for pointing accuracy and slew rate of an infrared
instrument, as a function of encounter distance (distance of
closest approach).

to space. The main price which would be paid is the addition of an extra ~ 1.5 kg for the cooler. For the radiometric experiment, this is not very helpful since one must either cool to ~ 4 K, which is not realistic, or restrict the spectral bandpass to the HgCdTe-sensitive region ($\lesssim$ 15 µm), which offsets the gain in S/N. For a near-infrared spectroscopy experiment, however, performance is improved by about an order of magnitude, due to increased detector sensitivity, by cooling to ~ 193 K. This is enough to make low (~ 2%) resolution spectroscopy energetically feasible with a modest aperture telescope (~ 15 cm, 6 in.) over the wavelength range 0.7 to approximately 4 µm. Provided qualitative and not quantitative spectroscopy is acceptable, the pointing problem could be overcome by using a field of view which is large enough so that the nucleus is always viewed in spite of the pointing uncertainty. Qualitative spectroscopy is unlikely to identify any parent molecules, by the argument presented above. It could, however, possibly identify the solid condensates on the nucleus if these are exposed. H_2O, H_2S, NH_4SH, NH_3, CH_4 and other interesting condensates all have spectral features in the 0.7 to 4 µm range. Infrared spectra of solid bodies are, however, notoriously difficult to interpret unambiguously. Experience with spectra of asteroids and the Jovian moons, for example, shows that the broad nature of the spectral features and the fact that they are substantially modified if the sample is impure, greatly complicate the analysis and a confident diagnosis is rarely possible. Another important point is that the instrument needed at Encke would have to be developed as no suitable flight instrument exists. Also, the energy flux from the nucleus would be high enough to obtain good data for only about 5 minutes before encounter; this is enough time for only one or two complete spectra. An estimate of the total size and weight of the instrument, based on a design study of a similar device for MJS, would be 30 x 25 x 25 cm and 7 to 8 kg. All

things considered, this experiment is not recommended as cost effective.

4. General

Assuming an approach distance of 5000 km, a spacecraft spinning at 2 rpm and uncooled detectors, neither infrared radiometry or near-infrared spectroscopy appears feasible. The problems are (i) the difficulty of pointing the narrow field of view accurately enough, (ii) the probable absence of an optically thick inner coma, (iii) the probable low column abundance of the species we want to detect, and (iv) energy limitations.

If the spacecraft spin axis is aligned along the sun-nucleus direction and the spacecraft is targeted as accurately as possible at the nucleus, the situation improves for spectroscopy but not for radiometry. The nucleus can be held in the field of view by making the latter sufficiently large and dropping the requirement that the nucleus should fill the field of view, and the detectors can be cooled by radiation. Low resolution qualitative spectroscopy of the nuclear surface is then energetically feasible. The experiment is not recommended on the grounds that the instrument would be quite large and heavy, and would be a new development, while the value of the results to be obtained is rather uncertain.

Qualitative radiometry is not useful and the pointing problem for an infrared radiometer is very difficult unless the encounter velocity is greatly reduced. It makes essentially no difference which way the spin axis of the spacecraft is oriented; some active pointing scheme capable of the precision described in Figure VIII-3 would be needed in any case.

C. VISUAL SPECTROMETER

High spectral resolution in the visible does not seem necessary; it can be obtained from earth. For good spatial resolution in various

visible bands, the Imaging Photometer with interchangeable spectral
filters should perform well.

D. ELECTRIC FIELD DETECTOR; A. C. MAGNETOMETER

The plasma wave detector provides similar data.

E. HIGH ENERGY CHARGED PARTICLES

Some consideration was given to this class of experiment since it
has been theorized that high energy ($\gtrsim$ 100 keV) electrons (or protons)
at sufficiently high fluxes could account for the ionization levels ob-
served in the coma and tail. Since no source for these energetic particles
has been suggested, it is not felt that sufficient justification exists
to warrant reorganizing the baseline science payload.

F. ALPHA BACK-SCATTERING AND X-RAY FLUORESCENCE

This technique would be of great interest in analyzing cometary
dust. The quantity of dust that can be collected, however, is limited
by the short time the spacecraft can spend near the nucleus, and by the
minimum distance of safe approach on a fast flyby (limited by the high-
velocity dust impacts on the spacecraft). Techniques for collecting dust
at 18 km/sec are not developed. Consequently, these measurements appear
more appropriate for a rendezvous mission.

G. GAMMA-RAY SPECTROSCOPY

This technique would be of interest in remotely analyzing some
elemental compositions of the comet nucleus. Again, the high velocities
mean both a large separation distance from the nucleus and a short in-
tegration time for the gamma-ray spectrum. This technique does not appear
feasible for a fast flyby; it should be suitable for a rendezvous.

H. MICROWAVE SPECTROSCOPY

Microwave spectroscopy might provide data on molecular abundances
in the coma or tail, supplementing UV spectroscopy. At present, it is

not clear that adequate performance could be obtained from a spacecraft instrument at Encke or that the data would be better than those attainable from Earth.

I. RADAR AND RADIO SCIENCE

Even though an active radar system is desirable for measurement of range and of nucleus surface properties, it does not seem possible to include a satisfactory instrument in the Pioneer payload because of the limitations on the weight, power, antenna size, and pointing requirements. Even if the bus will be targeted to encounter the nucleus, the time during which useful data could be collected will be so limited that the scientific pay-off would not be large enough to justify including a radar instrument with the payload.

In principle, a radio occultation experiment could be conducted to measure the plasma content and profile in the comet tail (and coma). It is definitely preferable to have a two frequency communication link between the spacecraft and the ground station, or one wide-bandwidth link (i.e., using chirped pulses). The plasma content and profile could then be determined from the differential dispersion effect of the ionized gas on signals of different frequencies. A detailed study would be required to evaluate the effect of the terrestrial ionosphere and to determine the optimum link frequencies based on a cometary plasma model. However, the estimated peak electron density is less than 600 e/cm^3 (as estimated by Biermann et al., Ref. VIII-5, for a model comet with 10^3 times more gas emission than Encke), and the total column density is estimated on the same basis to be $<2 \times 10^7$ e/cm^2. The indicated densities are not promising for measurements by radio transmission; the best chance would be to detect a sharp gradient (Ref. VIII-6) such as a contact surface if one exists. The radio frequencies needed for these measurements will be

much lower than the S- and X-band expected for deep-space communications. A separate transmitter would therefore be needed with appropriate low-frequency ground receiving equipment. At present, this is not considered warranted.

IX. SCIENCE PAYLOAD INTEGRATION

A. COMPATIBILITY OF PAYLOAD INSTRUMENTS

The primary area of incompatibility among the science instruments is that between the magnetometer and the mass spectrometer. On the bus, a short magnetometer boom will probably be needed in any case to reduce the spacecraft field at the magnetometer to within the specified limits. This technique should be adequate even if a magnetic-sector mass spectrometer is aboard the bus.

On the (optional) separable probe, use of a deployable boom is probably impractical. It complicates the otherwise simple probe and would not be needed if no mass spectrometer were aboard: the probe could be rather clean magnetically. With a magnetic-sector mass spectrometer a magnetometer boom would be needed; with an electric-quadrupole mass spectrometer the boom should not be necessary. Thus, the preferred mass spectrometer for the probe is the electric-quadrupole type. Since it is porbably undesirable (from the cost standpoint) to fly a different type of mass spectrometer on the bus than on the probe, electric-quadrupole instruments appear preferable for both vehicles if a probe is carried. On the other hand, if no separable probe is carried the magnetic-sector mass spectrometer may be best.

The data in Section VII centered on the magnetic-sector mass spectrometer, about which more detailed information is available. It is anticipated that similar performance characteristics could be obtained from an electric quadru- pole mass spectrometer with little impact on the mission if suitable trade- offs between weight and power were allowed. The engineering interface charac- teristics of the two types of instruments are expected to be very similar.

B. PAYLOAD CONFIGURATION

Since this study was limited to science aspects of the mission, it did not evaluate overall spacecraft configurations. To aid in visualization, however, Figure IX-1 has been prepared which shows the suggested science payload on a spacecraft similar to one of those proposed by Martin Marietta (Ref. IX-1).

Such features as the solar-array placement are copied from the Martin Marietta concept, though they probably would not be optimum for the concepts outlined in this study.

C. SPIN RATE

A very low spin rate increases the effective sensitivity of the framing camera and reduces its smear. It increases the spatial resolution of the ultraviolet spectrometer. On the other hand, a high spin rate increases the number of camera frames that can be obtained within a given short distance from the nucleus. The characteristics of the imaging photometer need to be tailored to the spin rate. Performance of the remaining recommended instruments is little affected by spin rate.

At long range, high camera sensitivity is important, and a low spin rate appears desirable. It is understood that a 2-rpm rate is likely to be satisfactory for the spacecraft (Refs. IX-2 and IX-3). This rate is tentatively recommended for the approach.

Spin-rate trade-offs for near-encounter science need more detailed examination. It appears simplest to keep the spin rate fixed for science portions of the mission, and the 2-rpm rate is therefore tentatively recommended for encounter as well as approach. If a serious attempt is made to obtain pictures of maximum resolution by imaging very close to the nucleus, the encounter spin rate should probably be raised to 3-1/3 or 4 rpm to permit more close-in pictures. Still higher spin and imaging rates will overload the data-channel capacity unless some of the proposed characteristics are changed.
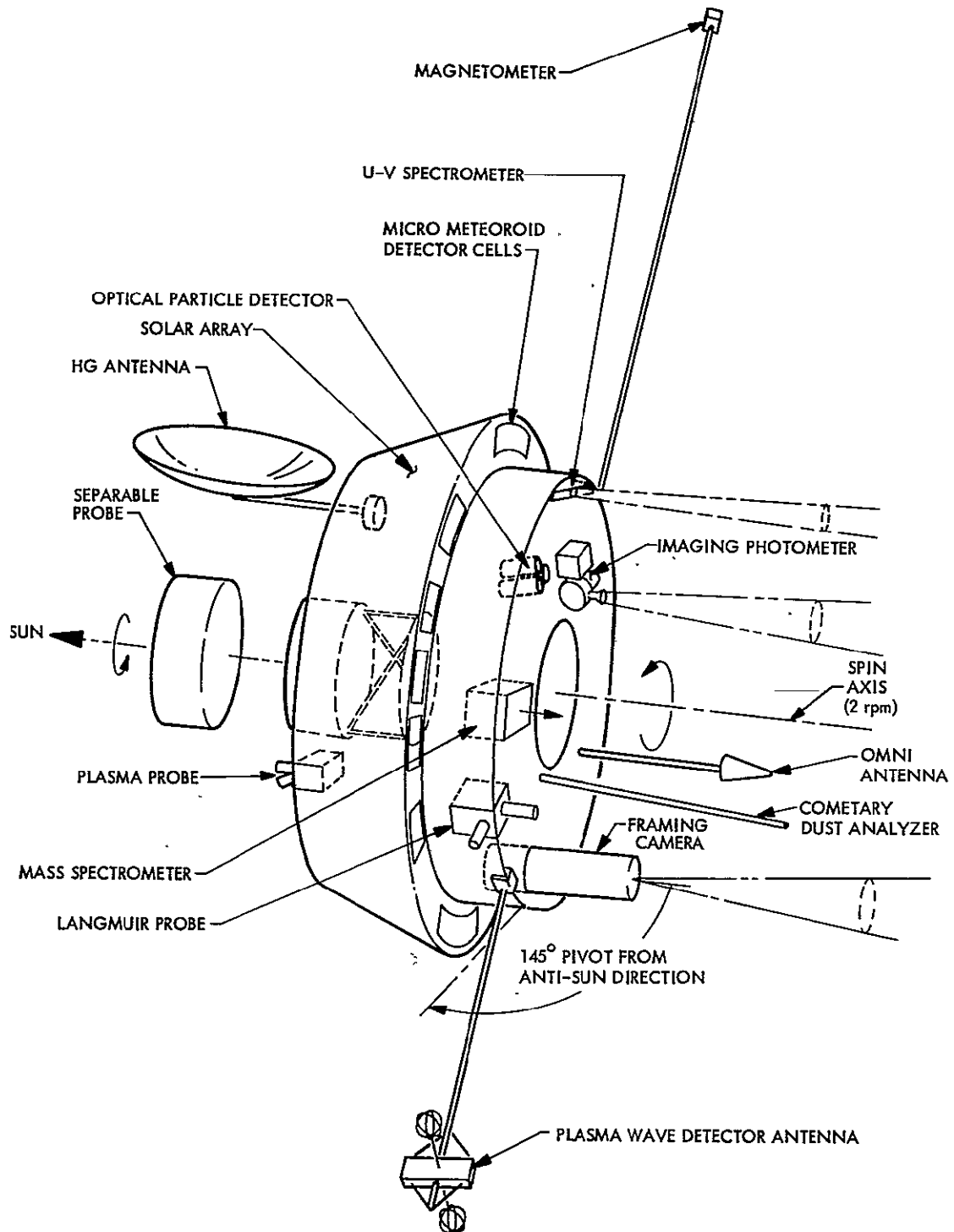
Figure IX-1. A configuration sketch.

D. INTERACTIONS OF PROPULSION AND ATTITUDE CONTROL GAS WITH SCIENCE

Direct chemical analysis of the cometary gas by mass spectroscopy is one of the most important measurements to be made. The primary elemental constituents are expected to be hydrogen, oxygen, nitrogen, and carbon, and the combinations in which these occur are of major interest. It is therefore important not to interfere with analysis of these elements. Although a retarding potential field in the mass spectrometer can be used, as described below, to discriminate against molecules travelling with the spacecraft, it nevertheless would be unwise to dump large quantitites of molecules containing H, O, N, or C, especially within the last few days prior to encounter.

There may be no feasible alternative to the use of maneuver propellants containing the elements listed. It may be possible to reduce interferences by avoiding impurities in the propellants; for example, by using hydrazine without the usual H_2O impurity. For attitude control, cold gas systems using non-interfering gas, such as xenon, seem feasible.

Whether these steps are necessary and practical to avoid interference with the mass spectroscopy should be a subject of further study.

E. INTERACTIONS OF NAVIGATION WITH SCIENCE

It is highly desirable to place the spacecraft within 500 km of the nucleus to permit mass spectrometer measurements of parent molecules. The estimated 3-sigma uncertainty of comet position is 3000 km at encounter on the basis of telescopic observations from Earth during the 1980 Encke apparition, prior to encounter (Ref. IX-4). This is clearly inadequate. Thus, terminal guidance is needed.

In planning navigation and guidance, the target is the nucleus. The nucleus is not at the center of the coma; it may be off by perhaps half the coma radius (Ref. IX-5), here taken as about 20,000 km, but the offset is not

known. A single observation of the coma thus may give the nucleus position
with an uncertainty of 10,000 km. Since most of the cometary mass is in the
nucleus (or the loose aggregation of solids misinterpreted as the nucleus),
tracking over a period of time and fitting the equations of motion will give
the nucleus position more accurately. Nevertheless, tracking of the nucleus
itself will apparently be necessary.

The framing camera described in Section VII has a pixel size of 50 micro-
radians. With proper filtering to discriminate against emission from the
coma, its sensitivity is adequate to detect the nucleus plus halo against the
bright background of the inner coma at a distance of 10^7 km (E-6 days). This is
for a spin rate of 2 rpm and the camera pointed $\frac{1}{2}^o$ from the spin axis. At
10^7 km, therefore, it should be possible to locate the nucleus, in camera
coordinates, to within 500 km, in the plane perpendicular to the line of
sight (essentially, the B-plane). At 2×10^6 km (E - 30 hours),
an image should locate the nucleus (in the B-plane) to 100 km; at 10^6 km
(E-15 hours), to 50 km, in camera coordinates.

Locating the nucleus in camera coordinates is not all that is required.
For terminal guidance it will probably be necessary to relate the observation
to celestial coordinates. The framing television system will detect stars
of magnitude 8 and brighter very close to the spin axis. On the average,
there is ~ 0.5 star of magnitude 8 or brighter per square degree of sky (see
Ref. IX-6). The camera field of view covers only 0.36 deg^2. Stars are there-
fore unlikely to be detected in the same frame as the nucleus. The accuracy
of the coordinate transformation may therefore be fixed by the accuracy with
which sun and rotational reference star (or sun and Earth) directions are
known for the spacecraft. For most spacecraft the accuracy of these direc-
tional references is much poorer than 50 microradians. If, for example, the
celestial references of the spacecraft were known only to $\frac{1}{2}^o$ (8 milliradians),

the nucleus position would not be measured to 500 km (perpendicular to the line of sight) until the spacecraft is within 60,000 km (E-1 hour); if they were known only to 0.2^o, the position would not be measured to this accuracy until within 150,000 km (e-2 hours).

If celestial reference is relatively poor, it may be possible to place the spacecraft within 500 km of the nucleus by making a series of comet observations and successively smaller homing maneuvers as the comet is approached. Maneuvers within the last few hours are undesirable, however, since they interfere with the science measurements. Thus, there is much incentive to use some means of sensing star positions and referencing the nucleus position to them. One possibility is to take many pictures of the sky with the framing camera. At 90° to the spin axis, the camera could detect stars to about magnitude 3.8. There are $\sim$ 400 stars of magnitude 3.8 or brighter in the sky (Ref. IX-7), or 0.01 deg^{-2}, on the average. Assuming random distribution, a 360° rotational sweep with the framing camera at 90° to the spin axis, requiring at least 600 frames and covering 216 square degrees, should detect 2 stars. The large number of pictures required to observe and confirm the star locations makes this approach unattractive. Also, the resulting accuracy would be limited by knowledge of the angle through which the camera was slewed, from comet to stars. An error of 0.03^o (500 μrad) in telemetry of the slew angle would mean that the nucleus would not be located to 500 km until the spacecraft was within 10^6 km (E-15 hours). Moreover, the spin axis might vary by more than 500 μrad during the hours necessary to take the pictures, further degrading the accuracy.
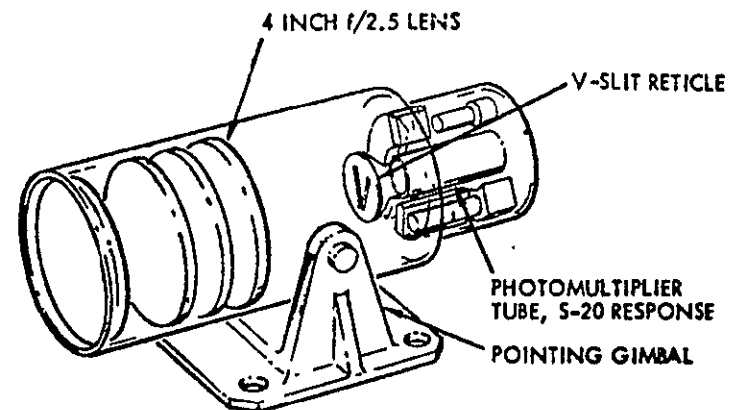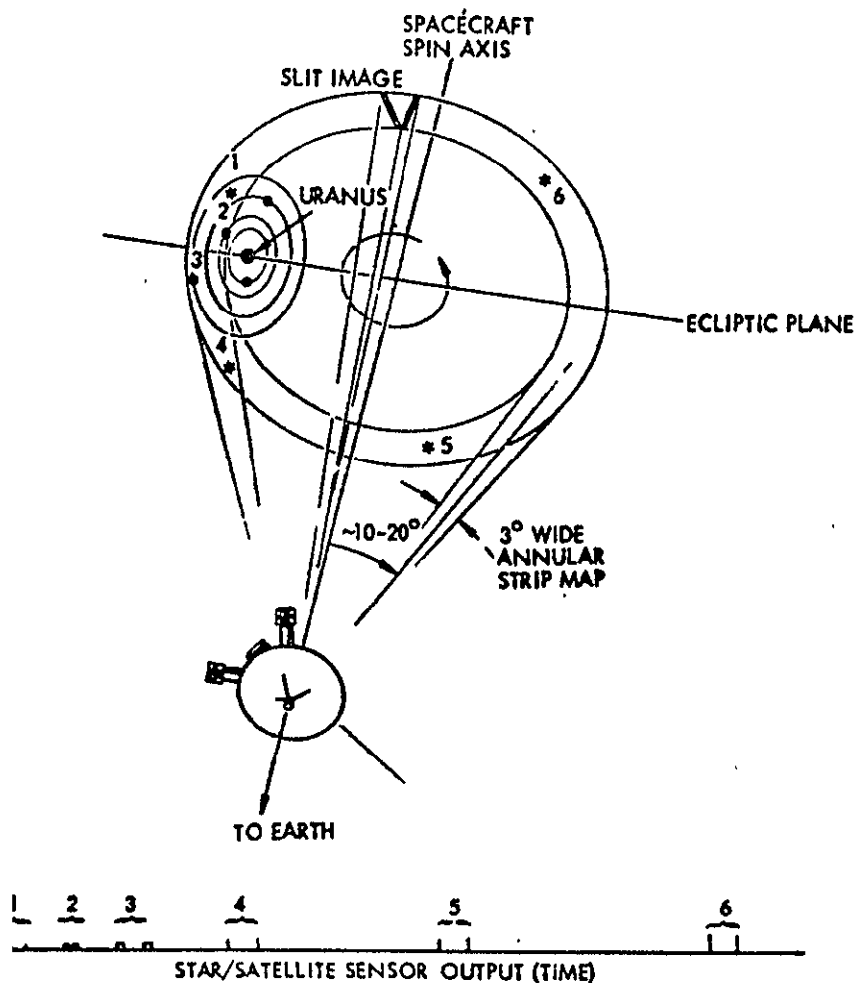
The Imaging Photopolarimeter (IPP) has been suggested as a navigation sensor for Pioneer outer planet missions (Ref. IX-8). At 2 rpm, this instrument can detect stars to about magnitude 3.8. As presently designed (Table VII-3), its spatial resolution is 500 μrad in the imaging mode. The area sampled in this mode is 0.03^o x 14°, or 0.42 deg^2, only slightly greater than

for the framing camera. Hundreds of such scan samples would be needed to find 2 or 3 stars, but the total number of bits transmitted would be much less than if the framing camera did this task.

By inserting a suitable mask in the 0.5° photopolarimetry-mode aperture of the IPP, adding suitable pulse-timing circuits, and making other modifications in the electronics, it should be possible to measure star positions with sufficient accuracy for location of the nucleus to ~ 400 μrad, and to scan an 0.5° x 360° swath during each spacecraft rotation (Ref. IX-8). At 30° from the spin axis, the area scanned in one rotation is 90 deg^2; an average of slightly < 1 star would be detected per scan. By scanning at several cone angles, it should be possible to find several stars. Alternativel optics of the instrument could be enlarged to increase its sensitivity. An accuracy of 400 μrad would permit locating the nucleus, in the B-plane, to 500 km at 1.2 x 10^6 km (E-20 hours).

A V-slit scanning navigational sensor, similar to those used on earth-orbiting spacecraft (Refs. IX-9, IX-10), is also under study for outer-planet Pioneer missions (Refs. IX-11, IX-12). One version (Figure IX-2) is designed to measure directions to better than 100 μrad and its photomultiplier is capable of detecting magnitude 4.0 stars at 5 rpm (Ref. IX-13). Its weight may be as little as 3 kg. It can scan a 3° x 360° strip in each spacecraft rotation, or, at 40° from the spin axis, 700 deg^2. About 500 stars would be detectable in the sky at magnitude 4.0, or perhaps, at 2 rpm, somewhat dimmer. This is equivalent to 0.012 star/deg^{-2}, so the device should locate an average of ~ 8 stars in one spacecraft rotation. The stated 100 μrad accuracy is equivalent to 500 km in nucleus position at 5 x 10^6 km (E-3 days).

The IPP or the V-slit sensor may serve to provide star positions for measurement of the nucleus position; the V-slit sensor seems particularly promising. If the V-slit sensor or IPP cannot itself reliably image the

SPACECRAFT
SPIN AXIS

SLIT IMAGE

URANUS

ECLIPTIC PLANE

~10-20°

3° WIDE
ANNULAR
STRIP MAP

TO EARTH

1 2 3   4   5   6

STAR/SATELLITE SENSOR OUTPUT (TIME)

4 INCH f/2.5 LENS

V-SLIT RETICLE

PHOTOMULTIPLIER
TUBE, S-20 RESPONSE

POINTING GIMBAL

- MINIMUM NUMBER OF REFERENCE
  STARS IS TWO

- STAR PATTERN IDENTIFIED IN
  ADVANCE OF TARGET DETECTION

- STAR MAPPER ALSO ACCURATELY
  DETERMINES SPIN AXIS POINTING
  ON CELESTIAL SPHERE

- PLANET'S SATELLITES ARE PREFERABLE
  AS NAVIGATIONAL REFERENCES:
  SMALLER IMAGE SIZE; MASS CENTER
  DETERMINATION SIMPLIFIED

- INTERFERENCE BY BRIGHT PRIMARY
  IMAGE TO BE AVOIDED

Figure IX-2.   V-Slit Terminal Navigation Sensor as designed for outer planet missions (Ref. IX-12).

cometary nucleus, it could presumably be mechanically mounted to the TV camera so that the nucleus imaged by the TV could be accurately related to star positions sensed by the V-slit sensor (or IPP). To reduce errors in the relative angles, the V-slit or IPP device would probably have to be mounted and aligned to the camera in a fixed position, so it could not be separately scanned in cone angle; this might rule out the idea of using multiple IPP scans to find sufficient stars.

Besides needing navigation to bring the spacecraft to the desired position, it will also be important to know accurately what the position of the space-craft was relative to the nucleus as a function of time for post-flight data reduction; an accuracy of 100 km or better is needed for interpretation of the science data. This presumably should be possible by triangulation from the imaging data obtained during encounter.

If a separable tail probe is carried, it should preferably be launched several days before encounter to keep the deflection maneuver small. For 5000 $\pm$ 3000 km offset between the probe and the bus, performing the deflection maneuver 2 days before encounter requires a velocity increment $\geq$ 30 m/s. Presumably, this would be done by bus propulsion. To design this maneuver, the nucleus position would need to be known, perpendicular to the trajectory, to better than 3000 km at 2 days before encounter. This presumably would be possible from the Earth-based measurements, without on-board observations, many weeks before encounter.

For post-flight analysis of the probe data, an accuracy of 500 km in probe position vs time is needed. This should be possible to obtain from the post-flight information on spacecraft trajectory together with the bus-probe separation velocity.

Clearly, navigation will need serious attention. Navigation is not within the scope of this study, and resources to study it were not provided; the above discussion points out problems, not solutions. In further development of the mission concepts, study of navigation should have high priority.

F. INTERACTIONS OF GUIDANCE WITH SCIENCE

To obtain high resolution pictures of the nucleus, it is necessary to point the camera at the nucleus when at close range, and within the 0.6° field of view of the camera, and to trigger the camera at the proper instant for each frame. If pictures are to be taken very close to the nucleus, the slew rates become very high and, as mentioned in Section VII C, an optical sensor system with onboard control of pointing will probably be needed. If a despun camera platform were employed, the Far Encounter Planet Sensor used by Mariners 6 and 7 could provide a closed-loop scan platform adjustment (Ref. IX-14). For a spinning system, it might be possible to develop analogous on-board pointing control using as sensor the Imaging Photometer or the V-slit device, mentioned in the preceding subsection.

There are also interactions of the mechanical systems of the spacecraft with science instruments. If the camera or other optical instruments are to be kept observing the nucleus during a 500-km flyby, a pointing mechanism that can handle a $126^{\circ}/min$ slew rate will be needed. Furthermore, either the camera will have to take pictures during slew or, if the slew is halted during exposures, the mechanism will have to slew even faster, stop, and then damp out resulting vibrations very quickly.

All of these problems need further study. Particularly difficult may be the decision as to how close to the nucleus imaging should be planned. Several spacecraft systems (mechanisms, attitude control, nucleus sensing, camera pointing) can be considerably simplified if imaging is not planned within 500 km or so of the nucleus. Note that only 2 frames could be obtained

within this distance at 2 rpm, since the spacecraft moves 550 km between frames. Omitting these frames means abandoning the possibility of 2 pictures with pixel size less than 25 m (feature resolution 60 m).

X. SCIENCE OPERATIONS PROFILE

A detailed breakdown of the science timeline is not warranted at this stage of mission definition. A general outline is as follows. Pictures for navigation are not covered here.

After separation from launch vehicle:

> Turn on, for cruise measurements, bus magnetometer, bus plasma probe, optical particle detector, micrometeoroid detector, dust analyzer.

Prior to Encounter - 5 days (E-5 days):

> Other instruments on briefly for calibration, background measurements, and to verify operation. This can be done one instrument at a time. Leave cruise instruments on.

E-5 days (8×10^6 km):

> Framing camera on for occasional pictures of nucleus to verify acquisition and camera operation. Normal rate: 4 frames/day.

E-2 days (3×10^6 km) or earlier:

> Launch flyby tail-probe if carried. Maneuver bus, targeting it for nucleus.

E-48 hr (3×10^6 km):

> Plasma wave detector and bus Langmuir probe on.

E-24 hr (1.5×10^6 km):

> Ultraviolet spectrometer on. Nominal rate: 1 scan/hr.

E-15 hr (1×10^6 km):

> Imaging photometer on in photometer mode, scanning through its spectral filters. Nominal rate: 1 set of scans per hour.

E-5 hr (3×10^5 km):

    Bus mass spectometer on.

E-2 hr (1.3×10^5 km):

    Increase framing camera rate to 1 frame per 5 minutes.

    Increase photometer rates to maximum.

    Increase UVS rate to 4 scan/hr.

E-1 hr (7×10^4 km) or preferably earlier:

    All tail-probe instruments on.

E-1 hr (7×10^4 km):

    All bus instruments to maximum rate.

E+5 minutes (5×10^3 km):

    Framing camera off. (Nucleus will be within a few degrees

    of the sun).

E + 1 hr (7×10^4 km):

    Lower UVS rate to 4 scan/hr.

E + 2 hr (1.3×10^5 km):

    Lower photometer rate to 1 scan per hour.

E + 10 hr (7×10^5 km):

    OK to exhaust probe batteries.

    Bus mass spectrometer of

    UVS and photometer off.

Note: The probe should be designed to provide data until it has exited

from the tail and begun to observe the interplanetary plasma again. This

may be as long as 10 hours after encounter (see discussion of tail passage

in Section V D). The probe instruments should be on and start sending data at least 1 hour before encounter to permit comparison of probe data with bus instrument data over a time interval prior to exposure of the bus to high risk from dust. Thus the probe should have a power supply capable of operating instruments and transmitter for 11 hours. An earlier turn-on, and correspondingly longer-lived power supply is desirable, in that it would provide simultaneous particle and field data from two positions between the shock front and the coma.

XI. PROBLEM AREAS AND RECOMMENDED STEPS TOWARDS SOLUTIONS

A. SCIENCE INSTRUMENT PROBLEMS

1. **Mass Spectrometer**

   Techniques for calibration of the mass spectrometer for neutral particles at velocities around 18 km/sec are not known. Development of such techniques is recommended.

2. **Framing Camera**

   Development towards a charge-coupled flight framing camera is needed. At the appropriate time, after some further development of terrestrial or aircraft CCD framing cameras, development of a spacecraft version should be initiated.

3. **Optical Particle Detector**

   Certain deficiencies have been identified in the instrument flown on Pioneer 10. In addition, adaptations for the Encke mission, such as discrimination against the coma background, will be needed. Development is recommended to correct the deficiencies and make the needed adaptations.

4. **Solid Particle Analyzer**

   Improvement over the Helios instrument is needed with respect to mass resolution and quantitative response. Development in these directions is recommended.

5. **Lyman-Alpha Photometer**

   More data are needed on the line-width of cometary Lyman-alpha emission, especially from Comet Encke, to permit better evaluation of the desirability of flying a Lyman-alpha photometer. Observations from Earth orbit are recommended.

B. SCIENCE INTERFACE PROBLEMS

1. Navigation

Study is recommended of sensors and techniques to permit navigation within 500 km of the nucleus of Encke, for the mission considered in this report.

2. High Resolution Pictures

A study is recommended of the problems and tradeoffs, including spacecraft and mission design and costs, involved in obtaining 100-m (or higher) resolution of the nucleus.

3. Guidance and Pointing

Study is recommended of the possible need for a sensor and for on-board control to point the camera at the nucleus during encounter. If it is concluded that such capabilities are needed, methods of implementing them should also be studied. (This item may overlap Item 2.)

4. Propulsion and Attitude Control Gas

Study is recommended to evaluate whether propellants and attitude control gas, or procedures for releasing them, should be chosen to minimize interference with mass spectroscopy. If so, appropriate techniques for propulsion and attitude control should also be studied.

XII. SUMMARY OF KEY CHOICES

Among the key choices made in the course of this study were the following:

Approach direction	Along sun-comet line
Nominal encounter	0.53 A.U. from sun
Nominal encounter velocity	18.3 km/sec
Spacecraft flyby distance	< 500 km from "nucleus"
Terminal guidance	Required
Science instruments despun	None
Suggested spin axis orientation	Toward sun
Separable probes	One, as optional add-on
Probe function	Tail data if bus is lost
Probe flyby distance (optional)	5000 km nominal
Tape Recorder	None
Science payload, spacecraft	Framing camera, CCD
	Imaging photometer
	Ultraviolet spectrometer
	Mass spectrometer
	Particles and fields instruments
	Dust detectors and analyzer
Science payload, optional probe	Mass spectrometer
	Particles and fields instruments

A further summary is given at the beginning of this document, under "Summary and Conclusions."

ACKNOWLEDGMENTS

APPENDIX A

IMAGING SENSOR TRADE-OFFS

Several studies of imaging from a spinning spacecraft have been conducted. Some of these are listed in the references. Of approximately twenty candidate sensors, there are three general categories:

I.   Non-integrating detector scanners; e.g., image dissector.

II. Integrating detector line array scanners; e.g., array of PMT's.

III. Integrating full-frame sensors; e.g., vidicon.

Category I instruments are not suitable to the Pioneer Encke Mission because of the high angular image motion near encounter. Far from encounter, the angular resolution degradation and geometric distortion are severe. Category II instruments are complex in design and exhibit sensor spacing requiring long focal length telescopes to meet the resolution criteria. Only the CCD linear array may be feasible; however, Section VII A suggests huge data readout rates ($\sim 10^7$ bps) are required for moderate spacecraft rotational velocities. Only integrating full-frame sensors are, therefore, considered practical for the Comet Encke flyby missions.

The maximum exposure time for a framing camera is determined by the spacecraft rotational rate and the science resolution criteria. Assuming image motion compensation, the maximum exposure is given by:

$$t = \frac{50 \ \mu r \quad \times 10}{R \times 10^6 \ \mu r/sec}$$

at 10 rpm = 5×10^{-4} sec

Where 50 μr = Minimum resolution element

$\times 10$ = IMC Compensation

R = Spacecraft rotation rate (radians/sec)

Figure A-1 displays various sensor thresholds (S/N = 10) and the predicted brightness of an image of the Comet Encke nucleus (at 0.53 AU sun
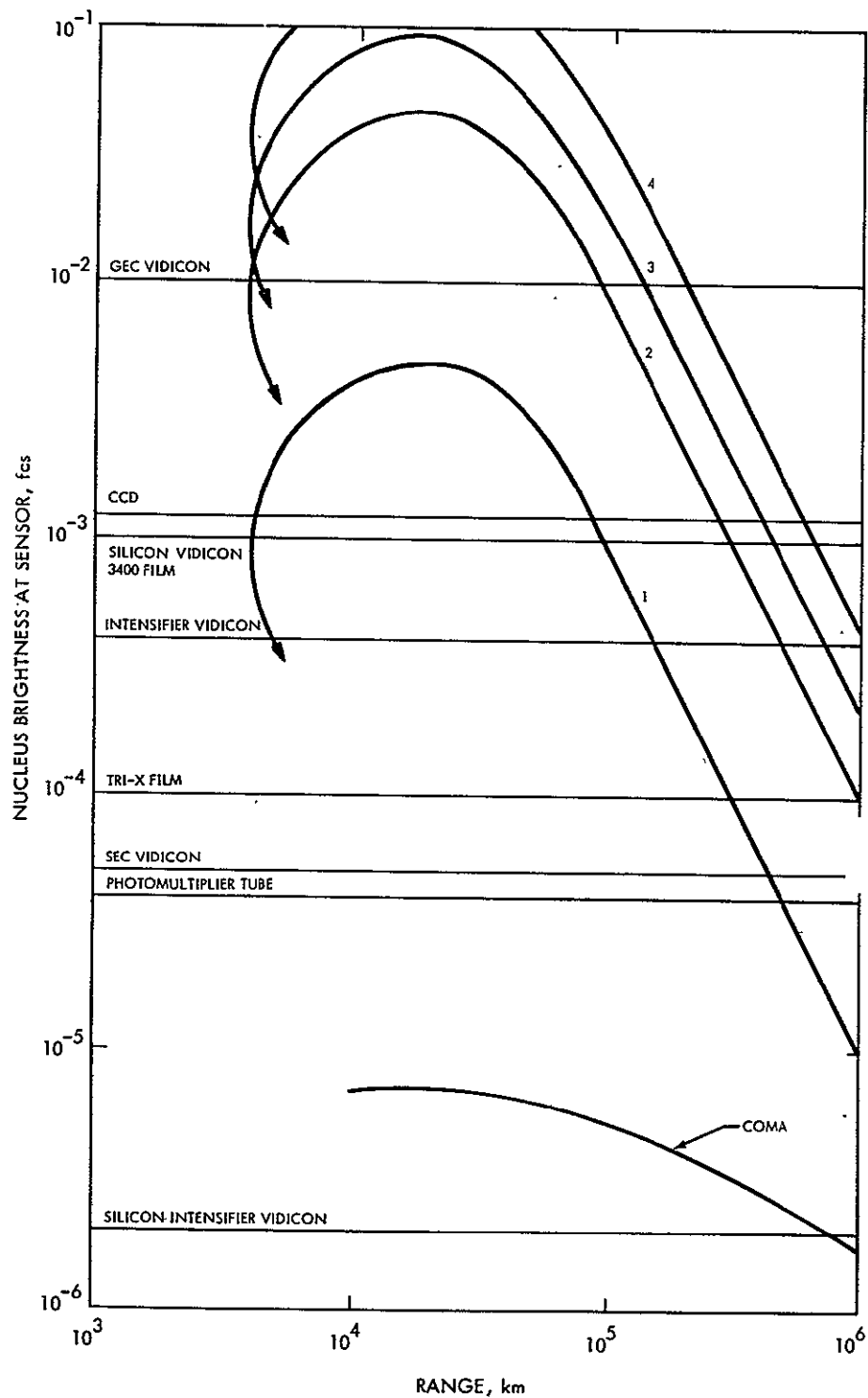
Figure A-1: Sensor thresholds (S/N = 10) vs. comet brightness.
1. 10 rpm; without IMC; f/2.35   2. 10 rpm; with IMC; f/2.35
3. 5 rpm; with IMC; f/2.35   4. 5 rpm; with IMC; f/1.5
Coma: 5 rpm; without IMC; f/2.35; 0.3 mrad from nucleus

distance) produced by a Mariner 9, f/2.35, 50 cm focal length telescope.
Discussion of the advantages and disadvantages of each of these sensors
may be found in the references and will not be dealt with here. Only the
solid-state camera combines minimal weight, power, and cost characteristics
with sensitivity, resolution, and simplicity.

APPENDIX B

CURRENT CHARGE-COUPLED DEVICE DEVELOPMENT

Experimental work with solid-state cameras is currently being pursued at a number of institutions; e.g., Fairchild Space and Defense Systems, Texas Instruments, RCA, and Bell Telephone Lab; JPL is presently testing a 1 x 500 array CCD camera for possible Pioneer-Venus application. A 64 x 64 two-dimensional array camera will also be tested in the near future. Several study contracts are being monitored by JPL and potential program applications are being reviewed; e.g., Large Space Telescope proposal (Ref. B-1).

Fairchild is presently the leading commercial producer of solid-state cameras. They are developing a 400 x 400 array for the U. S. Navy and are studying IMC techniques for the DOD. Their 100 x 100 element camera is now readily available (see Figure B-1). Development within the next few years relevant to the Pioneer Encke Mission is likely to include: larger arrays, extended ultraviolet response (reverse illuminance), and image-motion compensation by image transfer.
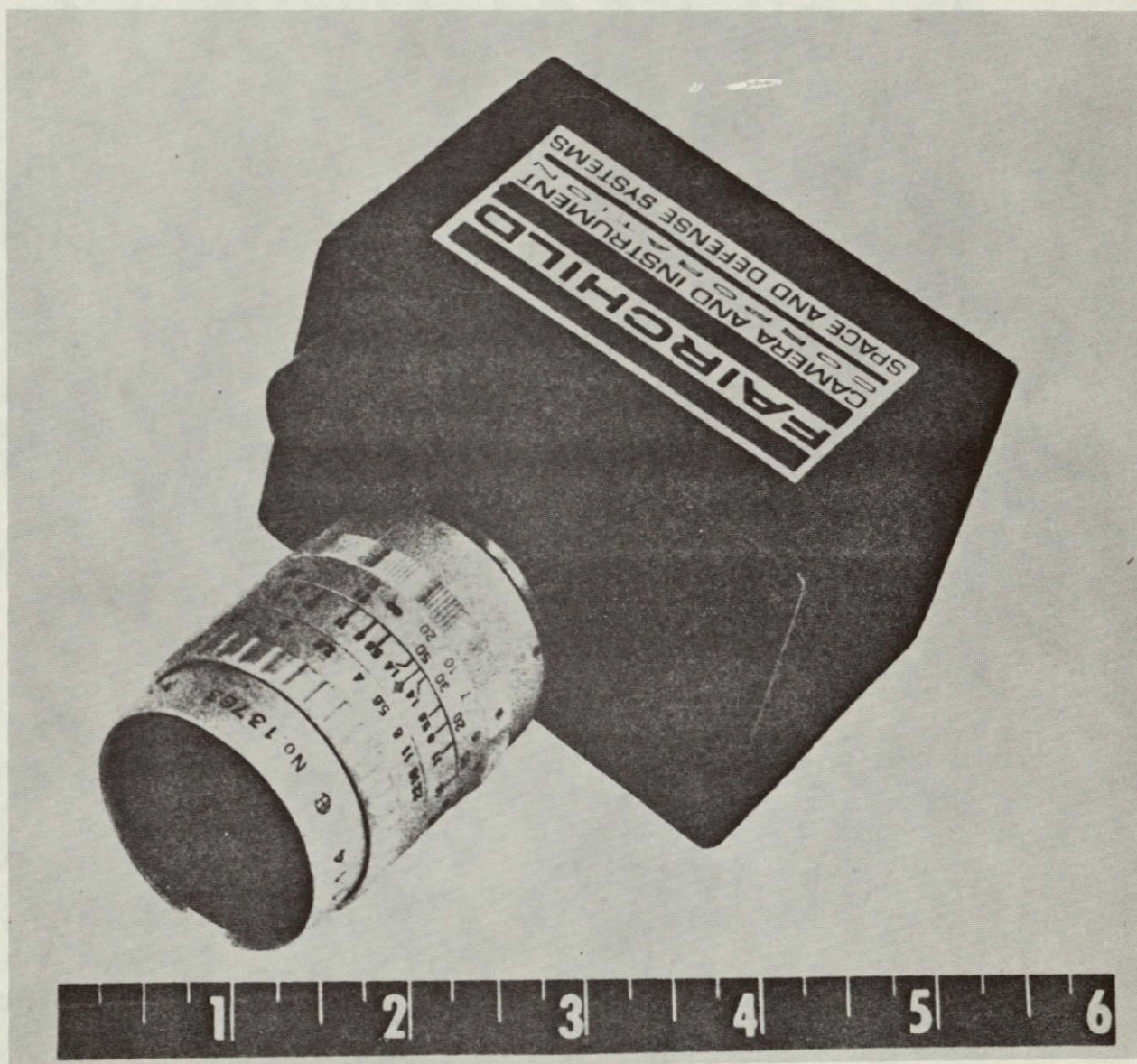
Figure B-1: CCD Camera, 100 x 100 element.

APPENDIX C
IMAGE MOTION COMPENSATION DEVICE

The following image-motion compensation device was initially proposed for a Viking camera design. The discussion has been extracted from Reference C-1.

MECHANICAL IMAGE MOTION COMPENSATION MECHANISM

The electromechanical system proposed for Image Motion Compensation (IMC) for a 25mm vidicon TV camera is shown in Figure C-1.

For simplification and reliability, two types of mechanisms are used - rotation and nod. This simplification is possible since the attitude of the spacecraft as it crosses a planet is nearly constant and only minor corrections are required to a rotational system to keep a nod axis at right angles to the line of flight. IMC can then be accomplished around a single axis (nod).

Rotational System

The system chosen to keep the nod axis at right angles to the line of flight is a conventional type system. A torque motor, gear train, angle sensor and bearing are the main components. Since this mechanism is used to maintain a heading and requires only infrequent small changes to maintain that heading, the system components were chosen for minimum weight and power consumption, speed and servo accuracy being of less importance. If the position sensor is mounted on the rotational axis as shown in Figure C-1, component and manufacturing tolerances are also relaxed.

Nodding System

The system chosen to compensate for motion of a scene as the spacecraft crosses a planet "nods" a flat quartz disc through a small angle. The nod servo system, unlike the rotational system, requires accurate rate and position control.

The components for the nod mechanism were chosen for their trouble free and anti-contamination characteristics. No bearings, electrical brushes, gears or lubricants are used. All the rotating components are bearingless; they are supported by two flexural pivots (torsion bars). See Figure C-1.
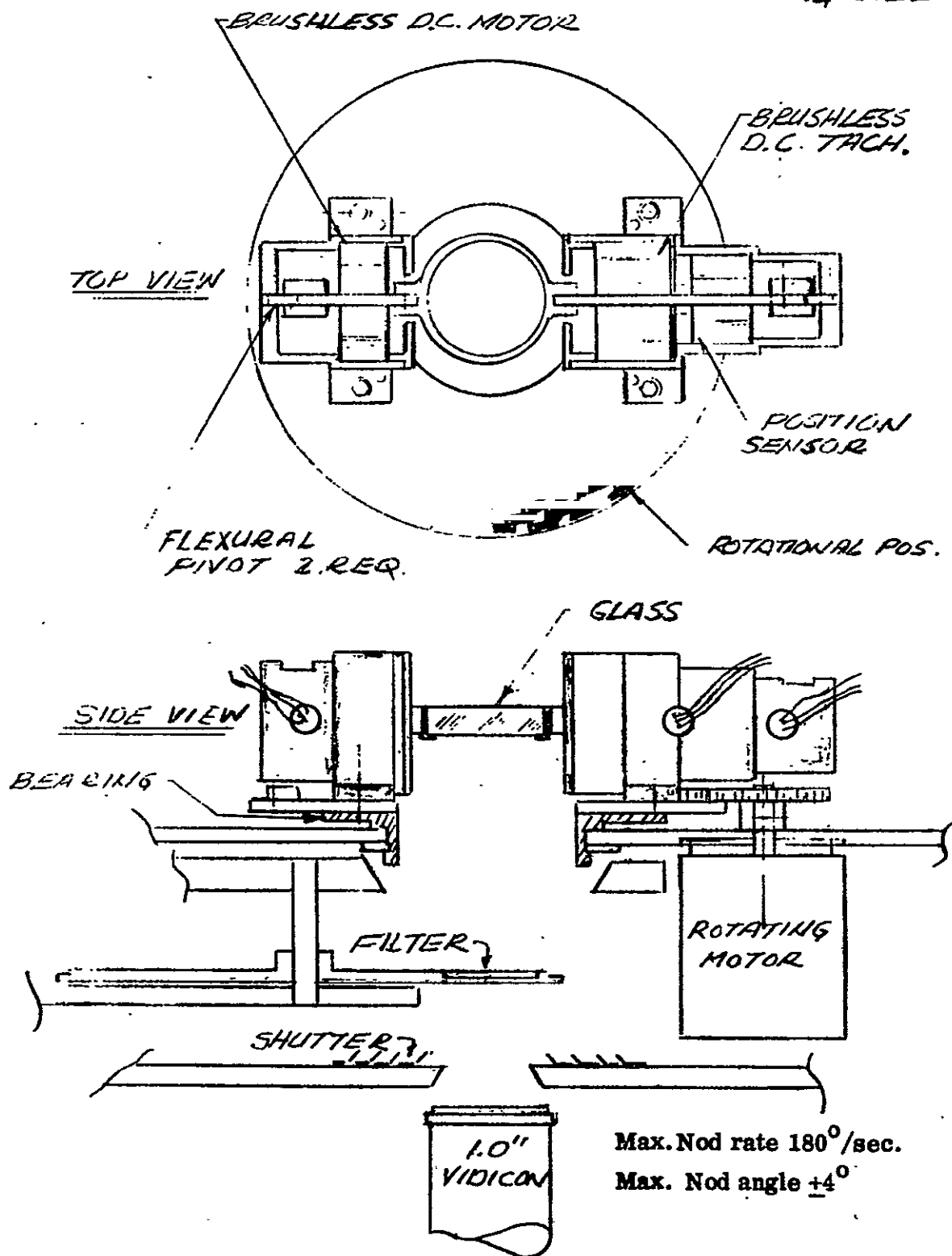
Figure C-1:   Mechanical Image Motion Compensator

The design parameters for the nodding mechanism are:

1. Maximum nod rate $180^{\circ}/\text{sec}$.

2. Maximum nod angle $\pm 4^{\circ}$.

3. Minimum weight.

4. Long life.

Discussion of Nod System Components

The components chosen for the nod mechanism are zero friction devices developed for gyro stabilized aerial camera platforms and have been found dependable in operation.

The lack of gearing and bearings enables the mechanical system to achieve a high mechanical stiffness and, consequently, higher resonant frequencies resulting in superior servo performance. The elimination of gear backlash and bearing runout also provides increased accuracy and a higher resolution system.

The image displacements available are a function of the slab thickness and the total tilt. Table C-1 indicates the magnitude of displacement obtained with various combinations using a quartz slab. Using half-angle pre-positioning, the displacements are effectively doubled. The values are derived from the relationship.

$$D = \frac{A}{\cos (\sin^{-1} [\sin I / n])} \sin (I - \sin^{-1} [\sin I / n])$$

where

D = Image Displacement (mm)
A = Slab Thickness (mm)
I = Tilt Angle (Deg.)
n = Index of Refraction

		$\lambda = 350$ nm n = 1.4771	$\lambda = 550$ nm n = 1.4598	$\lambda = 800$ nm n = 1.4532
A = 4mm	I = 1°	D = 22.55 μm	D = 21.99 μm	D = 21.77 μm
	2	45.12	44.00	43.57
	3	67.72	66.04	65.39
	4	90.37	88.13	87.26
	5	113.09	110.29	109.20
	6*	135.89	132.53	131.23
6mm	1	33.83	32.99	32.66
	2	67.68	66.00	·65.35
	3	101.58	99.06	98.09
	4	135.56	132.20	130.90
	5*	169.64	165.44	163.81
	6*	203.84	198.80	196.84
8mm	1	45.10	43.98	43.55
	2	90.24	88.00	87.13
	3	134.45	132.08	130.78
	4*	180.75	176.27	174.53
	5*	226.18	220.58	218.41
	6*	271.79	265.06	262.45

*Exceeds 0.5 pixel chromatic image separation.

Table C-1. Image Motion Compensator Displacements

REFERENCES

Section I

I-1. Martin Marietta Corporation, "Study of 1980 Comet Encke-Asteroid
      Missions using a Spin-Stabilized Spacecraft".   NASA-CR-114670
      and 114671.   Report to N.A.S.A. Ames Research Center.   Contract
      NAS 2-7564.   Denver, 1973

I-2. F. W. Taylor, C. M. Michaux, and R. L. Newburn, Jr., "A Model of
      the Physical Properties of Comet Encke", JPL Tech. Rpt. 32-1590, 1973.

I-3. D. Clay, C. Elachi, C. E. Giffin, W. Huntress, L. D. Jaffe, R. L.
      Newburn, R. H. Parker, P. W. Schaper, F. W. Taylor, T. E. Thorpe,
      B. Tsuritani, "Science Rationale and Instrument Package for a Slow
      Flyby of Comet Encke", JPL Doc. 760-90, 1973.

I-4. D. F. Bender, K. L. Atkins, C. G. Sauer, Jr., "Mission Design for
      a 1980 Encke Slow Flyby using Solar Electric Propulsion", presented
      at AAS/AIAA Astrodynamics Conf., Vail, Colo., 1973.   R. L. Newburn
      and J. B. Weddell, "Encke Flyby Science Package", Paper 73-1125,
      Am. Institute of Aeronautics and Astronautics, New York, 1973.
      J. H. Duxbury, "An Integrated Solar Electric Spacecraft for the
      Encke Slow Mission", Paper 73-1126, ibid. K. L. Atkins et al.,
      "A Study of the Solar Electric Slow Flyby of Comet Encke in 1980",
      JPL Doc. 760-90 Rev. A, 1974.

Section I

I-5. R. W. Farquhar, D. K. McCarthy, D. P. Muhonen, and D. K. Yeomans, "Mission Design for a Ballistic Slow-Flyby of Comet Encke 1980", Paper 74-219, Am. Institute of Aeronautics and Astronautics, New York, 1974.

Section III

III-1. R. A. Lyttleton, "The Comets and Their Origin", Cambridge, 1953.

III-2. Comet and Asteroid Mission Study Panel, "Comets and Asteroids. A Strategy for Exploration", NASA TM X-64677, 1972.

III-3. D. Clay, C. Elachi, C. E. Giffin, W. Huntress, L. D. Jaffe, R. L. Newburn, R. H. Parker, P. W. Schaper, F. W. Taylor, T. E. Thorpe, B. Tsuritani, "Science Rationale and Instrument Package for a Slow Flyby of Comet Encke", JPL Doc. 760-90, 1973.

Section V

V-1. G. R. Hook, E. G. Howard, J. M. van Pelt, W. J. Bursnall, "Study of 1980 Comet Encke-Asteroid Missions using a Spin-Stabilized Spacecraft", Martin Marietta Corp., MCR 73-180, "Mid-Term Review" and MCR 73-260, "Final Oral Presentation", 1973.

V-2. K. Wurn, "Die Natur der Kometen", Mitt. Hamburger Sternw. 8, No. 51, 1943, as quoted by N. Richter, "The Nature of Comets", transl. and rev. edition, p. 58, Methuan, London, 1963.

Section V

V-3.   Z. Sekanina, "Secular Decrease in the Absolute Brightness of Comet Encke", in Astrometriya i Astrofizika, 4, Fizika Komet, ed. V.P. Konoplena, Naukova Dumka, Kiev, 1969. English translation NASA TT F-599.

V-4.   F. W. Taylor, C. M. Michaux, R. L. Newburn, Jr., "A Model of the Physical Properties of Comet Encke", JPL Tech. Rpt. 32-1590, 1973.

V-5.   J. C. Brandt and P. Hodge, "Solar System Astrophysics", McGraw-Hill, New York, 1964.

Section VI

VI-1.   G. R. Hook, E. G. Howard, J. M. van Pelt, W. J. Bursnall, "Study of 1980 Comet Encke-Asteroid Missions using a Spin-Stabilized Spacecraft", Martin Marietta Corp., MCR 73-180, "Mid-Term Review" and MCR 73-260, "Final Oral Presentation", 1973.

Section VII

VII-1.   D. Clay, C. Elachi, C. E. Giffin, W. Huntress, L. D. Jaffe, R. L. Newburn, R. H. Parker, P. W. Schaper, F. W. Taylor, T. E. Thorp, B. Tsuritani, "Science Rationale and Instrument Package for a Slow Flyby of Comet Encke", JPL Doc. 760-90, 1973.

VII-2   F. W. Taylor, C. M. Michaux, and R. L. Newburn, Jr., "A Model of the Physical Properties of Comet Encke", JPL Tech. Rpt. 32-1590, 1973.

Section VII

VII-3.   E. Roemer, "Comet Notes", Mercury, 1, No. 6, 18-19 (1972).

VII-4.   Fairchild Space and Defense Systems, "Charge Coupled Device Image
         Sensor Study", Proposal No. ED-CJ-75 to JPL, Mountain View, Ca.,
         13 April 1973.

VII-5.   Santa Barbara Research Center and Lunar and Planetary Laboratory,
         Univ. of Arizona, "Study of Spin-Scan Imaging for Outer Planet Missions",
         Presentation to NASA Ames Research Center. Contract NAS 2-7096,
         24 July 1973.

VII-6.   CBS Laboratories, "The Applicability of Frame Imaging from a Spinning
         Spacecraft", Presentation to NASA Ames Research Center. Contract
         NAS 2-7101, 24 July 1973.

VII-7   M. Tomasko, "Spin Scan Imaging Capabilities Grigg-Skjellerup
         Flyby", Univ. of Arizona, Presentation to NASA Ames Research
         Center, 1973.

VII-8.   T. Reilly, "Comparison of Imaging System Performance Capabilities
         from Spinning and Stabilized Spacecraft for the Outer Planets
         Missions", JPL Inter-office Memorandum, 2 Jan. 1971.

VII-9   Santa Barbara Research Center, "Evaluation of a Digicon-Type
         Detector Suitable for Advanced Spin-Scan Imagers", Tech. Proposal
         SM028/73a, 7 May 1973.

Section VII

VII-10.   Univ. of Wisconsin, Space Science Engineering Center, "Line Scan
          Radiometer for MVM Flyby Imaging Mission", 12 Nov. 1969.

VII-11.   M. C. Clary, "Mariner Venus-Mercury 1973 Viking Orbiter 1975
          Visual Imaging Subsystem Commonality Study", JPL Interoffice
          Memorandum, 12 June 1970.

VII-12.   Santa Barbara Research Center, "Detailed Instrument Description:
          Pioneer F/G Imaging Photopolarimeter Instrument", Cont. NAS
          2-5605 for NASA Ames Research Center, 1 Oct. 1971.

VII-13.   J. F. Friichtenicht, N. L. Roy, and L. W. Moede,"Cosmic Dust
          Analyzer", Final Report, 10735-6002-R0-00, TRW Systems Group,
          Redondo Beach, Calif., 1971.

VII-14.   H. Fechtig, and J. Weirauch, as quoted by J. Friichtenicht, TRW.
          Personal communication (1973).

VII-15.   R. N. Grenda, W. A. Shaffer, and R. K. Soberman, "Sisyphus -
          A New Concept in the Measurement of Meteoric Flux", XIX Inter-
          national Astronautical Congress, Vol. 1 Spacecraft Systems,
          245 (1970).

VII-16.   A. M. A. Frandsen, R. E. Holzer and E. J. Smith, "OGO Search Coil
          Magnetometer Experiment", IEEE GE-7, #2, 61 (April 1969).

Section VII

VII-17. H. Rosenberg, Pioneer 10 and 11; "Final Technical Report Vector Helium Magnetometer", JPL Contract #952691, Time Zero Corporation (1971).

VII-18. C. T. Russell, and R. E. Holzer, "Fluctuating Magnetic Fields in the Magnetosphere-1.ELF and VLF Fluctuations", Space Science Rev., Vol. 12, #6, 810 (January 1972).

VII-19. A. Hasegura, "Plasma Instabilities in the Magnetosphere", Rev. Geophysics and Space Physics, 9, 703 (1971)

VII-20. R. M. Thorne, "The Importance of Wave Particle Interactions in the Magnetosphere", Critical Problems of Magnetospheric Physics, COSPAR/IAGA/URSI (1972)

VII-21. W. B. Hanson, S. Sanatani, D. Zuccaro, and T. W. Flowerday, "Plasma Measurements with Retarding Potential Analyzer on OGO-6," JGR, 75, 5483 (1970)

VII-21. Instruments and Spacecraft, NASA SP-3028, pp 753-755 (1966).

VII-22. R. H. Parker, J. Ajello, A. Bratenahl, D. Clay and B. Tsurutani, "A Study of the Compatibility of Science Instruments with the Solar Electric Propulsion Space Vehicle", JPL Tech. Memo TM33-641 (1973)

Section VII

VII-23. W. C. Knudsen and K. K. Harris, "Ion-Impact-Produced Secondary
         Electron Emission and Its Effect on Space Instrumentation",
         J.G.R. 78, 1145, (1973).

VII-24. C. W. Snyder, D. R. Clay, and M. Neugebauer, "The Solar Wind
         Spectrometer Experiment", Apollo 12 Preliminary Science Report,
         NASA SP-235 pp 75-81 (1970)

VII-25. R. A. Graham, and F. E. Vescelus, "OGO-E Plasma Spectrometer",
         Proc. 13th National Instrument. Soc. Am. Aerospace Instrument
         Symposium, pp 111-153 (1967)

VII-26. "Pioneer F/G Technical Plan", Pioneer Document P-201, NASA Ames
         Research Center.

Section VIII

VIII-1. H. U. Keller, "Lyman-α Radiation in the Hydrogen Atmospheres
         of Comets. A Model with Multiple Scattering", Astron. Astrophys.,
         23, 269-280 (1973).

VIII-2. F. W. Taylor, C. M. Michaux, and R. L. Newburn, Jr., "A Model
         of the Physical Properties of Comet Encke", JPL TR-32-1590, 1973.

VIII-3. J. L. Bertaux, J. E. Blamont, and M. Festou, "Interpretation of
         Hydrogen Lyman-α Observations of Comets Bennet and Encke",
         Astr. Astrophys. 25, 415 (1973).

Section VIII

VIII-4.   W. H. Ip and D. A. Mendis, "Development of an H_2O Atmosphere
          Around Comet Kohoutek (1973) and its Possible Detection",
          Nature 245, 197 (1973).

VIII-5.   L. Biermann, B. Brosowski, and H. U. Schmidt, "The Interaction
          of the Solar Wind With a Comet," Solar Physics, 1, 254 (1967).

VIII-6.   Personal Communication, A. J. Kliore, JPL.

Section IX

IX-1.   G. R. Hook, E. G. Howard, J. M. van Pelt, W. J. Bursnall,
          "Study of 1980 Comet Encke-Asteroid Missions Using a Spin-
          Stabilized Spacecraft," Martin Marietta Corp., MCR 73-180,
          "Mid-Term Review" and MCR 73-260, "Final Oral Presentation," 1973.

IX-2.   Personal Communication, L. Evans, NASA Ames Research Center, 1973.

IX-3.   Personal Communication, W. J. Bursnall, Martin Marietta Corp., 1973.

IX-4.   B. G. Marsden, as quoted in Ref. IX-1.

IX-5.   E. Roemer, "Comet Notes," Publ. Astron. Soc. Pacific, 73 (1961)
          pp. 170-174 (1961).

IX-6.   R. J. Trumpler, and H. F. Weaver, "Statistical Astronomy," p. 418
          Univ. of California Press, Berkeley, 1953.

IX-7.   H. N. Russell, R. S. Dugan, and J. Q. Stewart, "Astronomy,"

        p. 622, Ginn & Co., Boston, 1927.

IX-8.   "Feasibility of Using The Pioneer 10/11 Imaging Photopolarimeter

        as a Navigation Sensor in Future Pioneer Missions," Report to

        NASA Ames Research Center, Contract NAS 2-6859, TRW Systems Group,

        Redondo Beach, Calif., 20 Dec. 1973.

IX-9.   C. B. Grosch, A. E. LaBonte, and B. D. Vanelli, "The SCNC Attitude

        Determination Experiment on ATS-III," Proc. Symp. on Spacecraft

        Attitude Determination, Aerospace Corp., El Segundo, Calif., 1969.

IX-10. D. L. Mackinson, R. L. Gutshall, and F. Volpe, "Star Scanner Attitude

        Determination for the OSO-7 Spacecraft," J. Spacecraft Rockets,

        10, 262 (1973).

IX-11. R. A. Park, K. R. Jenkin, and D. M. Layton, "Terminal Guidance

        Sensing from a Spinning Spacecraft," AAS Preprint 17-121,

        Am. Astronautical Soc., Tarzana, Calif. 1971.

IX-12. "Saturn Uranus Atmospheric Entry Probe Mission: Spacecraft System

        Definition Study," TRW Final Report, Contract NAS 2-7297, to

        NASA Ames Research Center, TRW Systems Group, Redondo Beach,

        Calif. 1973.

IX-13.   R. F. Gates, J. V. Flannery, and J. T. Cragin, "Feasibility Test

for a V-slit Star Mapper for Pioneer Spacecraft Terminal Navigation,"

Final Report R7537-2-451 to NASA Ames Research Center. Contract

NAS 2-7597. TRW Systems Group, Redondo Beach, Calif. Nov. 1973.

IX-14.   "Mariner Mars 1969 Final Project Report." JPL Technical Report

TR 32-1460. Volume 1, "Development, Design, and Test," pp. 360-373,

1970.

Appendix B

B-1.   G. M. Smith, "Participation in the Large Space Telescope Working

Group Solid State Camera Study," JPL proposal to NASA, 1973.

Appendix C

C-1.   "Mariner Venus-Mercury 1973 Viking Orbiter 1975 Visual Imaging

Subsystem Commonality Study," compiled by M. Clary, JPL, 1970.